Materials Research Report **October 2012**
Final Report

UNF Project
Contract No. BDK82 977-03

The Repair of Damaged Bridge Girders with Carbon-Fiber-Reinforced Polymer "CFRP" Laminates

Principal Investigator: **Adel ElSafty, P.E., Ph.D.**

Graduate Research Assistant: **Matthew K. Graeff**

School of Engineering
College of Computing, Engineering, and Construction
University of North Florida
Jacksonville, Florida 32224

DISCLAIMER

The opinions, findings, and conclusions expressed in this publication are those of the authors and not necessarily those of the State of Florida Department of Transportation.

SI CONVERSION FACTORS

SYMBOL	WHEN YOU KNOW	MULTIPLY BY	TO FIND	SYMBOL
LENGTH				
in	inches	25.4	millimeters	mm
ft	feet	0.305	meters	m
yd	yards	0.914	meters	m

SYMBOL	WHEN YOU KNOW	MULTIPLY BY	TO FIND	SYMBOL
AREA				
in^2	square inches	645.2	square millimeters	mm^2
ft^2	square feet	0.093	square meters	m^2
yd^2	square yard	0.836	square meters	m^2

SYMBOL	WHEN YOU KNOW	MULTIPLY BY	TO FIND	SYMBOL
VOLUME				
ft^3	cubic feet	0.028	cubic meters	m^3
yd^3	cubic yards	0.765	cubic meters	m^3
NOTE: volumes greater than 1000 L shall be shown in m^3				

SYMBOL	WHEN YOU KNOW	MULTIPLY BY	TO FIND	SYMBOL
MASS				
oz	ounces	28.35	grams	g
lb	pounds	0.454	kilograms	kg

SYMBOL	WHEN YOU KNOW	MULTIPLY BY	TO FIND	SYMBOL
FORCE and PRESSURE or STRESS				
lbf	pound force	4.45	newton	N
lbf/in^2	pound force per square inch	6.89	kilopascals	kPa
kip	1000 pounds force	4.45	kilonewton	kN

1. Report No. BDK82 977-03	2. Government Accession No.	3. Recipient's Catalog No.
4. Title and Subtitle The Repair of Damaged Bridge Girders with Carbon-Fiber-Reinforced Polymer "CFRP" Laminates		5. Report Date July 2012 6. Performing Organization Code
7. Author(s) Adel ElSafty, P.E., Ph.D., and Matthew Graeff		8. Performing Organization Report No.
9. Performing Organization Name and Address University of North Florida School of Engineering 1 UNF Drive Jacksonville, FL 32224		10. Work Unit No. (TRAIS) 11. Contract or Grant No. BDK82 977-03
12. Sponsoring Agency Name and Address State of Florida Department of Transportation 605 Suwannee St. MS 30 Tallahassee, FL 32399		13. Type of Report and Period Covered Draft Final Report (4/20/2010) to (9/30/2012) 14. Sponsoring Agency Code
15. Supplementary Notes		

16. Abstract

This research study aims at assessing the repair options for prestressed concrete bridge girders laterally damaged by overheight vehicle collisions. It investigates the effectiveness of different Carbon-Fiber-Reinforced Polymer (CFRP) repair configurations (longitudinal strips and U-wrapping) for the impact-damaged prestressed concrete bridge girders. The study includes both experimental and analytical investigations of the prestressed concrete girders and reinforced concrete beams that were laterally damaged and then repaired with CFRP laminates. It investigates the behavior of both full-scale and half-scale impact-damaged prestressed concrete bridge girders (American Association of State Highway and Transportation Officials (AASHTO) Type II) repaired with CFRP repair systems to restore their flexural capacity. The simulated impact damage in the field included a concrete damage and presetressing force reduction by cutting some of the prestressing strands. The repair systems for eight 40-ft-long AASHTO Type II PSC girders and thirteen half-scale 20-ft-long PS girders were designed to restore the original ultimate flexural capacity. In addition to the static load tests, some of the girders were tested under fatigue loading to examine the behavior under simulated traffic conditions. Test results showed that, with proper detailing, CFRP systems can be designed to restore the flexural capacity and maintain the desired failure mode. Test results indicate that the capacity of the repaired girder was restored and even exceeded the capacity of the control undamaged girder in both strength and ultimate displacement. The study also suggested the optimum configuration of CFRP repair systems (longitudinal strips and U-wrapping).

17. Key Word	18. Distribution Statement
Bridge Girders, CFRP, Repair, Lateral Damage, Static, Fatigue	No restrictions.

19. Security Classif. (of this report)	20. Security Classif. (of this page)	21. No. of Pages	22. Price
Unclassified	Unclassified	119	

Form DOT F 1700.7 (8-72)

ACKNOWLEDGEMENTS

The authors would like to thank the Florida Department of Transportation for their support of this research project. In particular, special thanks go out to Rodney Chamberlain (the project manager), Sam Fallaha (Assistant State Structures Design Engineer, FDOT Structures Research Center in Tallahassee, Florida), David Wagner (engineer of FDOT Structures Research Center in Tallahassee, Florida), and William Potter (engineer of FDOT Structures Research Center in Tallahassee, Florida). We would also like to express our special thanks to the laboratory staff at the FDOT Structures Research Center, including Paul, Steve, Chris, Frank, Tony, Dave, all of the technicians, and OPS staff. Also, appreciation is extended to both the Gate Precast Concrete Company and the Fyfe Company for their participation and support in this experimental research investigation.

EXECUTIVE SUMMARY

A significant number of concrete bridges have been struck by overheight vehicles, and the impact of a vehicle collision may result in bridge system failure. This research study aims at assessing the repair options for prestressed concrete bridge girders laterally damaged by overheight vehicle collisions. The use of externally bonded carbon-fiber-reinforced polymers (CFRP) to repair bridge girders has proven to have numerous advantages; yet it also has limitations. Therefore, this research investigates the CFRP repair option and the effectiveness of different CFRP repair configurations (longitudinal strips and U-wrapping) for the impact-damaged prestressed concrete bridge girders.

The American Concrete Institute (ACI) 440.2R-08 and the NCHRP Report 514 provide the guidelines for strengthening or repairing structural members using FRP composites. In addition, ACI 440.2R-08 refers to debonding behavior as an area that still requires more research. This research project addressed the application of CFRP laminates to repair the laterally damaged prestressed concrete girders and the debonding mitigation.

The study includes both experimental and analytical investigations of the prestressed concrete girders and reinforced concrete beams that were laterally damaged and then repaired with CFRP laminates. The study investigates the behavior of both full-scale and half-scale impact-damaged prestressed concrete bridge (American Association of State Highway and Transportation Officials (AASHTO) Type II) girders repaired with CFRP repair systems to restore their flexural capacity. Impact damage was simulated in the field by (1) concrete damage and (2) reducing the prestressing force by cutting some of the prestressing strands. The repair systems for eight 40-ft-long AASHTO Type II PSC girders and thirteen half-scale 20-ft-long PS girders were designed to restore the original ultimate flexural capacity. In addition to the static load tests, some of the girders were tested under fatigue loading for 2 million cycles to examine the behavior under simulated traffic conditions. The study investigated and recommended the proper CFRP repair design in terms of the CFRP longitudinal layers and U-wrapping spacing to obtain flexural capacity improvement and desired failure modes for the repaired girders.

Test results showed that with proper detailing, CFRP systems can be designed to restore the lost flexural capacity and maintain the desired failure mode. Test results indicated that the capacity of repaired girder was restored and even exceeded the capacity of the control undamaged girder in both strength and ultimate displacement. The study also suggested the optimum configuration of CFRP repair system (longitudinal strips and U-wrapping). The CFRP system composed of longitudinal CFRP laminate applied to the girder soffit along with U-wrapping anchored with a longitudinal CFRP strip at the top ends of U-wrappings proved to be an excellent repair alternative for damaged girders. This repair option restored and increased the load-carrying capacity of the girders. The evenly spaced transverse U-wrappings provided an efficient configuration to mitigate debonding. The original capacity of a damaged bridge girder was restored and enhanced using non-prestressed fabric CFRP repair applications. The damaged prestressed bridge girders repaired using the CFRP laminates withstood over 2 million cycles of fatigue loading with little degradation. The optimum spacing for transverse anchoring is recommended to be between a distance of one half to two thirds the height of the AASHTO girder (or one half the height of the entire composite cross-section). It was also necessary to

cover the damaged section (loss of concrete and ruptured prestressing strands) with transverse and longitudinal strips to restrain the crack opening and propagation in the critical region which initiates early debonding. The CFRP repair restored the lost flexural capacity of the damaged girders. The CFRP repair also enhanced the flexural capacity for the full-scale repaired girders by a range of 23% to 28% compared to that of the control damaged girder. The CFRP repair not only restored the lost flexural capacity of the damaged girders but also enhanced their flexural strength more than that for undamaged control girder by about 10% to 16%. Significant improvements were also reported in the performance of CFRP repaired the half-scale girders. The evenly spaced transverse U-wrappings were successfully implemented to mitigate debonding and performed in a comparable way to fully-wrapped girders.

TABLE OF CONTENTS

LIST OF FIGURES

LIST OF TABLES

1. INTRODUCTION

Uncontrollably, concrete structures are affected by deterioration or damage. A significant number of concrete bridges have been struck by overheight vehicles, and the occurrence of such accidents keeps rising. The impact of vehicles with bridge components may result in failure of the bridge system and loss of lives.

Bridges in New York State are experiencing close to 200 bridge hits a year. From the analysis of bridge hits data provided by the NYSDOT, it has been observed that these accidents could be attributed to numerous factors, including improperly stored equipment on trucks, violation of vehicle posting signs, illegal commercial vehicles on parkways, etc. According to the Federal Highway Administration (FHWA), over 600,000 bridges are registered in the National Bridge Inventory (NBI). By a wide margin, most bridges that collapse do so during floods. Overweight vehicles, usually crossing a bridge in violation of posted weight limits, are the second biggest cause of bridge collapses. According to Federal Highway Administration, a third leading cause of bridge failure or collapse is collision damage when a vehicle or a vessel hits a bridge.

A research conducted in Virginia showed that an inadequate vertical clearance was listed as a key contributing factor in 4% and 6% of the total bridges cited by police officers and highway engineers, respectively. Overheight loads were the leading cause of damage (81%) to prestressed concrete, as reported in another study (Shanafelt and Horn 1980). An analysis of U.S. bridge failures over a 38- year period from 1951 to 1988 was conducted (Harik et al. 1990). Of the 79 bridge failures considered in the study, 11 were precipitated by truck collisions (14%) between superstructure and substructure collisions. The Michigan Department of Transportation reported a 36% increase in overheight collisions over one year (“Span” 1988). The Mississippi State Highway Department installed overheight warning systems on some rural bridges after intensification in bridge damage by overheight logging trucks (Hanchey and Exley 1990).

Despite the persistent and increasing occurrence of bridge collisions, few studies have focused on the assessment of the structural damage, suitable repair material, optimum repair method and repair configuration. A multitude of procedures have been developed in order to restore any structures seriously affected by such influences. However, as technology advances and new materials are utilized for innovative applications, more desirable procedures for restoration become available. Yet, when new materials are introduced, it is necessary to investigate the effectiveness and performance of those new materials and the most efficient manner to implement them. Carbon-Fiber-Reinforced Polymers (CFRP) is one of those fairly new materials that are being utilized in different innovative applications. The unique properties of this material have made it appealing for structural repairs and/or structural member strengthening applications. The use of CFRP laminates for restoring or enhancing the performance of reinforced concrete (RC) and prestressed concrete (PSC) bridge girders has become a more commonly acceptable repair method (ElSafty and Graeff 2011). However, there is still a great need to investigate the effectiveness of using CFRP systems in the repair of damaged PSC girders due to a vehicle impact/collision.

The literature shows a lot of experimental and analytical information on the effectiveness of CFRP systems for strengthening or retrofitting both RC and PSC girders (Shanafelt and Horn

1985). Yet, most of the published experimental work that addresses external strengthening of concrete girders with composite materials is focused on specimens without preexisting damage. Little investigation has been conducted on repair of impact damaged girders; which is important due to the high frequency of bridge collisions in the United States. Also, many previous research tests experienced debonding of the longitudinal CFRP laminates attached to the concrete tension surface. The debonding problem associated with FRP laminates hinders the ability to utilize the full tensile strength of the FRP thereby decreasing the efficiency of the repair. Therefore there was a demand for researching behavioral aspects of externally bonded CFRP used for repairing laterally damaged bridge girders.

The following research investigates the effectiveness of using CFRP laminates in repairing both RC and PSC girders damaged primarily by impacts that cut through the steel reinforcement and/or prestressing cables (Figure 1-1). Included in the investigation is an evaluation of the proper configuration and spacing of CFRP U-wrappings to mitigate the debonding problem. Other repair application and design considerations such as cross-section, reinforcement ratio, and the level of strengthening (number of CFRP soffit layers) were also addressed in the experimental program and the resulting recommendations are ultimately presented.

Figure 1-1: Example of severe impact damage to prestressed concrete bridge girder

1.1. BACKGROUND

Currently there exists a multitude of options for viable methods to repair structurally deficient reinforced concrete (RC) and prestressed concrete (PSC) bridge components. The use of externally bonded carbon-fiber-reinforced polymers (CFRP) to repair bridge girders has proven to have numerous advantages in comparison. CFRP has a high strength to weight ratio, is resistant to chemicals, and the repair methods are usually inexpensively and rapidly applicable in the field with little to no disturbance to traffic; the repairs also maintain the overheight clearance and original configuration of the structure (Shin and Lee, 2003). Yet, in spite of their benefits, the use of externally bonded FRP systems is hampered by the lack of nationally accepted design specifications for their use in the repair and strengthening of concrete bridge elements (NCHRP R-655, 2010).

The American national specifications for designing externally bonded CFRP laminates is the American Concrete Institute (ACI) 440.2R-08. This document provides a large array of guidelines for strengthening structural members. However, it does indicate some limitations in its contents and refers to durability and debonding behaviors as “areas that still require research”.

It continues to state specifically that "more accurate methods of predicting debonding are still needed" (ACI Committee 440 2008). Similarly, this document also does not provide deflection provisions specific for FRP-strengthened beams but instead refers the designer to ACI 318-99 which does not address post-yielding deflections for strengthened beams.

The ability of bonded CFRP to enhance the capacity of RC or PSC girders is well established with conservative documents such as the ACI 440 reporting enhancement possibilities up to 160% and multiple independent research papers reporting enhancements up to 200% including Ramana et al. 2001, Grace et al. 1999, and Grace et al. 2003. However, these documents and most others do not address strengthening concrete members with existing damage. Furthermore, none of the design references and very few research papers address the effects of intermediate transverse anchoring and the corresponding design considerations. Therefore, with the limitations or lack of research and nationally accepted design specifications it was determined that more investigation was required to develop an efficient CFRP repair design procedure for prestressed concrete bridge girders (Charkas et al. 2003).

1.2. STATEMENT OF HYPOTHESIS

It was found that the lack of existing design information was primarily related to implementing the repairs on girders with pre-existing damage, more specifically, lateral damage. It was hypothesized that through conducting an extensive experimental program of testing real structural components with simulated lateral damage and various CFRP repairs, an accurate and justified design procedure could be compiled. That design procedure will assist the state transportation department in designing cost effective CFRP repairs for future incidents of damaged prestressed concrete bridge girders.

1.3. OBJECTIVES

The experimental program consisted of testing both prestressed and reinforced concrete girders with lengths ranging from 8 ft to 40 ft. A total of 55 beams of various sizes and reinforcement ratios were tested and observed in order to achieve the following objectives.

1. To investigate the feasibility and performance of an innovative repair using CFRP laminates to restore the capacity of laterally damaged concrete and prestressed concrete girders.

2. To investigate experimentally and analytically the CFRP laminate performances and their potential debonding.

3. To investigate the effectiveness of using the transverse U-wrappings to anchor and mitigate the longitudinal CFRP debonding problem.

4. To investigate different configurations of both longitudinal and transverse CFRP laminates to constitute a repair.

5. Develop a recommended spacing of the CFRP U-wrappings for repairing laterally damaged prestressed concrete girders.

6. Investigate the fatigue behavior of CFRP repaired prestressed concrete girders.

The research also presents the flexural behavior of the repaired girders including load-deflection characteristics, strain development, and modes of failure. Similarly, an analytical design model is established and proposed to more effectively design CFRP repairs for laterally damaged prestressed and reinforced concrete bridge girders.

2. LITERATURE REVIEW

2.1. BRIDGE IMPACT STUDIES AND ASSESSMENTS

FRP has been used to repair several impact-damaged prestressed concrete girders in the field (Stallings et al. 2000, Schiebel et al. 2001, Tumialan et al. 2001, Di Ludovico 2003). However, a very limited number of studies were conducted in a laboratory setting to describe the overall behavior and nature of failure (Klaiber et al. 1999, Green et al. 2004, Di Ludovico et al. 2005).

A study conducted by Rosenboom et al. (2011) indicated that the field studies have shown that FRP repair systems can reduce displacements at service load levels (Stallings et al. 2000), successfully restore the capacity after large losses of concrete section (Schiebel et al. 2001), and perform well under service loads after loss of a small number of ruptured prestressing strands (Tumialan et al. 2001, Di Ludovico 2003).

The study by Rosenboom et al. also indicated that laboratory testing of impact-damaged prestressed concrete bridge girders has reported mixed results. Premature debonding of the longitudinal CFRP occurred due to poor detailing in some studies. One study indicated that a combination of inadequately detailed transverse CFRP anchorage and insufficient CFRP development length led to debonding failure of the CFRP system (Klaiber et al. 1999). Other studies concluded that proper detailing of the CFRP repair system, especially at the CFRP termination points, was critical for good bond performance (Di Ludovico et al. 2005, Green et al. 2004).

One of the most influential publications investigating damaged PSC bridges was published in 1980 by Shannafelt and Horn. In this report, known as NCHRP Report 226, an extensive compilation of statistics provided by cooperating states is presented documenting damaged PSC bridges all over the nation. It is reported that of the 23,344 PSC bridges in those participating states, an average of 201 were damaged each year. Furthermore, it was discovered that 80 percent of the damage to the PSC bridges was due to overheight vehicle collisions. Similarly, more recent studies have been conducted in the same manner to evaluate the frequency of current PSC bridge conditions. In 2003, Fu, Burhouse, and Chang published a study of overheight vehicle collisions reporting that of the 29 state departments participating, 62% considered overheight vehicle collisions a significant problem; including Florida (Fu et al. 2003). Additionally, it was stated that on average, between 25 and 35 PSC bridges are damaged each year, in every state. Furthermore, in 2008 Agarwal and Chen reported that, of the bridges that are damaged by overheight collisions each year many are impacted multiple times (Agarwal and Chen 2008). Providing an example in NY State where 32 bridges have been struck a total of 595 times since the mid-1990s.

Sixty one percent of the damaged girders surveyed by a study (Feldman et al. 1998) were assessed as having minor damage, defined as isolated cracks, nicks, shallow spalls, or scrapes. Moderate damage, defined as cracks or spalls large enough to expose undamaged prestressing tendons, was found in 25% of the girders. Severe damage, consisting of damaged tendons, significant concrete section loss, or lateral misalignment, made up the remaining 14% of cases (Chung et al.). The resulting statistics from the previously mentioned surveys led to the

understanding that there was a need to standardize a method to evaluate damaged PSC bridge members and possible associated repair methods. Shannafelt and Horn followed up their previous investigation with a second publication in 1985 researching the appropriate repairs for different amounts of damage; it is known as NCHRP Report 280. This document classified possible damages into three categories.

Minor Damage: is defined as; concrete with shallow spalls, nicks and cracks, scraps and some efflorescence, rust or water stains. Damage at this level does not affect a member's capacity. Repairs are for aesthetic or preventative purposes.

Moderate Damage: includes; larger cracks and sufficient spalling or loss of concrete to expose strands. Moderate damage does not affect a member's capacity. Repairs are intended to prevent further deterioration.

Severe Damage: is classified as; any damage requiring structural repairs. Typical damage at this level includes significant cracking and spalling, corrosion and exposed and broken strands.

The repair methods experimentally tested by Shannafelt and Horn investigated external post-tensioning, externally bonded reinforcing bars, mild steel external sleeves, and internal strand splicing. However, in 2009 Kasan published a similar, updated study which subdivides the "Severe Damage" classification into three different categories and introduces FRP systems as repair methods (Kasan 2009). The three categories proposed to represent the "Severe Damage" classification are:

Severe I: the experienced damage requires structural repair that can be affected using a non-prestressed or post-tensioned method. This may be considered as repair to affect the strength (or ultimate) limit state.

Severe II: the experienced damage requires structural repair involving replacement of prestressing force through new prestressing or post-tensioning. This may be considered as a repair to affect the service limit state in addition to the ultimate limit state.

Severe III: the experienced damage is too extensive. Repair is not practical and the member or element must be replaced.

The author continues to provide the appropriate or best fitting repair method for a variety of experienced amount of damage; including additional CFRP repair system methods ranging from preformed CFRP strips to non-prestressed CFRP fabrics, near-surface mounted (NSM) CFRP, prestressed CFRP, or post-tensioned CFRP. This information is presented and available in Table 2-1.

2.2. DESIGN CRITERIA AND EXISTING CODES

Since the emergence of CFRP usage as a structural repair or enhancement efforts have been made to standardize both the predicted behaviors and needed design calculations for

implementation. The American Concrete Institute (ACI) 440.2R-08 addresses the design criteria and calculations for designing externally bonded CFRP systems to repair both RC and PSC bridge girders. However, the ACI document indicates some limitations in its contents and refers to durability and debonding behaviors as "areas that still require research". It continues to state specifically that "more accurate methods of predicting debonding are still needed". Furthermore, this document also does not provide deflection provisions specific for FRP-strengthened beams but instead refers the designer to ACI 318-99 which does not address post-yielding deflections for strengthened beams (Charkas et al. 2003). Similarly, the AASHTO and AASHTO Load and Resistance Factor Design (LRFD) provisions (which provide specifications for structural design parameters including design loading criteria, impact factors, and reduction factors) do not contain appropriate values or calculations for concrete members strengthened with CFRP laminates.

Some of the aforementioned limitations have been previously addressed by other researchers. El-Tawil and Okeil developed a fiber section model that accounts for inelastic material behavior, composite action between deck and girder, CFRP bonding properties, and various parameters involved with the construction sequence (El-Tawil and Okeil 2002). Using this model to conduct thousands of Monte Carlo simulations the pair ultimately proposes an equation for the flexural strength reduction factor for PSC girders strengthened with CFRP in their 2010 publication. Likewise, Charkas, Rasheed, and Melhem present a rigorous procedure for accurately calculating the deflections of RC beams strengthened with FRP systems (Charkas et al. 2003). Their method of calculation is based on a moment curvature relationship which is idealized to be trilinear addressing precracking, post-cracking, and post-yielding stages. Lastly, a 2008 publication by Rosenboom and Rizkalla investigates the common debonding problem associated with bonded CFRP laminates. This document identifies and discusses the most common premature debonding concern, referred to as intermediate crack debonding. This is where the crack propagations through the interface of the bond are initiating at the toes of intermediate flexural cracks. Through experimental testing and analysis they first provide compelling evidence that the current calculation modes do not correlate to results.

Table 2-1: Appropriate Repair Methods for Various Levels of Damage, from Kasan 2009

Damage Assessment Factor	Repair Method								
	Preform CFRP strips	**CFRP fabric**	**NSM CFRP**	**Prestressed CFRP**	**PT CFRP**	**PT Steel**	**Strand Splicing**	**Steel Jacket**	**Replace Girder**
Damage that may be repaired	Severe I	low Severe I	Severe I	Severe II	Severe II	Severe II	low Severe I	Severe II	Severe III
Active or Passive repair	passive	passive	passive	marginally active	active	active	active or passive	active or passive	n/a
Applicable beam shapes	all	all	IB, limited otherwise	all	all	all	IB, limited otherwise	IB	all
Behavior at ultimate load	excellent	excellent	excellent	excellent	excellent	excellent	excellent	uncertain	excellent
Resistance to overload	limited by bond	limited by bond	good	limited by bond	good	excellent	excellent	uncertain	excellent
Fatigue	limited by bond	limited by bond	good	limited by bond	excellent (unbonded)	excellent	poor	uncertain	excellent
Adding strength to undamaged girders	excellent	good	excellent	excellent	excellent	excellent	n/a	excellent	n/a
Combining splice methods	possible	possible	unlikely	possible	good (unbonded)	good	excellent	excellent	n/a
Number of strands spliced	up to 25%	limited	limited by slot geometry	up to 25%	up to 25%	up to 25%	few strands	up to 25%	unlimited
Preload for repair	no	no	no	no	no	no	possible	possible	n/a
Preload for patch	possible	no	yes	possible	possible	possible	yes	no	n/a
Restore loss of concrete	patch prior to repair	patch prior to repair	patch prior to repair	patch prior to repair	patch prior to repair	patch prior to repair	excellent	patch prior to repair	n/a
Constructability	easy	easy	difficult	difficult	moderate	moderate	difficult	very difficult	difficult
Speed of repair	fast	fast	moderate	moderate	moderate	moderate	fast	slow	very slow
Environmental impact of repair	VOC's from adhesive*	VOC's from adhesive	adhesive VOC's & dust	VOC's from adhesive	minimal	minimal	minimal	welding	erection issues
Durability	environmental protection	environmental protection	excellent	environmental protection	environmental protection	corrosion protection	excellent	corrosion protection	excellent
Cost	low	low	moderate	moderate	moderate	low	very low	moderate	high
Aesthetics	excellent	excellent	excellent	excellent	fair	fair	excellent	excellent	Excellent

* (VOC) Volatile organic compound

Then ultimately, a discussion is provided regarding a more accurate proposed model for debonding predictions.

2.3. MATERIAL PROPERTIES AND BENEFITS

Since the emergence of interest in using FRP products to restore/retrofit structural components, a great deal of research has been done to evaluate benefits of both the material and the cost of implementation. The resulting consensus from the industry is that FRP products and the applications in which they are implemented are much more desirable methods for repairing or restoring degraded structural components. In agreement with many other publications, Shin and Lee give a good description in their 2003 publication stating that, with CFRP's high strength-to-weight ratio, its resistance to chemicals, and its ease of application, inexpensive and rapid restorations can be implemented in the field with little to no disturbance to traffic flow while maintaining the structure's original configuration and overheight clearance. Similar praises of the material's effectiveness after application have also been documented. R. Alrousan reports that the use of CFRP composites to rehabilitate structural components can greatly reduce maintenance requirements, increase safety, and increase the service life of the overall structure (Alrousan 2011). Other researches were also conducted to investigate the strengthening of impact-damaged bridge girder using FRP laminates (Nanni et al. 2001, Tumialan et al. 2001)

In addition to benefits of the material properties, it is also commonly reported that the use of CFRP is cost effective. Though it should be known that CFRP materials do carry a hefty price tag, application/labor costs are so greatly reduced that it becomes effective. In 1999, Grace et al. made a comparison and concluded that, in combination with the savings in the repair cost, and the elimination of future maintenance cost, FRP applications are economically competitive with their steel counterparts.

However, the intent of this project is specifically geared towards non-prestressed fabric CFRP repair applications; whereas the previous statements are directed towards the benefits of FRP applications in general. Kasan and Harries addressed these aspects in their 2009 document by concluding that, even though it has been demonstrated that prestressed and post-tensioned CFRP repairs utilize the carbon fiber material more efficiently, the difficulties and cost of implementation are more significant than the cost of extra CFRP material needed for non-prestressed applications (Kasan and Harries 2009, Harries 2009).

2.4. FLEXURAL REPAIR DESIGNS AND CONSIDERATIONS

A discussion of design considerations for implementing efficient structural repair using non-prestressed fabric CFRP laminates logically begins with the current American standards for the design of externally bonded FRP systems. This reference is the ACI 440.2R-08 previously mentioned, and appropriately, one of the first considerations it addresses is the scope and limitations of implementing various FRP repair systems. Each FRP repair system, whether it is prestressed FRP, post-tensioned FRP, non-prestressed FRP, or near surface mounted FRP bars, has its own abilities and limitations. This is why the ACI document first advises the execution of a detailed and thorough condition assessment of the existing structure which is to receive the repair or retrofit. The primary information that should be established during the assessment

includes the existing load-carrying capacity of the structure, any structural deficiencies and their causes should be identified, and the condition of the concrete substrate should be determined. The document continues further and elaborates, recommending that a multitude of items be determined. These items include, the existing dimensions of the structural members; the location, size, and causes of cracks and spalls; the location and extent of any corrosion of reinforcing steel; the presence of any active corrosion; the quality and location of existing reinforcing steel; the in-place compressive strength of the concrete; and the soundness of the concrete, particularly the concrete cover in all areas where the FRP system is going to be bonded to the concrete.

The second major consideration raised by the ACI document is the strengthening limitations that should be followed to prevent sudden failure of the repaired member in case the FRP system is damaged. The philosophy of the guidelines used to specify these strengthening limitations is that a loss of the FRP system should not cause member failure under a sustained service load. These imposed limitations are specific to each repair project and should consider aspects such as the calculated load limitations, the rational load paths, effects of the temperature and environment on the FRP system, and any effects of reinforcing steel corrosion on the repair. The document further discusses the importance of these considerations and limitations as they relate to fire codes because FRP materials are known to degradate under high temperatures. The degradation of the material is to the point that, in the instance of fire the FRP system is usually assumed to be completely lost.

Other design aspects mentioned in the document that should be considered relate to the installation of the FRP system. The first aspect related to installation addressed is substrate repair and surface preparation. Where, in the case of bonded fabric CFRP, it recommends that all problems associated with the substrate should be repaired; including both corrosion-related deterioration in the substrate and crack control/crack injection. Similarly, in the case of bond-critical applications such as CFRP fabrics, a number recommendations are made related to surface preparation that facilitate a strong bond between the FRP material and the concrete surface. The recommendations related to the surface preparation include, but are not limited to: rounding off any sharp outside corners of the member; cleaning the surface so it is free of any dust, dirt, oils, or anything else that could interfere with the bond of the FRP system; filling in any variations that could cause voids between the two materials, such as extrusions or bug holes, with an approved putty material; and lastly, the repaired surface should be roughly ground or sanded to help insure an adequate bond. The design aspects related to the installation that address the FRP material itself include considerations such as the alignment of the FRP materials, lap splices used when multiple layers are applied to a member, and temporary protection needed during the curing process of the resins used to bond FRP materials to concrete.

Lastly, the quantified design considerations for flexural strengthening calculations are detailed in chapter ten of the ACI document. This chapter first gives a reasonable range of increases in flexural strength from 10 to 160% which was adopted from other supporting documents. It continues to describe verbally and mathematically the required aspects of its recommended strength design approach. The aforementioned aspects include the nominal strength considerations as they would pertain to each failure mode, the assumptions used when designing repairs for either reinforced concrete or prestressed concrete members, shear strength

requirements, existing substrate strains, strain and stress levels that are developed in the FRP reinforcements, strength reduction factors that could be applicable, serviceability design requirements, creep-rupture and fatigue stress limits, stresses developed in steel reinforcements under service loads, and the ultimate strength of the designed repair section. To summarize, the document provides guidance on proper detailing and installation of FRP systems to strengthen and repair structural members to prevent any undesirable failure modes. Though the ACI document includes a vast number of design considerations and calculations, the limitations which it contains and considerations not mentioned in the document have been researched by several independent entities.

Most all are in general agreement with the ACI, documenting the ability of CFRP to increase the capacity of a bridge girder by gaining maximum enhancements around 200% as reported in Ramana et al. 2001, Grace et al. 1999, and Grace et al. 2003. Similarly, the ACI 440.2R-08 concludes that debonding behaviors will require more research, as many investigative efforts resulted in the same conclusion; Di Ludovico et al. 2005, Green et al. 2004, Klaiber et al. 1999, and Klaiber et al. 2003 all reported issues with premature debonding failures due to either inadequate transverse CFRP anchors or development lengths. Though several papers report debonding issues, a number of conducted researchers have demonstrated successful cases of repairing damaged bridge girders. As a result the general conclusions accepted to constitute a satisfactory are summarized well in a 1999 publication by Grace et al. which states that by providing both horizontal and vertical FRP laminates coupled with the proper epoxy can decrease the deflection and possibly double the ultimate carrying capacity of a repaired girder. They continue to state that the vertical layers are used to prevent rupture or early debonding failures in the flexural horizontal laminates.

Then, in more recent publications by Rosenboom et al. the design issues concerning the presents of lateral damage which cut through prestressing reinforcements on one side of the girder is addressed. In their 2010 publication they present a study of five laterally damaged full-scale AASHTO type II girders repaired with CFRP tested under both static and fatigue loading. Concluding the research it was determined that PSC girders having a significant loss of concrete cross-section and up to 18.8 percent loss of prestressing can be repaired using CFRP laminates to restore the original capacity of the member. It continues to suggest that detailing of the CFRP repair configuration should be carefully considered to restrain the opening of cracks in the damaged region and to prevent debonding; which in their research included a longitudinal laminate on the side of the bottom flange of the girders. Other conclusions provided information into fatigue and shear behavior, claiming that AASHTO girders repaired with CFRP withstood over 2 million cycles of fatigue loading with very little degradation and the ACI 440 document combined with the Precast Prestressed Concrete Institute (PCI) design manual provides accurate predictions to the shear behavior of the section.

As for the implications that the established shear design aspects are already very accurate for designing CFRP laminate repairs, this has been proven and documented in several studies and therefore will not be addressed in the following conducted research. However, the same does not apply for the fatigue implications raised in the publication by Rosenboom et al. In a previous study by Rosenboom and Rizkalla they state that “The effect of the CFRP strengthening on the induced fatigue stress ratio in the prestressing strands during service loading conditions is not

well defined." (Rosenboom & Rizkalla, 2006). Yet, in a 2001 publication by El-Tawil et al., it was concluded that fatigue cycle loading leads to a redistribution of stresses similar to that obtained under static creep (El-Tawil et al. 2001). They specify that the stresses in the steel can display an increase in stress of approximately five percent due to fatigue cycling. They follow up by recommending a limitation that the service steel stresses should not exceed eighty-five percent of the yield strength to account for the increase in stress displayed, shrinkage, creep under dead loads, and any variability in the reinforcing steel strength. Though there exists some conflicts between some previous researches there seems to be a general agreement that CFRP repairs can sustain increased load levels under fatigue cycling.

2.5. SUMMARY OF STATE OF THE ART

Recent studies and surveys have established that a large number of vehicles collide with bridge structures all over the United States and the majority of those are due to overheight vehicles impacting bridge girders. The lateral damage that is common in these cases has been well documented at various levels of damage and appropriate methods to repair those damages have been established. Through analysis of efficiency versus cost, previous work in the field has revealed that externally bonded non-prestressed CFRP has a more desirable cost-to-benefit ratio when strengthening or repairing bridge girders. The use of CFRP as repair or strengthening option has several advantages due to its noncorrosive nature, ease of installation, and high strength-to-weight ratio.

The current standards for designing externally bonded CFRP laminates provide an immense amount of information required for design. However, being a fairly new material there are some behavioral aspects that have limited understanding and need more investigation such as the debonding stresses and debonding failures. Other research has addressed some of these limitations in the standard codes as they relate to flexural design, but results from their study should be confirmed. As for the shear design of girders repaired with externally bonded CFRP fabrics, the ACI procedure combined with considerations from the PCI design manual as well as similar procedures have been validated and confirmed through multiple independent research projects.

3. METHODOLOGY

This research study aims at assessing the repair options for the laterally damaged prestressed concrete bridge girders by overheight vehicle collisions with highway bridges. This study includes both experimental and analytical investigations of full-scale prestressed concrete AASHTO II girders, half-scale prestressed concrete beams, and reinforced concrete beams that were laterally damaged and then repaired with CFRP laminates.

3.1. EXPERIMENTAL PROGRAM

The proposed experimental program consisted of testing both prestressed and reinforced concrete girders; including control girders and CFRP flexural repaired concrete girders. The girder lengths ranged from 8 ft to 40 ft and were subjected to simulated lateral damage that cut through the steel reinforcements. They were pre-damaged by saw-cutting through the concrete and the flexural steel reinforcement and/or strands in the girder's side before installing the CFRP laminates. Several repair methods and considerations were evaluated by designing multiple different configurations of CFRP laminates with various numbers of longitudinal CFRP layers while changing the number and spacing for transverse CFRP U-wrappings for a number of test specimens having different dimensions.

Material Properties used for designing Test Specimens: All of the included test specimens were designed using considerations and calculations from the ACI 440.2R-08 document. To complete those calculations and evaluate the designed specimens, the property values provided by the manufactures for each material were used. All of the design values provided for both the CFRP and steel reinforcement properties used are listed in Tables 3-1 and 3-2.

Table 3-1: Properties of CFRP Materials Utilized in Repair Methods

CFRP Material Properties	Typical Dry Fiber Properties	*Composite Gross Laminate Properties
Tensile Strength	550 ksi (3.79 GPa)	121 ksi (834 MPa)
Tensile Modulus	33.4 x 10^6 psi (230 GPa)	11.9 x 10^6 psi (82 GPa)
Ultimate Elongation	1.70%	0.85%
Density	0.063 lb/in^3(1.74 g/cm^3)	N/A
Weight per Sq yd.	19oz. (644 g/m^2)	N/A
Nominal Thickness	N/A	0.04 in. (1.0 mm)
*Gross laminate design properties based on ACI 440 suggested guidelines will vary slightly		

Table 3-2: Properties Of Steel Reinforcements Used to Design Test Specimens

Steel reinforcements	Prestressing Strands	#3 mild steel rebar	#4 mild steel rebar
Diameter	0.4375 in. (11.1mm)	0.375 in. (9.53 mm)	0.5 in (12.7 mm)
Steel area	0.115 in^2 (96.9 mm^2)	0.11 in^2 (71.3 mm^2)	0.2 in^2 (126 mm^2)
Steel Grade	270	60	60
Young's mod.	$27.5x10^3$ ksi	$29x10^3$ ksi	$29x10^3$ ksi
Weight	0.367 lb/ft	0.376 lb/ft	0.683 lb/ft
Yield Strength	243 ksi (1676 MPa)	60 ksi (345 N/mm^2)	60 ksi (345 N/mm^2)
Ult. Strength	270 ksi (1862 MPa)	90 ksi (621 N/mm^2)	90 ksi (621 N/mm^2)

The CFRP product decided upon for this research was Tyfo® SCH-41, a unidirectional carbon fiber fabric product from the Fyfe Company, as shown in Figure 3-1. It was used in conjunction with their Tyfo® S, a saturating epoxy designed by the manufacturer specifically for the CFRP product. A unidirectional fiber was desired for the research because of its affordability and efficiency. The specific unidirectional fiber product chosen was selected based on the various properties of materials and the outcomes reported in previous research documents.

Figure 3-1: Picture of carbon fiber fabric material used in test specimen

3.1.1. REINFORCED CONCRETE BEAMS

The primary purpose of the RC series of testing was to quickly manufacture relatively small test specimens that were easy to work with and could be tested to gain an immediate informed understanding of the mechanics surrounding the scope of the investigations. The RC series included a total of thirty-four beams, all 8 ft long with cross-section dimensions of 5.5 in by 10 in. However, the first fifteen beams were manufactured with #4 mild steel rebar as the main flexural reinforcements and the remaining nineteen beams were manufactured with #3 mild steel rebar. The intention was to gather information regarding the behavioral difference pertaining to the reinforcement ratios. The first fifteen beams had an undamaged reinforcement ratio of 0.0128 and a damaged ratio of 0.0086 while the last nineteen RC beams had reinforcement ratios of 0.0071 for undamaged beams and 0.0047 for damaged beams. Figure 3-2 shows a sketch and a picture of the test specimen cross-section dimensions and reinforcements.

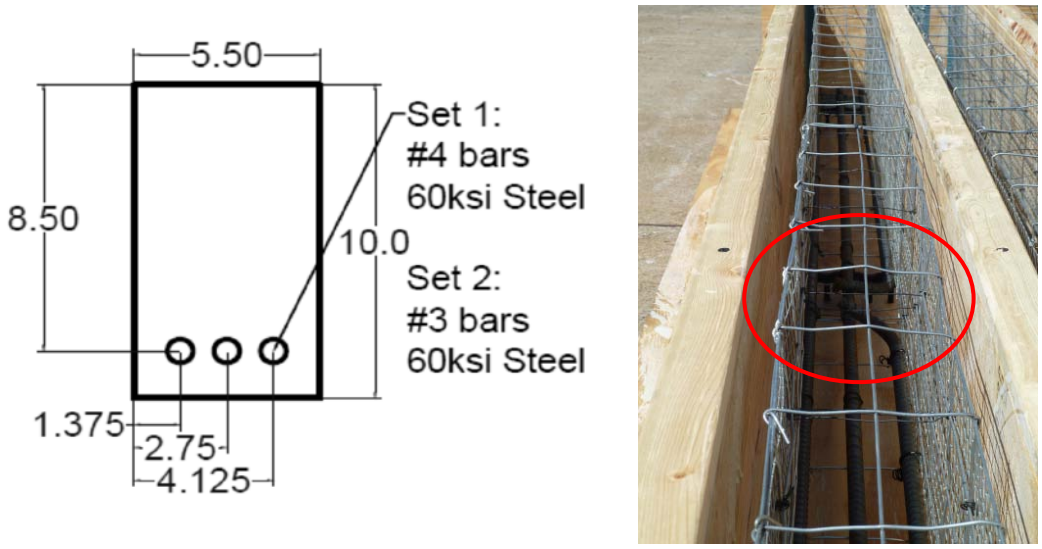

Figure 3-2: (left) Cross-section dimensions of RC test specimens; (right) Example of RC casting forms and internal steel reinforcements.

It should be evident by looking at the example photo presented in Figure 3-2 that a welded wire steel mesh was used as the shear reinforcements; this is true for all thirty-four RC beams. Similarly, in the photo of Figure 3-2, it can be seen that the outermost longitudinal rebar is cut and bent inward at mid-span. This is how the simulated lateral damaged was achieved for the RC test specimen.

The method of simulating the lateral damage during the manufacturing process provided the benefit of quick production and repair application. By cutting and bending the longitudinal rebar then casting the concrete, the resulting product simulated a laterally damaged RC beam with an excellent concrete repair.

Having all RC beams cast with simulated damage imposed, CFRP repairs were applied in various configurations specifically designed for the investigative purposes. For the first fifteen beams containing the larger #4 mild steel rebar, only one ply of longitudinal CFRP was used to

maintain the limits in the ACI-440.2R-08, whereas two plies of longitudinal CFRP were applied to the last nineteen having the smaller #3 rebar. The configurations of the transverse CFRP U-wrappings designed for each set are presented in Figures 3-3 and 3-4. The first fifteen beams have #4 rebar and one layer of CFRP and are designated set 1 or the "TB" set since the beams were cast in Tallahassee. And, the last nineteen beams with the #3 rebar and two layers of CFRP are designated as set 2 or the "JB" set since the beams were cast in Jacksonville.

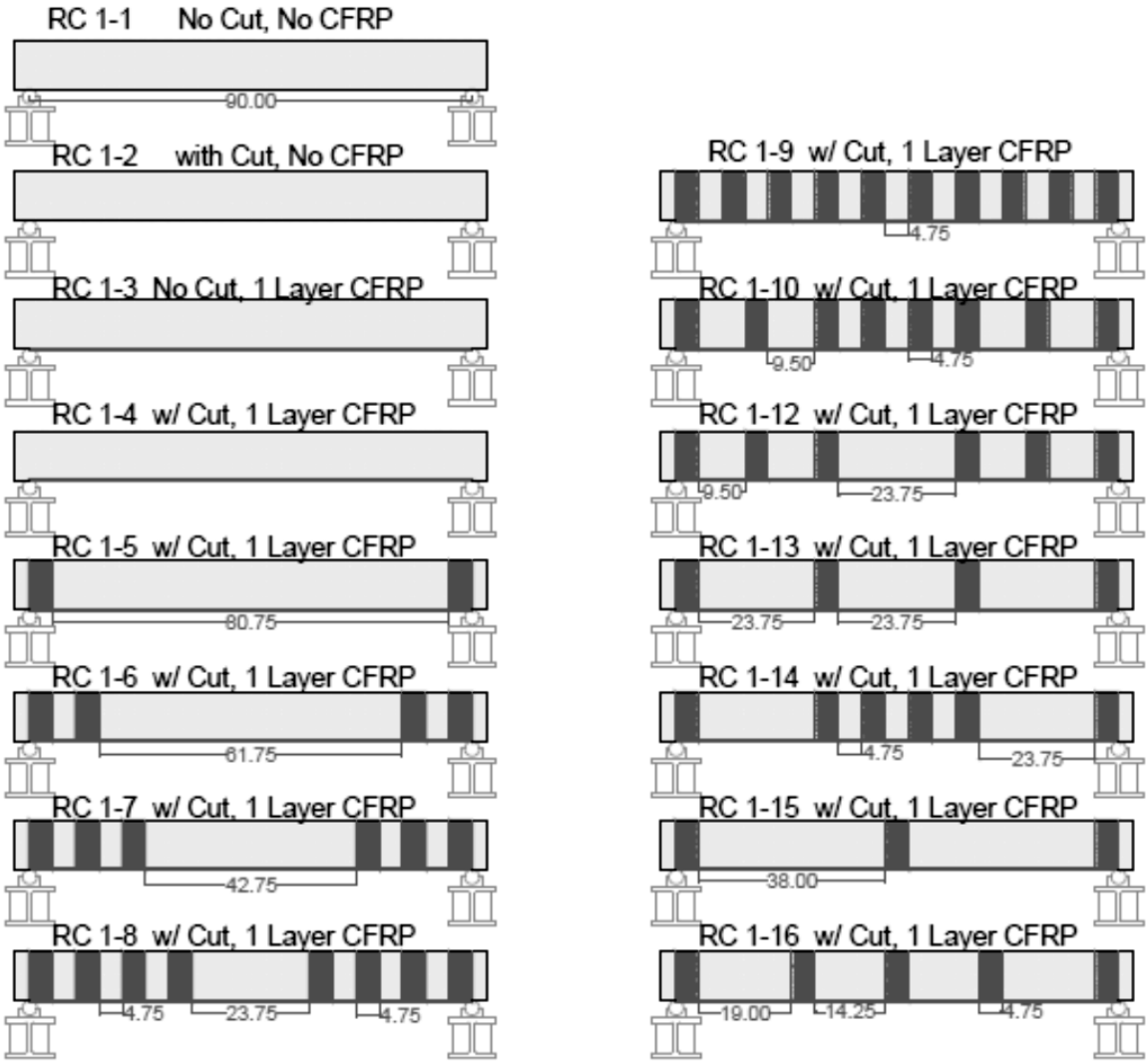

Figure 3-3: CFRP repair configuration layout for set 1 containing #4 rebar and one ply

The first set, shown previously in Figure 3-3, was designed based on the implications in the ACI440.2R-08 that specify the end areas or termination points of the longitudinal laminate as critical points for stress development. Upon observation of testing a handful of the beams included in this set, it was evident that the flexural cracks which developed during loading would initiate some early debonding behaviors by the longitudinal CFRP laminate. Furthermore, after analyzing the results from the first set, it was confirmed that a different approach to designing the transverse CFRP U-wrapping was needed.

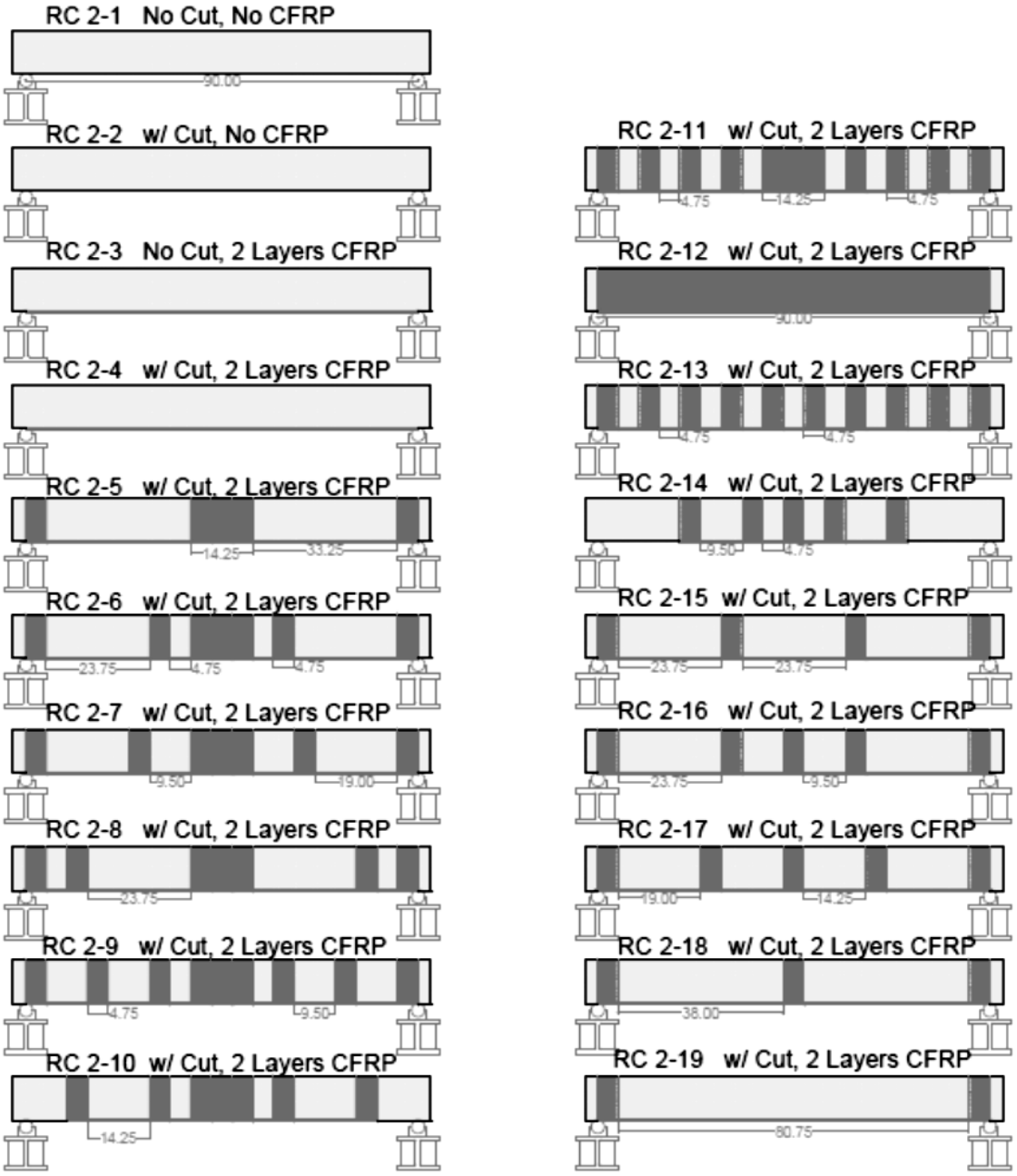

Figure 3-4: CFRP repair configuration layout for set 2 containing #3 rebar and two plies

The second set of nineteen beams was then designed to not only address the issues with end pealing stresses but also to address the issues with the flexural cracks initiating debonding. To address the later, it was believed that the section at the mid-span of the beams needed to be wrapped with transverse U-wrappings to prevent early debonding in that region and to hinder crack propagation in the damaged zone. The resulting designed configurations for the transverse U-wrappings were as they are presented in Figure 3-4 above.

3.1.2. HALF-SCALE PRESTRESSED CONCRETE (PS) GIRDERS

The tested half-scale prestressed concrete girders were 20 ft long and had cross-sectional dimensions set at exactly half-scale of an AASHTO type II girder. An additional decking 4in. thick was also cast on top to simulate a bridge deck composite with the PS girders. The concrete used for manufacturing the girders ended up having an average compressive strength of approx. 10,000 psi on the days of testing. A total of five low-relaxation grade 270 seven-wire prestressing strands were used to reinforce each girder. In addition, three non-prestressed rebar were provided in the girder flanges and two rebar in the deck topping. To insure full composite action, half of the steel stirrups provided for shear extended vertically from the girder to the decking while the other half remained entirely in the girder. They were spaced every six inches alternating between the two height sizes, providing nearly the maximum amount of shear reinforcement for the cross-section. The girders were designed to be heavily reinforced in shear in order to avoid any premature failures which could jeopardize the test results and the investigations into the debonding issues. A sketch of the cross-section and the reinforcements is shown in Figure 3-5.

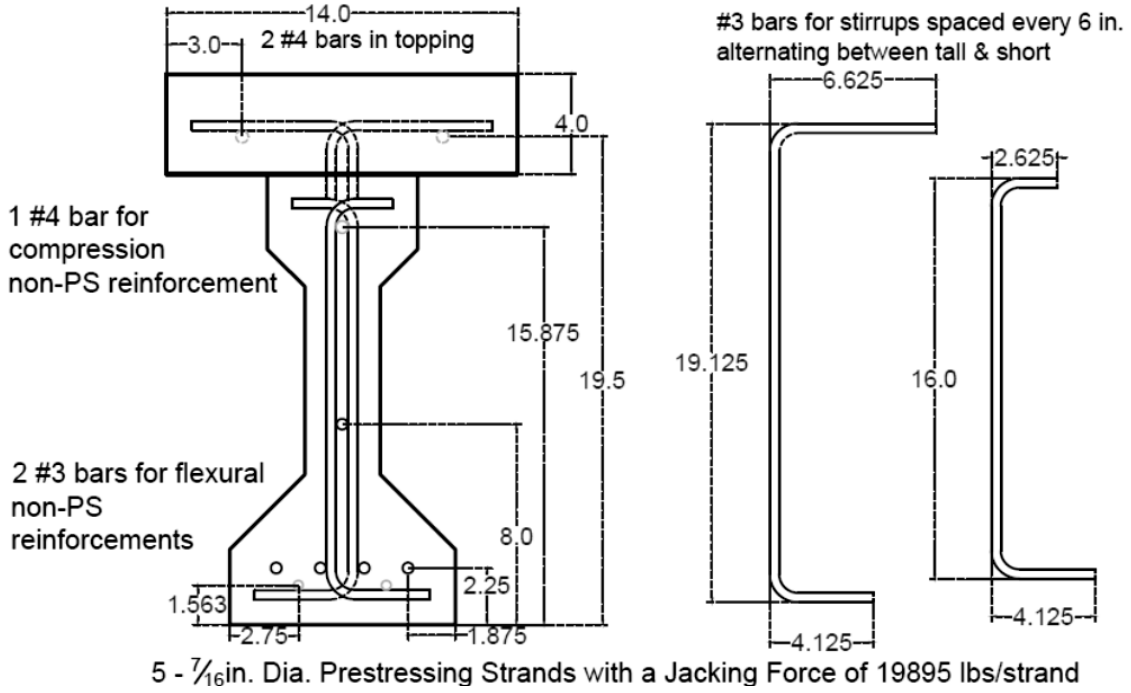

Figure 3-5: Cross-section dimensions and reinforcement dimensions of half-scale girders

The lateral damage simulation for each girder was achieved by sawing through the concrete of the bottom flange and slicing through one of the prestressing strands. A schematic of this procedure and a picture of the resulting cut are shown in Figure 3-6.

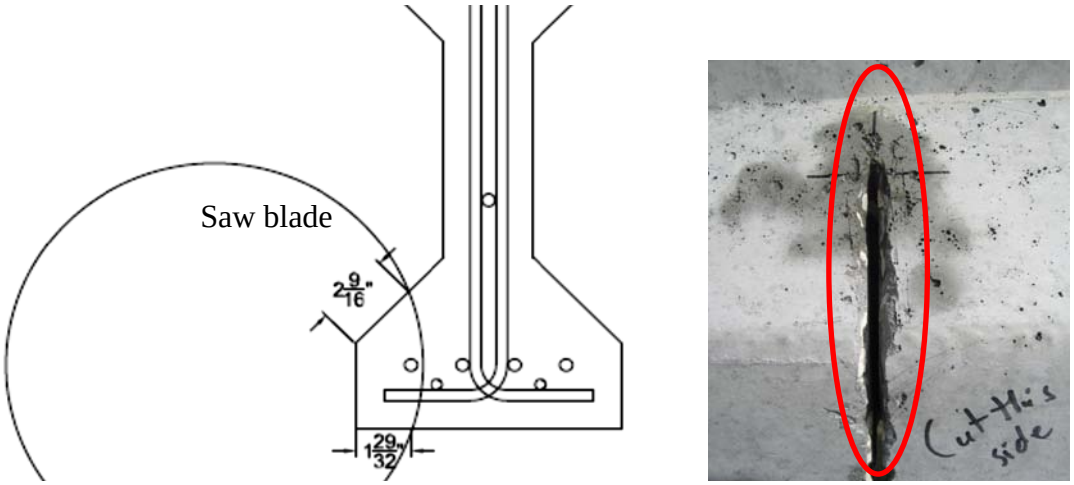

Figure 3-6: (left) Diagram of sawing used to simulate damage in the girders; (right) Photo showing resulting cut in actual girder sample

To repair the cut, the surfaces exposed by cutting were first roughened with chisels to improve bonding quality. These surfaces were then thoroughly cleaned with a water jet and pressurized air, as specified in both NCHRP 514 (NCHRP R-514) and ACI 440.2R-08. The cleaned cut was filled with a high-strength cementitious repair mortar, and a high-pressure epoxy injection procedure was performed after the mortar set. The procedure resulted in a near-perfect repair of the concrete cross-section. A repaired concrete section is shown in Figure 3-7.

Figure 3-7: Picture of half-scale girder with cut strands and concrete repair

Using the measured results from the RC testing series, a more refined design approach was utilized to design the CFRP configurations for the half-scale AASHTO type II PS girders. Fewer but more effective CFRP configurations and strengthening levels were designed to repair the ten half-scale girders which were statically tested. The longitudinal strips were all 8 in. wide and started at 17 ft long, reducing 6 in per each additional layer applied. The transverse U-wrappings were 12 in wide and extended to the top of the web of each girder.

The longitudinal CFRP reinforcement was extended beyond the location of the damage and ruptured prestressing strand a distance greater than the needed full development length of the prestressing strands. On top of the main longitudinal sheets, transverse wet layup U-wrappings were placed throughout the girder length and the length of the repaired region. The U-wrappings were provided at the termination points of longitudinal CFRP sheet and at several locations between the first cutoff point for the longitudinal CFRP and the damaged region. The U-

wrappings encircled the bottom flange and extended the full depth to on each side of the girder. Figures 3-8 and 3-9 show the CFRP configurations of the ten half-scale AASHTO type II girders tested statically.

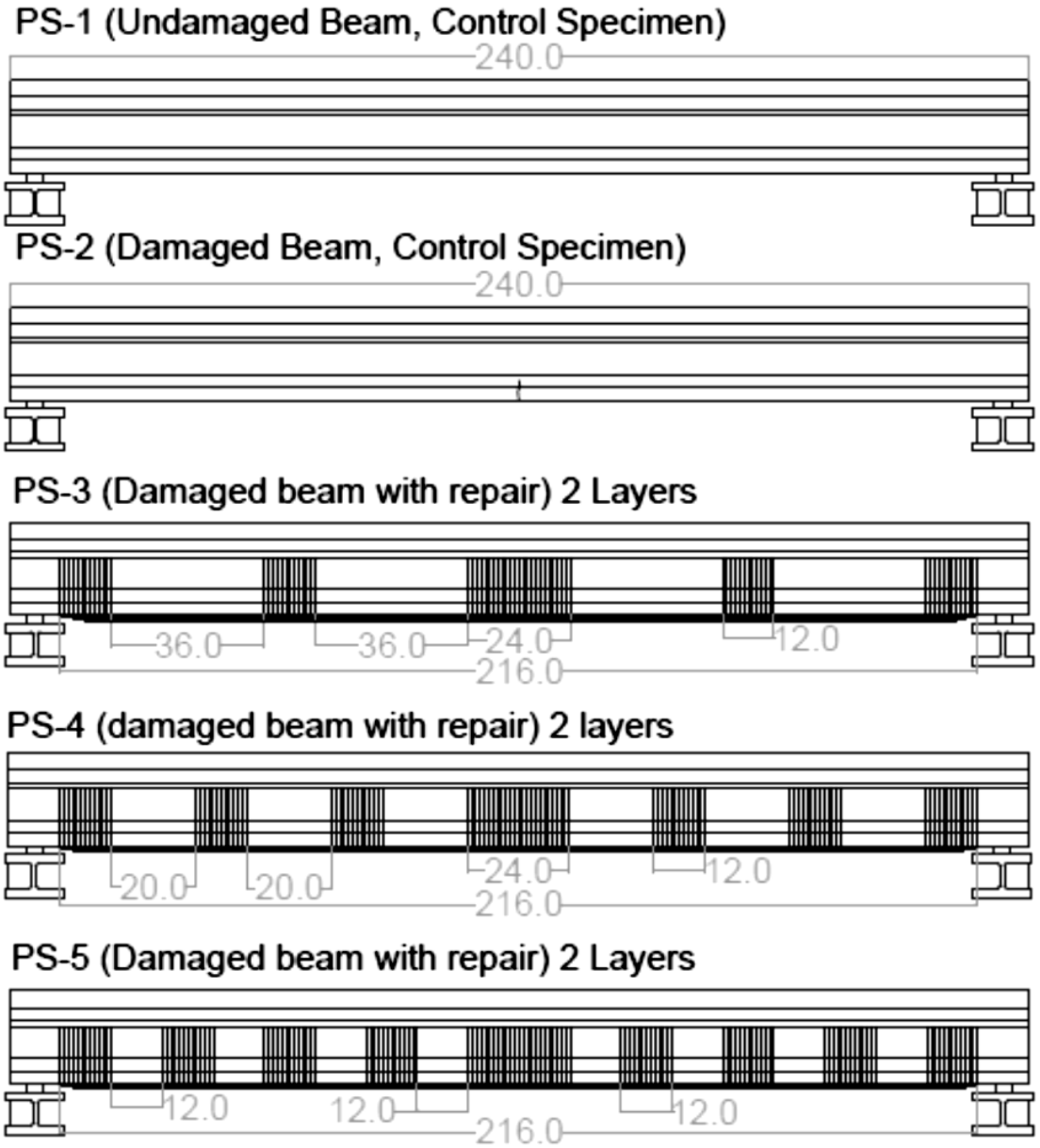

Figure 3-8: CFRP repair configuration layout for first five half-scale PS girders statically tested in flexure

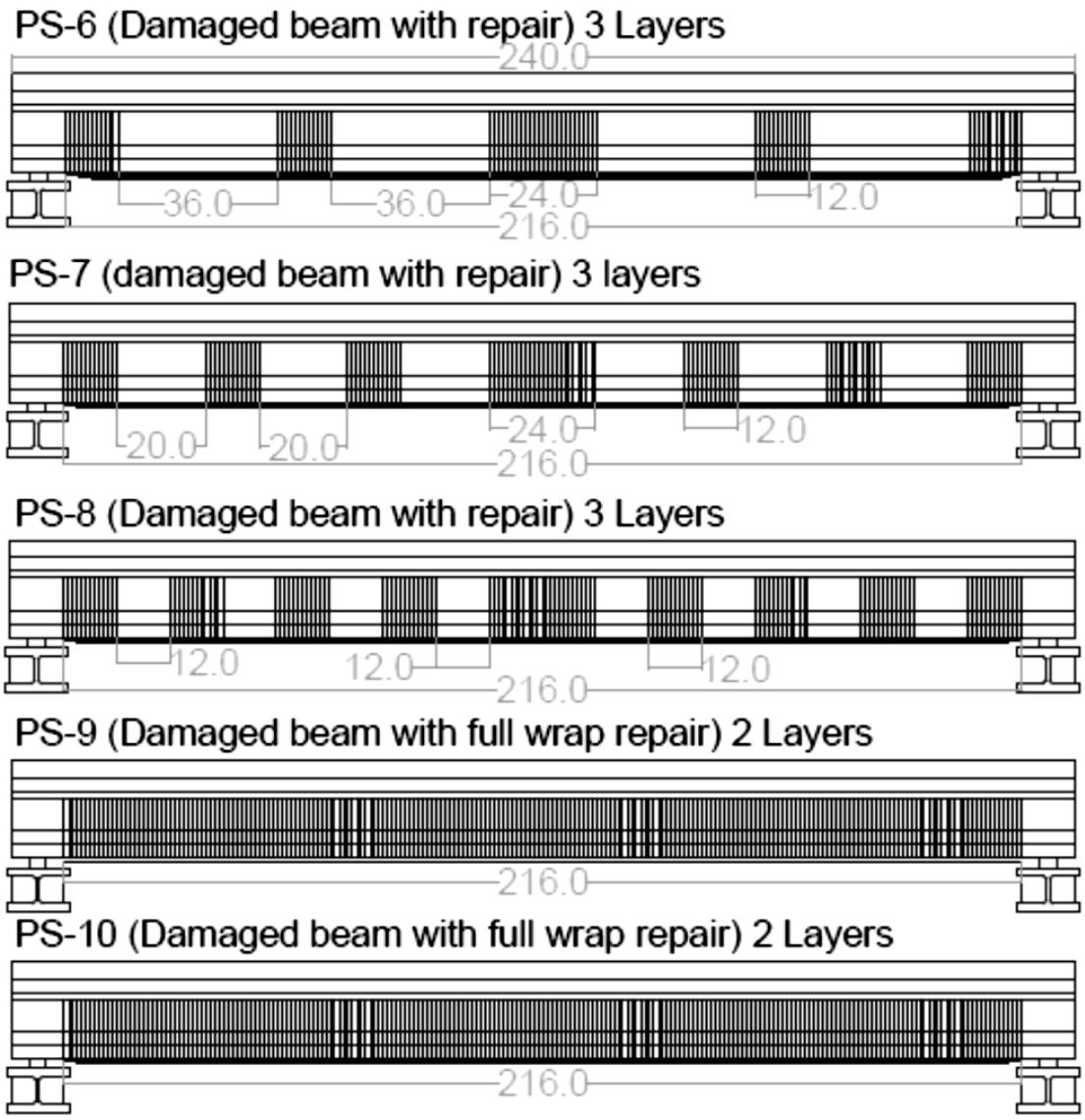

Figure 3-9: CFRP repair configuration layout for second five half-scale PS girders statically tested in flexure

The first girder (PS-1) is a control girder that represents an undamaged and unrepaired specimen. Similarly, the second girder (PS-2) is a damaged specimen which has received no CFRP repair (only concrete repair) representing the lower bound of the tested samples. The remaining girders (PS-3 to PS-5) had both simulated impact damage imposed on them, concrete repair, and two layers of CFRP at various spacing to constitute the repair. The spacing between U-wrappings was set at a distance of twelve inches, twenty inches, or thirty-six inches.

In figure 3-9, the three girders (PS-6 through PS-8) are damaged and repaired with three layers of CFRP at the girder soffit and U-wrappings at spacings of twelve inches, twenty inches, or thirty-six inches. The final two beams (PS-9 and PS-10) are fully wrapped girders (U-wrappings cover entire beam) using 2 layers of CFRP for the repairs (soffit and U-wrapping). However, the U-wrappings applied to PS-10 were overlapped by inch, whereas those applied to PS-9 were not

overlapped. This was intended to investigate the effect of continuity in the direction opposite to that of the fibers.

The three best performing repairs from the initial ten half-scale girders that were chosen for fatigue testing were the 2 layer and 3 layer repairs with 20 inches spacing and the 2 layer with 36 inches spacing. These configurations were recreated exactly, maintaining the 8 inch wide longitudinal laminates which started at 17 ft while reduced 6in. per each additional layer applied and the 12 inches wide transverse U-wrappings which extended to the top of the web of each girder. Figure 3 shows the CFRP configurations for half- scale girders.

Upon the completion of testing the ten half-scale girders under static loading and analyzing the results, the three top performing repair configurations from this set were duplicated and applied to the remaining three half-scale girders for dynamic loading tests (PS-11 to PS-13) to investigate fatigue properties of the repairs. The three best performing repairs from the initial ten half-scale girders that were chosen for fatigue testing were the 2 layer and 3 layer repairs with 20 in spacings and the 2 layer with 36 in spacings. These configurations were recreated exactly, maintaining the 8in. wide longitudinal laminates which started at 17 ft while reduced 6in. per each additional layer applied and the 12 in wide transverse U-wrappings which extended to the top of the web of each girder. Figure 3-10 shows a sketch of the CFRP configurations used for the three half-scale AASHTO type II girders tested under fatigue loading conditions.

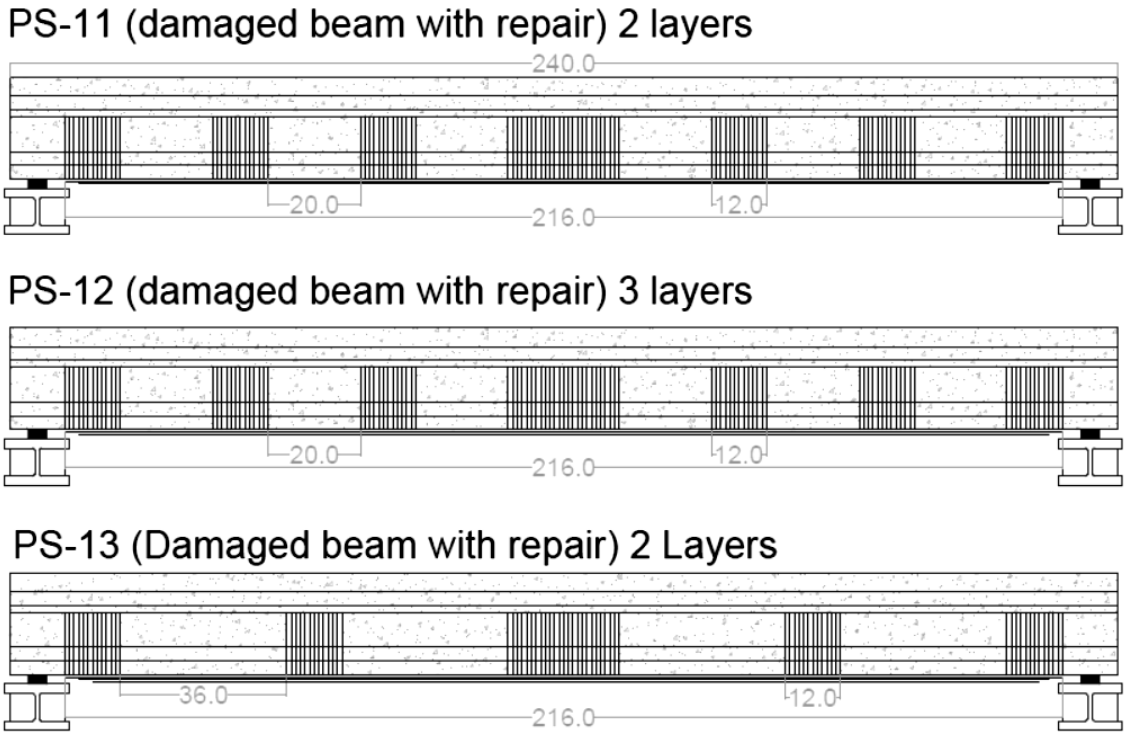

Figure 3-10: CFRP repair configuration layout for half-scale PS girders tested in fatigue

3.1.3. FULL-SCALE PRESTRESSED CONCRETE (PSC) GIRDERS

The full-scale prestressed test specimens were 40 ft long AASHTO type II girders which were taken from a previously existing bridge. An 8in thick decking remained atop the girders after removal and was in need of slight repairs due to the destructive nature of deconstruction. The compressive strength of both the concrete decking and the AASHTO girder itself were unknown. Likewise, the strand layout was estimated by using penetrating radar and a prestressing force had to be assumed in order to complete design calculations for an adequate repair. However, after completing the testing, the prestressing locations were verified. It was discovered that the majority of the girders had unique placements of longitudinal reinforcements, both prestressed and non-prestressed steel reinforcements. Each girder's cross-section is shown in order in Figure 3-11 where girders PSC-1 through PSC-3 were used for fatigue testing and PSC-4 through PSC-8 were tested statically.

The lateral damage simulation was achieved by sawing through the concrete at the bottom flange of each girder and slicing through three of the prestressing strands. To repair the cut, the opening left from the saw was first roughened up using chisel tools to help improve the bonding area. The surface of the concrete exposed by the cut was then thoroughly cleaned with a water jet and pressurized air. The cleaned opening was filled with a high strength cementitious repair mortar, and a high-pressure epoxy injection procedure was performed after the mortar set. The procedure resulted in a near-perfect repaired concrete cross-section.

The longitudinal CFRP also extended beyond the location of the damage and ruptured prestressing strand. Transverse U-wrappings were also provided throughout the girder length and the length of the repaired region. The U-wrappings covered the bottom flange and extended the full girder depth on each side of the girder. A horizontal CFRP strip was bonded to anchor the ends of U-wrappings. To control flexural cracks and prevent premature crack opening, additional CFRP sheets were provided longitudinally along the length of the repaired area. The CFRP sheets were attached to the angled portion of the bottom flange and to part of the web of the girder on each side. This CFRP sheet/strip acted as tension struts and as a crack growth inhibitor in the damaged region to prevent premature failure especially under fatigue loading. In order to provide adequate anchorage, the sheets were extended beyond the damaged region.

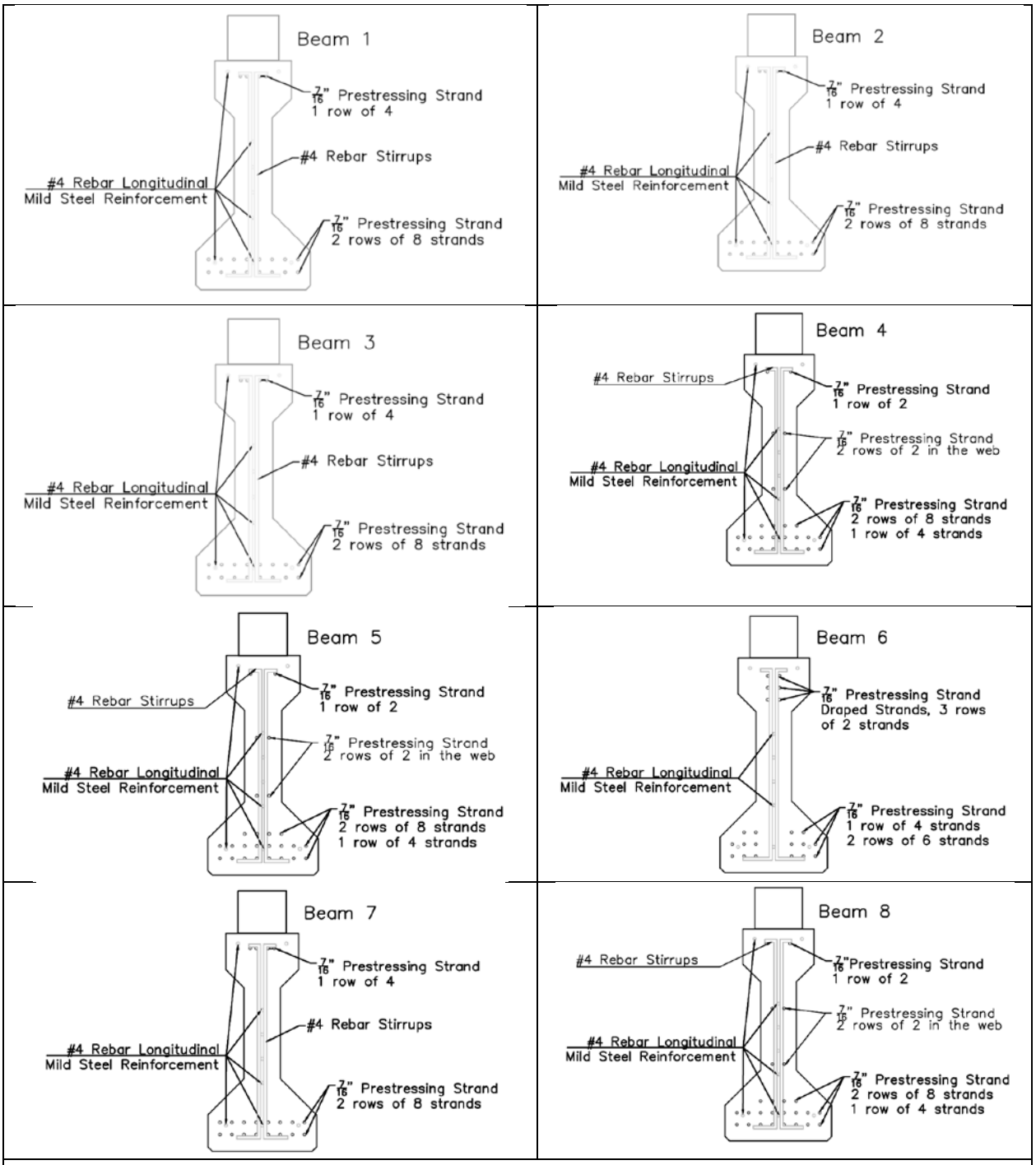

Figure 3-11: Cross-section designs of the full-scale PSC girders extracted from an existing bridge

The CFRP repair design configurations designed using the assumed values are presented in Figures 3-12 and 3-13; where it can be seen that the general spacing and configuration of the transverse U-wrapping remain constant. The forty-seven tests resulted in compelling evidence to determine appropriate values of these two parameters; though the designs are used to investigate the level of strengthening by utilizing two, three, and four layers of longitudinal CFRP laminates

on selected girders. Similar to the half-scale girders, the full-scale girders were also separated into two sets; one set of three beams to be dynamically tested under fatigue loading and the other to be tested under static loading conditions. The fatigue set is presented first in Figure 3-12 and the remaining static set follows in Figure 3-13.

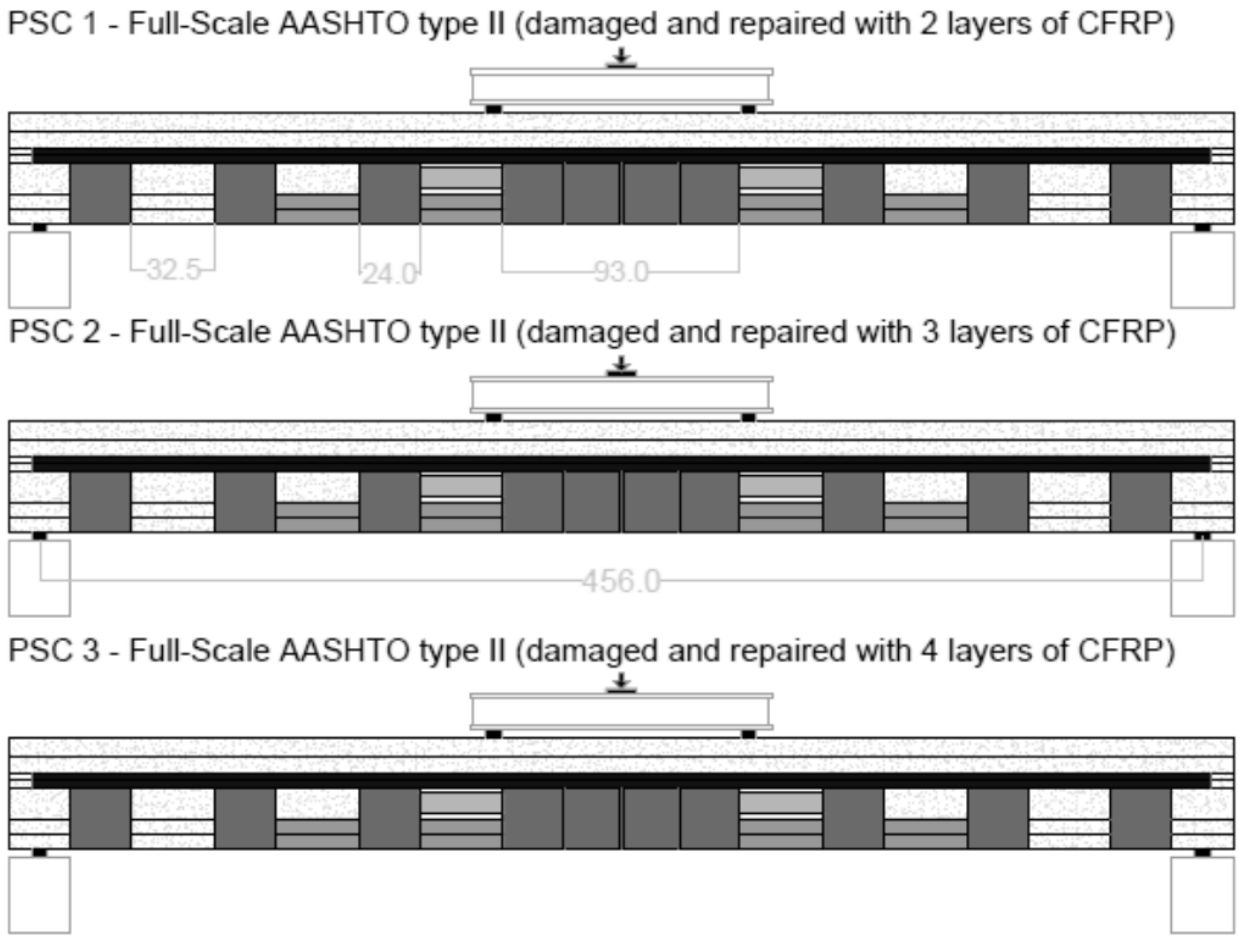

Figure 3-12: CFRP repair configuration for full-scale AASHTO type II girders dynamically tested

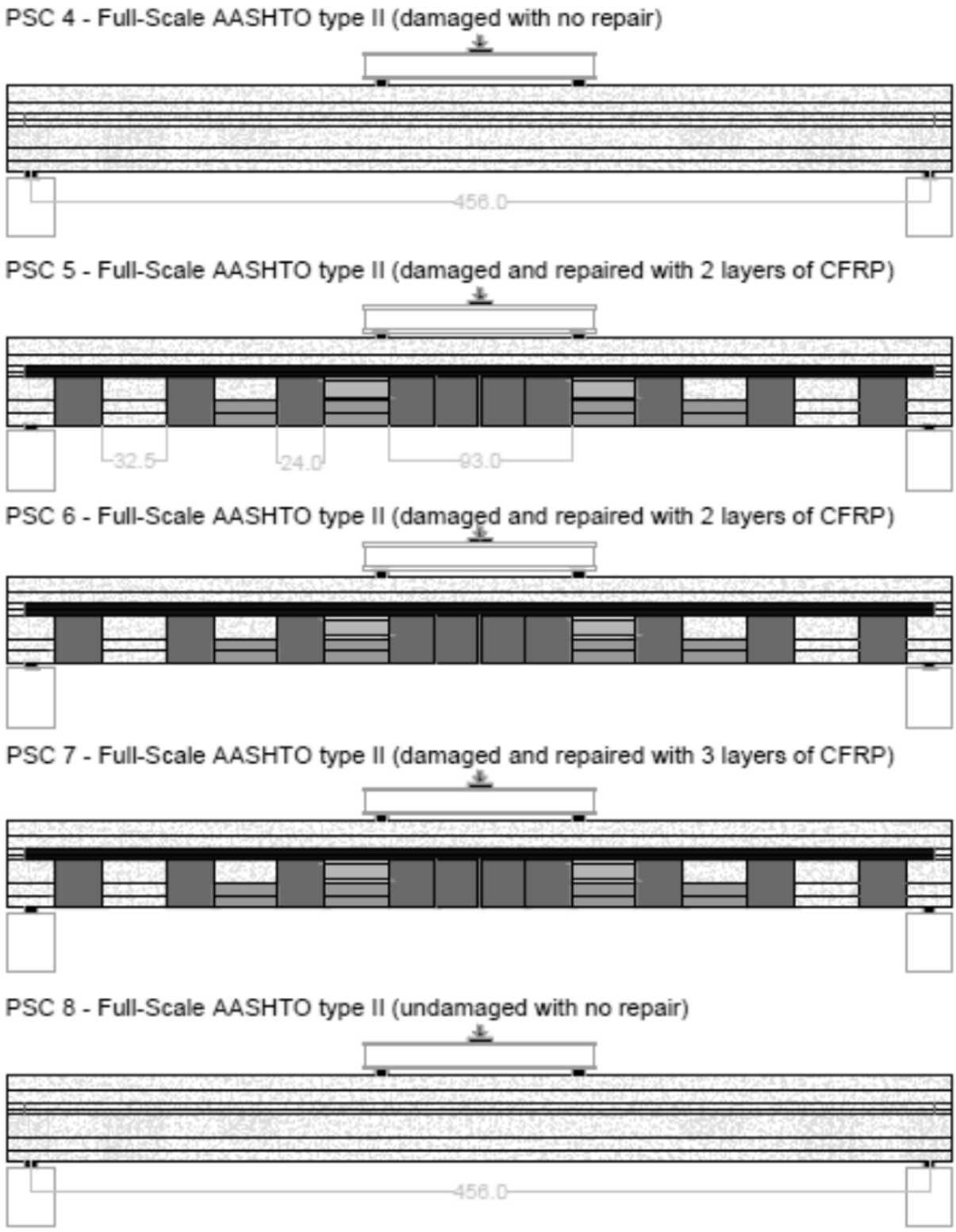

Figure 3-13: CFRP repair configuration for full-scale AASHTO type II girders statically tested

3.2. EQUIPMENT

Testing was carried out at the FDOT structures research center in Tallahassee, Florida, where access to professional technicians and accurate machines was given to complete all required testing and measurements. The equipment utilized at the state structures research laboratory included:

- Strong Floor
- 100 Kip actuator (used for smaller specimens with low ultimate capacities)
- 500 Kip actuator (used for larger test specimen with high load capacities)
- MTS 110 Kip dynamic loading actuator (used for fatigue testing)
- MTS 55 Kip dynamic loading actuator (used for fatigue testing)
- Compression testing load frame (used for concrete cylinders and grout cubes)
- Data Acquisition Systems with multiple channels available for recording measurements.
- Laser and Linear variable differential transformer (LVDT) deflection gauges.
- Strain gauges

The displacements of the repaired AASHTO girders were measured using string potentiometers placed at several points along the girder length. The compressive strain in the concrete was measured by electrical resistance strain gauges. The tensile strain in the CFRP reinforcement was also measured using electrical resistance strain gauges. The instrumentation was selected to determine the strain profile of the section at mid-span, the behavioral differences between the damaged and undamaged sections, and the tensile strain in the CFRP to determine the bond characteristics throughout the longitudinal CFRP.

3.3. CFRP REPAIR PROCEDURES

After conducting the concrete repair for the damaged parts of the girders, all of the test specimens were repaired using the traditional wet layup methods associated with CFRP fabric laminates. The repair procedures for applying the CFRP were done in accordance with the traditional methods for this approach. The procedures for this method, as described by the manufacturer, are discussed in three primary sections; surface preparation, mixing, application, and quality control. The description of each is provided below.

Surface Preparation: In general, the surface must be clean, dry and free of protrusions or cavities, which may cause voids behind the Tyfo® composite. Discontinuous wrapping schematics typically require a light sandblasting, grinding or other approved methods to prepare for bonding.

Mixing: Pour the contents of component B into the pail of component A. Mix thoroughly for five minutes with a low speed mixer at 400-600 RPM until uniformly blended. If material is too thick, heat unmixed components by placing containers in hot tap water or sunlight until desired viscosity is achieved. The Tyfo® S epoxy may also be thickened in the field to the desired consistency by adding fumed silica.

Application: Apply Tyfo® S epoxy to surface as a primer coat. Then, uniformly saturate the fabric by hand and apply to the surface. Next, using a roller or a trowel, press the fabric to surface, and work out any air voids or pockets of thick epoxy.

Quality Control: If voids behind the cured CFRP laminates are present, use the Tyfo® S epoxy, and inject it into voids using traditional injection methods.

3.3.1. RC BEAM REPAIR PROCEDURES

CFRP application to repair the reinforced concrete beams followed all major recommendations proposed by the company. The beams were first sanded and cleaned in order to achieve the proper surface condition for applying the CFRP materials. Following this, the beams were flipped onto a set of wooden planks so that the laminates could be applied in a much more convenient fashion. A priming layer of the mixed Tyfo® S epoxy was next applied to the bare beam using a regular paint roller. Then, the pre-cut CFRP laminate strips were drawn through a pool of the epoxy held in a paint tray; the excess epoxy was squeezed out of the material by hand. To bond the CFRP strips, the saturated laminates were gently placed in their proper positions, and a plastic trowel was used to straighten the fibers and to force out any air pockets behind the laminates. A collection of repaired beams is shown in Figure 3-14.

Figure 3-14: Picture of CFRP repairs applied to RC beam specimens

3.3.2. PS CONCRETE GIRDER REPAIR PROCEDURES

The repair procedures conducted to constitute the CFRP application for the prestressed concrete (half-scale and full-scale) girders also followed all major recommendations proposed by the company. The girders' surfaces were first ground down and cleaned in order to achieve the proper surface condition for applying the CFRP materials. Following this, the girders were primed by applying a layer of the mixed Tyfo® S epoxy to the bare girders using a regular paint roller. Then, the pre-cut CFRP laminate strips were laid out on a plastic sheet where they saturated with epoxy using the same regular paint roller. To bond the saturated strips of CFRP, the end of the laminates were gently placed in their proper positions the thickened epoxy was applied as the laminate was rolled out onto the bottom surface. The epoxy was thickened by mixing in some fumed silica; as recommended by the manufactures. The picture of the fumed silica used and the resulting thickened epoxy are presented in Figure 3-15.

Figure 3-15: (left) Fumed silica used to thicken epoxy; (right) Thickened epoxy

Like previous beams, plastic trowels were scraped along the surface of the laminates in order to straighten the fibers and to force out any air pockets behind the laminates. Lastly, after the longitudinal laminates were appropriately fixed to the soffit, the transverse U-wrappings were applied in the same manner. An example of a girder being repaired is shown in Figure 3-16.

Figure 3-16: Wet layup application of CFRP fabric laminates on PS girder

3.4. TESTING PROCEDURES

All beams reported in this research have been tested at the Florida Department of Transportation (FDOT) structural research center in Tallahassee, Florida. The girders that were statically tested were done so under a four point loading setup using either a 100 kip or 500 kip load actuator mounted on a steel frame. On the other hand, the fatigue testing was carried out under a three point loading arrangement using a 200 kip MTS dynamic load actuator. Each test specimen spanned a certain length and the bearing surfaces rested on either stationary steel cylindrical supports or neoprene bearing pads. The four point loading was applied by using a steel spreader I-beam centered on top of the test specimens and resting on a second set of bearing pads. In addition, most of the beams were instrumented with two laser deflection gauges, multiple linear variable differential transformer (LVDT) deflection gauges, and a multitude of strain gauges.

3.4.1. STATIC TESTING PROCEDURES

The 8 ft long RC samples were arranged for static testing with a span of 7.5 ft and each bearing surface rested on stationary steel cylinders that were welded to support blocks. The four point setup was implemented by positioning a steel I-beam spreader bar at the mid-span of the beam and resting it on two neoprene bearing pads having a center to center distance of 20 in (10 in on either side of beam's centerline). The actuator then applied and measured the load to the top surface of the spreader beam. Other than load measurements read by the actuator, two laser deflection gauges were placed at the mid-span, both above and below the beam. Likewise, two LVDT deflection gauges were positioned over the supported areas and two more at quarter points in the beam. Strain gauges were also utilized both along the cross-section height and on the tension face of the beam along the span. The diagram illustrating the RC static testing setup is shown in Figure 3-17.

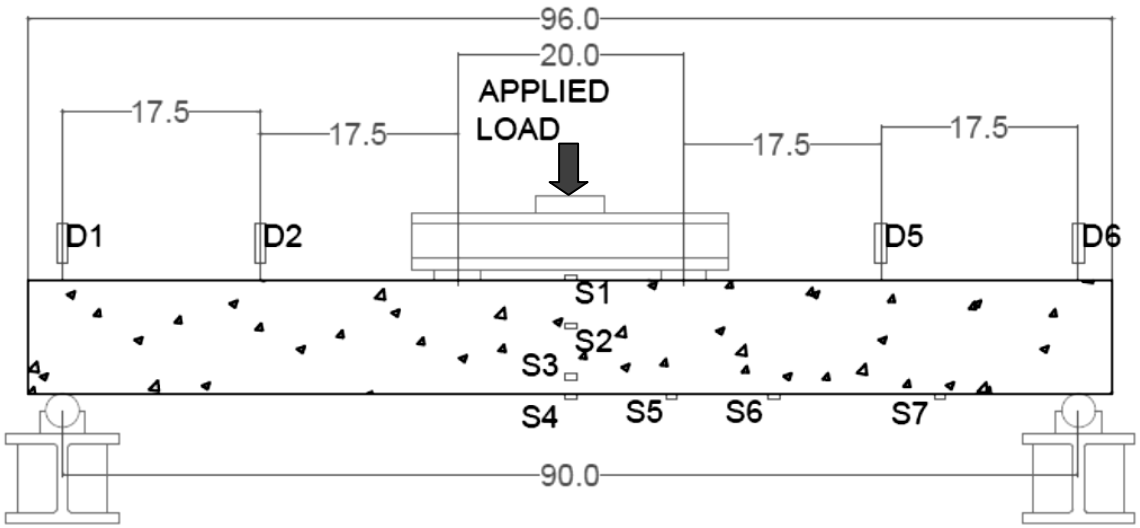

Figure 3-17: Static loading setup arrangement for all RC test specimens

The half-scale PS girders statically tested were arranged in a similar manner to the RC specimens. However, the 20 ft long PS girders spanned 19 ft and rested on neoprene pads instead of steel cylinders. The spreader beam was also increased to apply a load at 25 inches on either side of the beam's centerline. Also similar to the RC setup, load measurements were read by the actuator, but dissimilarly the two deflection gauges positioned at mid-span were LVDT deflection gauges not laser gauges. The LVDT deflection gauges were also placed both above the supported areas and quarter points. Again, strain gauges were attached to the girders along the cross-section height and on the tension face of the beam along the span of the girder; yet, in the testing of the half-scale girders a much larger amount of strain gauges were applied. Each half-scale girder utilized an average of twelve strain gauges, where the RC test specimens only had an average of seven applied. A depiction of the test setup for the statically tested half-scale girders and the relevant dimensions is visible in Figure 3-18.

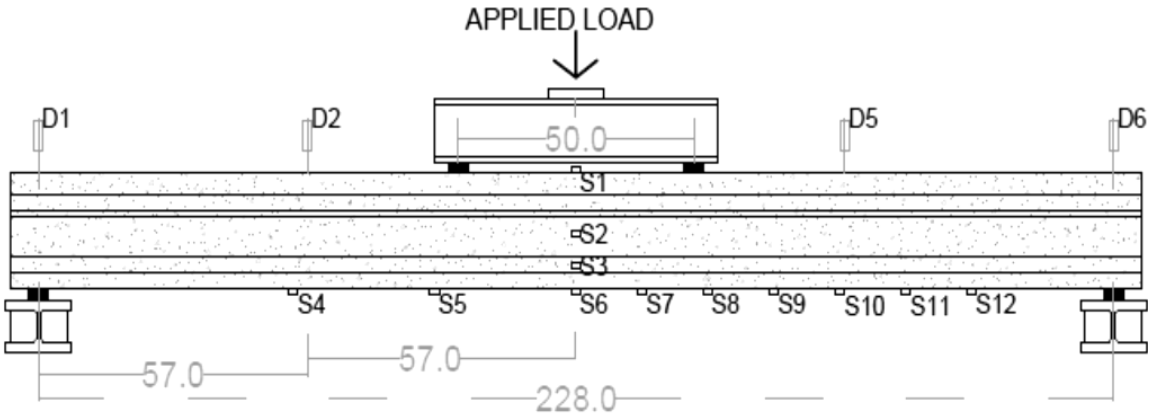

Figure 3-18: Static loading setup arrangement for half-scale AASHTO PS girders

The full-scale PSC girders statically tested were arranged in a similar manner to the half-scale specimens. However, the 40-ft-long PSC girders spanned 38 ft but similarly rested on neoprene pads. The girder loading was applied using a steel spreader beam resting on another set of two pads. Also, load measurements were read by the data acquisition connected to the actuator. The two deflection gauges positioned at mid-span were LVDT deflection gauges not laser gauges. The LVDT deflection gauges were also placed both above the supported areas and at quarter points on the girders. Again, strain gauges were attached to the girders along the cross-section height and on the tension face of the beam along the span of the girder; yet, in the testing of the full-scale girders more of the strain gauges were applied. Each full-scale girder utilized an average of fifteen strain gauges, where the half-scale test specimens only had an average of twelve applied. A schematic of the test setup for the statically tested full-scale girders and the relevant dimensions is visible in Figure 3-19.

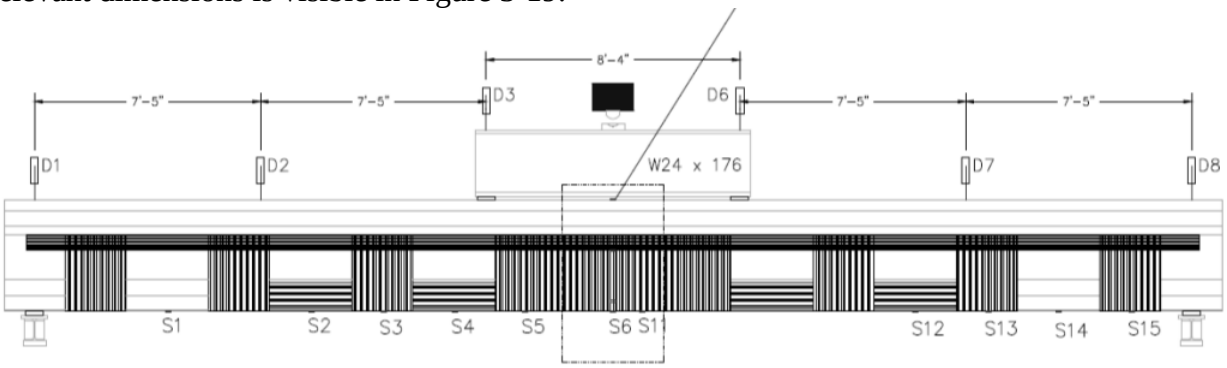

Figure 3-19: Static loading setup arrangement and gauge placement locations for full-scale AASHTO PSC girders

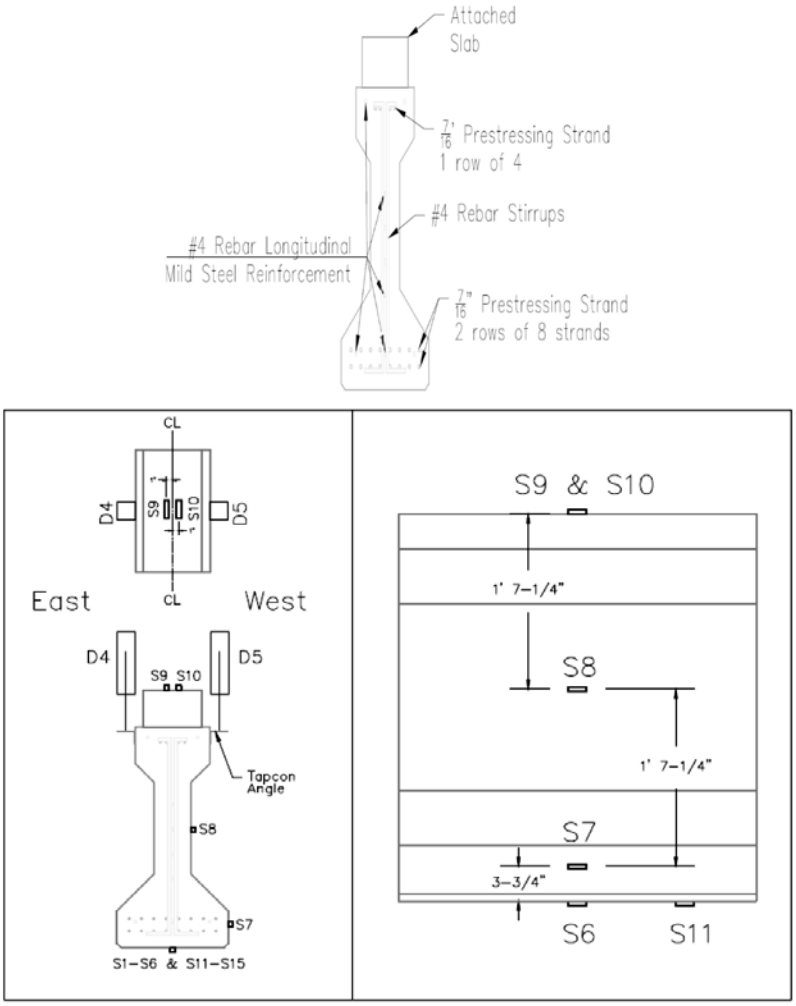

Figure 3-20: Cross-section diagram of full-scale girders

3.4.2. FATIGUE TESTING PROCEDURES

Unlike reinforced concrete, prestressed concrete members are susceptible to strand fatigue problems under elevated strand stress range. This presents itself as a critical point to investigate, since the lateral damage of concern usually harms some of the prestressing strands. ACI 440.2R-02 limits the service steel stress to 0.8fy, which is expected to allow for very high strand stress range levels when applied to prestressed concrete members. AASHTO 1998, on the other hand, limits the strand service stress range to 69 MPa or 10 ksi for harped strands and 124 MPa or 18 ksi for straight strands. Therefore, it was desirable to test sets of both the half-scale and full-scale prestressed members under fatigue loading conditions. The loading arrangements for the two sets are shown in Figure 3-21 for the half-scale members and Figure 3-22 for the full-scale members.

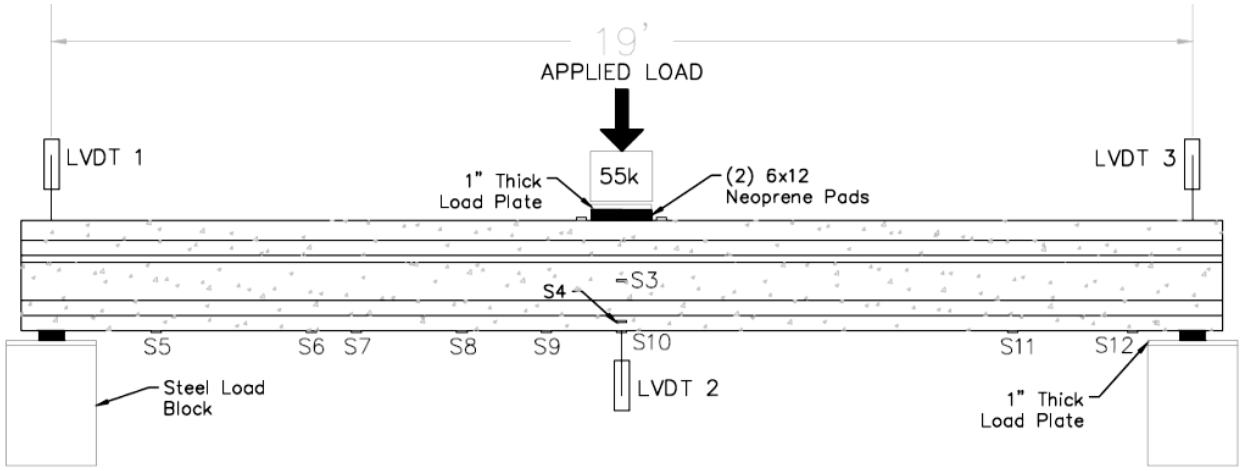

Figure 3-21: Fatigue loading setup arrangement for half-scale AASHTO PS girders

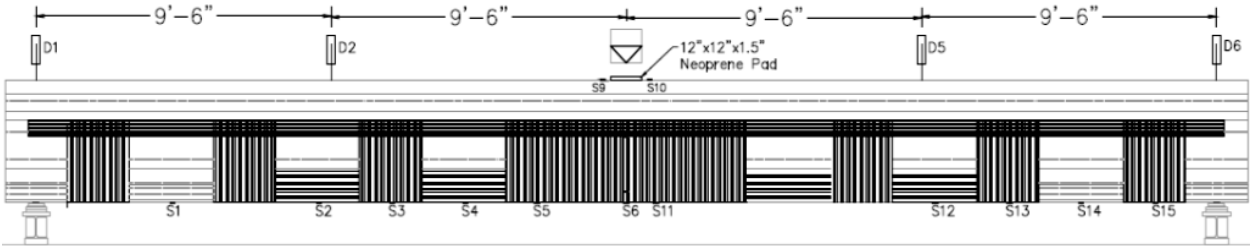

Figure 3-22: Fatigue loading setup arrangement for full-scale AASHTO PSC girders

The experimental testing presented in this study investigated the behavior and analysis of three full-scale and three half-scale AASHTO type II prestressed concrete girders with imposed simulated lateral damage and CFRP repair applications under fatigue loading. Ten half-scale AASHTO type II PS girders were investigated under static loading. Following the testing of the ten half-scale PS girders in flexure under static loading, three identical girders were tested under fatigue loading to evaluate residual strengths and longevity. That served as a preliminary investigation for the testing of eight full-scale AASHTO type II girders; five of which under static loading and three under fatigue loading. The half-scale and full-scale AASHTO type II PSC girders had an imposed simulated damage and applied CFRP laminates. The repaired girders varied in both CFRP configurations and levels of strengthening.

The girders were tested using the hydraulic actuator mounted to a steel frame at mid-span. The fatigue testing of AASHTO II girder was performed using the 110 Kip MTS hydraulic actuator selected based on its large capacity servo valve which permitted testing of the girder using a frequency of 2 to 4 Hz. The loading contact area was a 250 mm by 500 mm steel plate specified by AASHTO (AASHTO 2004). Neoprene pads were used at girder supports to simulate field supporting conditions.

The half-scale girders were intended to be tested under fatigue for 2 million cycles but using a high fatigue load range of 10 kip to 35 kip. This high load level was applied to investigate the behavior under overloading condition. The loading was applied at a rate of 2 to 3 Hz. Yet the half-scale girders failed prematurely at less than 1 million cycles under this overload condition. The repaired half-scale beams were tested in several stages to failure. After several initial loading cycles to simulate possible overloading conditions, the half-scale beams did not survive the desired 2 million cycles of loading. A photograph of the fatigue loading tests is shown in Figure 3-23 for the half-scale girders.

On the other hand, the full-scale PS girders were tested under the typical fatigue loading indicated in AASHTO LRFD Specifications for 2 million cycles of 2 and 3 Hz. The loading range used for the full-scale AASHTO type II girders was calculated using the standard range of an applied fatigue truck on the span of the girders assuming a girder spacing of 10 ft. The fatigue loading simulated a range from the dead load that would be present with a complete deck to a total load including the dead load and live load of a fatigue truck including factors of load factor (CE) of 0.75, distribution factor, and impact factor of 15%. These calculations for the full-scale girders resulted in a range from 20 kip to 45 kip. The girder loading was cycled between the loads of 20 kip and 45 kip to simulate the dead load to the dead load plus factored fatigue live load at a rate of approximately 2 to 3 Hz. However, after the testing of the first two full-scale girders, very little degradation was apparent. Therefore, the last full-scale girder was loaded to a higher load range of 25 kip to 50 kip for 2 million cycles at 3Hz. The full-scale AASHTO II girders successfully survived the 2 million cycles of fatigue loading with a very small amount of residual deformation and little change in stiffness. Then, the girders were tested in flexure until failure under a four point loading arrangement.

Load, deflection, and strain measurements were recorded for all girders during their testing. Similarly, the modes of failure and observed behaviors were also documented during testing.

According to the data files, the test measurements indicated the following:

- Half-scale PS-11 started at 4 Hz then went to 3 Hz after 2,000 cycles, then 2 Hz after 214,000 cycles.
- Half-scale PS-12 started at 4 Hz then went to 3 Hz after 6,000 cycles, then 2Hz after 69,000 cycles.
- Half-scale PS-13 started at 2 Hz and stayed at that rate.
- Full-scale PSC-2 appears to have started at 1 Hz, then 0.5 Hz after 110,000 cycles, then 1 Hz after 282,000 cycles, then 2 Hz after 289,000 cycles.
- Full-scale PSC-1 started and stayed at 2 Hz.
- Full-scale PSC-3 started and stayed at 3 Hz.

After the testing, the girders were examined confirming that all fatigue beams (PSC-1, PSC-2, and PSC-3) had only the two rows of 8 strands at the bottom and one row of 4 strands at the top. The same goes for PSC-7 from the 4-point tests. For girder PSC-3, the centroid of tension prestressing was at about 3.875 inch from the bottom. The four strands at the top were at 33.5" from the bottom.

Tables 3-3 and 3-4 show the fatigue test information for half-scale and full-scale girders.

Table 3-3: Fatigue Test Results for Half-Scale Girders

Fatigue Testing Results for the Half-scale AASHTO type II Girders			
Half-scale Girder designations	Loading Level Ranges	Loading Rates	Number of Loading Cycles Completed
PS-11	10 kip-35 kip	started at 4 Hz then to 3 Hz after 2,000 cycles, then 2 Hz after 214,000 cycles	322,000
PS-12	10 kip-35 kip	started at 4 Hz then to 3 Hz after 6,000 cycles, then 2Hz after 69,000 cycles	296,000
PS-13	10 kip-35 kip	2Hz	635,000

Table 3-4: Fatigue Test Results for Full-Scale Girders

Fatigue Testing Results for the Full-scale AASHTO type II Girders			
Full-scale Girder designations	Loading Level Ranges	Loading Rates	Number of Loading Cycles Completed
PSC-1	20 kip-45 kip	2Hz	2,000,000
PSC-2	20 kip-45 kip	started at 1 Hz, then 0.5 Hz after 110,000 cycles, then 1 Hz after 282,000 cycles, then 2 Hz after 289,000 cycles	2,000,000
PSC-3	25 kip-50 kip	3Hz	2,000,000

Figure 3-23: Fatigue loading setup arrangement for half-scale PS girders

4. EXPERIMENTAL FINDINGS

The summary of the data introduced in this section describes the flexural behavior of the tested girders. Measurements and comparisons were made and analyzed based on the load-deflection characteristic values, the development of strains along the beam soffit, the strains developed along the cross-section height at mid span, and the resulting modes of failure. However, first it is appropriate to report the findings of the material testing performed on the steel reinforcements used in the RC test specimens. This was executed to verify the properties of the reinforcements with intentions to ensure the analytical evaluations were as accurate as possible. The design values from the manufacturer and the values resulting from ASTM testing for all steel reinforcements used in the RC beams are presented in Tables 4-1 and 4-2.

4.1. METHOD OF EXPERIMENTAL ANALYSIS

The primary methods of analysis for evaluating the experimental results were conducted through comparisons of behavioral properties such as stiffness, maximum capacity, maximum deflection, developed strains, and deflections at service loads. By comparing the behavioral qualities associated with each unique repair configuration to each other, the most beneficial CFRP design was determined and verified through multiple stages of testing.

Table 4-1: Test Results of Tensile Strengths for Mild Steel Reinforcement

Rebar Tensile Specimens			Ultimate Load (kip)	Ultimate Tensile Stress (ksi)
Specimen	Size	Area (in^2)		
Design values	#3	0.11	6,600	60,000
1	#3	0.11	7,920	72,000
Design values	#4	0.2	12,000	60,000
2	#4	0.2	15,090	75,450

Table 4-2: Test Results of Tensile Strengths for RC Welded Wire Reinforcing Cage

1/16" Welded-Wire Frame Tensile Specimens			Ultimate Load (kip)	Ultimate Tensile Stress (ksi)
Specimen	Wire Dia. (inch)	Area ($inch^2$)		
Design values	0.073	0.0042	252	60,000
1	0.073	0.0042	280	66,899
2	0.072	0.0041	275	67,543
3	0.073	0.0042	272	64,988

4.2. REINFORCED CONCRETE BEAMS TESTING DATA

4.2.1. RC LOAD-DEFLECTION RESULTS

Values of the maximum loads, the corresponding deflections, and percent increases for the first set of RC beams with the #4 reinforcing bars and one layer of CFRP are given in Table 4-3. The first set of beams B1-1 to B1-15 is also referred to as TB-1 to TB-15. The beams designated as TB were fabricated in Tallahassee. The second set of beams B2-1 to B2-19 is also referred to as JB-1 to JB-19 and was fabricated in Jacksonville.

Table 4-3: Max Load-Deflection Values and Percent Gained for the First RC Set

Beam designation	max load (kip)	corresponding deflection (in)	% gained from damaged beam B1-2	% gain from undamaged beam B1-1
B1-1	14.160	0.958	38%	0%*
B1-2	10.245	1.661	0%*	-28%**
B1-3	20.910	1.185	104%	48%
B1-4	16.450	0.914	61%	16%
B1-5	15.589	0.682	52%	10%
B1-6	16.654	0.864	63%	18%
B1-7	16.578	1.020	62%	17%
B1-8	18.710	0.904	83%	32%
B1-9	19.717	0.879	92%	39%
B1-10	17.122	0.843	67%	21%
B1-11	18.866	0.931	84%	33%
B1-12	19.641	1.050	92%	39%
B1-13	17.948	0.748	75%	27%
B1-14	18.407	0.860	80%	30%
B1-15	18.683	0.891	82%	32%
* Control specimen gives values of 0%; **Signifies % capacity lost due to simulated damage				

A comparison between the failure load of the damaged control beam B1-2 (damaged beam with no CFRP) and the control beam B1-1 (undamaged beam with no CFRP) signifies that the simulated damage caused a 28% reduction in the ultimate capacity. Furthermore, the CFRP repaired beams B1-3 through B1-15 shows that the CFRP repairs enhanced the flexural capacity of a control damaged beam (1-2) by a range of 52% to 92%. Similarly, increases in the failure load above the original capacity of 10% to 39% were observed for the CFRP repaired pre-damaged beams (B1-3 to B1-15) when compared to the undamaged control specimen (B1-1).

To continue, the values of the maximum load, corresponding deflection, and percent increases for the second set having the #3 reinforcing bars and two layer of CFRP are given in Table 4-4.

Table 4-4: Max Load-Deflection Values and Percents Gained for Second RC Set

Beam designation	max load (kip)	corresponding deflection (in)	% gained from damaged beam B2-2	% gain from undamaged beam B2-1
B2-1	9.310	2.350	30%	0%*
B2-2	7.141	0.699	0%*	-23%**
B2-3	15.215	0.401	113%	63%
B2-4	14.327	0.357	101%	54%
B2-5	21.216	0.630	197%	128%
B2-6	22.813	0.671	219%	145%
B2-7	16.840	0.554	136%	81%
B2-8	26.879	1.160	276%	189%
B2-9	27.248	1.546	282%	193%
B2-10	22.907	0.686	221%	146%
B2-11	32.366	1.068	353%	248%
B2-12	31.987	0.923	348%	244%
B2-13	27.758	0.923	289%	198%
B2-14	18.007	0.958	152%	93%
B2-15	24.549	0.487	244%	164%
B2-16	23.818	0.859	234%	156%
B2-17	23.266	0.694	226%	150%
B2-18	21.613	0.710	203%	132%
B2-19	22.321	0.825	213%	140%

* Control specimen gives values of 0%; **Signifies % capacity lost due to simulated damage

A comparison between the failure load of the damaged control beam B2-2 (damaged beam with no CFRP) and the control beam B2-1 (undamaged beam with no CFRP) signifies that the simulated damage caused a 23% reduction in the ultimate capacity. Furthermore, the CFRP repaired beams B2-3 through B2-19 shows that the CFRP repairs enhanced the flexural capacity of a control damaged beam (B2-2) by a range of 101% to 353%. Similarly, increases in the failure load above the original capacity of 54% to 248% were observed for the CFRP repaired pre-damaged beams (B2-3 to B2-19) when compared to the undamaged control specimen (B2-1).

Figures 4-1 to 4-3 show load deflection graphs including the four tested beams which experienced the largest maximum load capacity compared with the two control beams. The control beams being B2-1, an undamaged beam and B2-2, a damaged beam with only a simulated concrete repair. It can be seen in this figure that the repaired beams maintained approximately the same stiffness but experienced a less ductile behavior and a large increase in capacity when compared to the control beams**.**

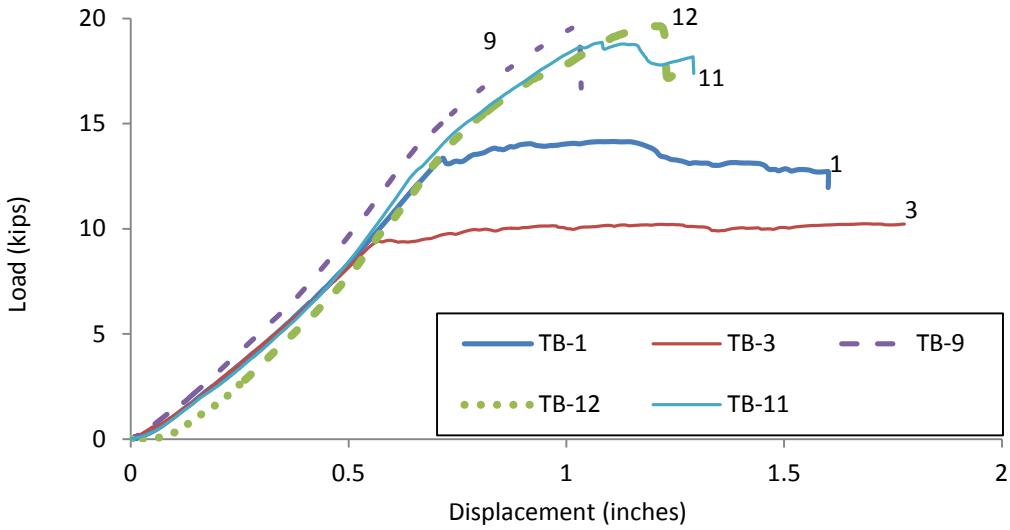

Figure 4-1: Load-deflection comparison of best performing repairs and control beams (first set)

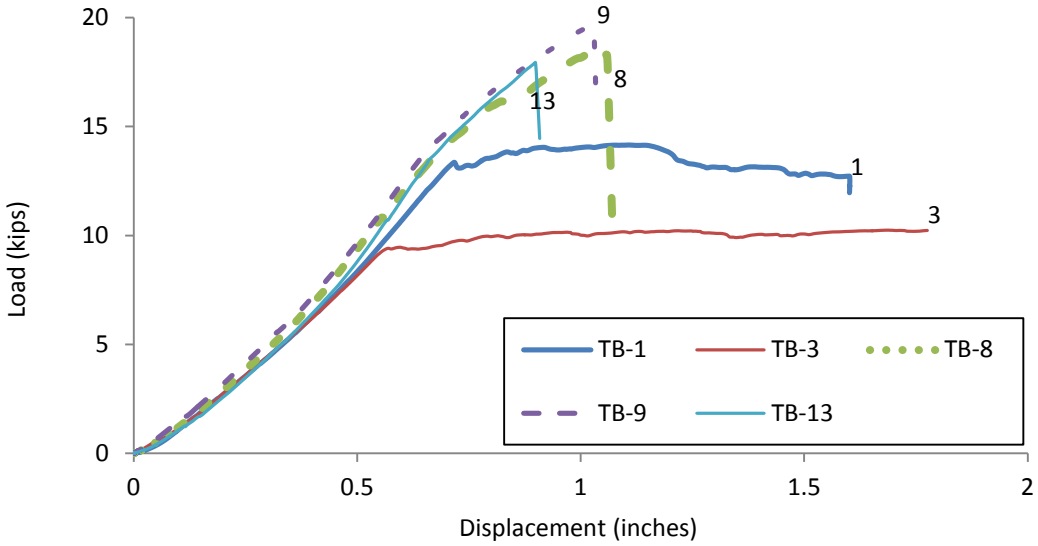

Figure 4-2: Load-deflection comparison of beams in the first set (TB-1, TB-3, TB-8, TB-9, and TB-13)

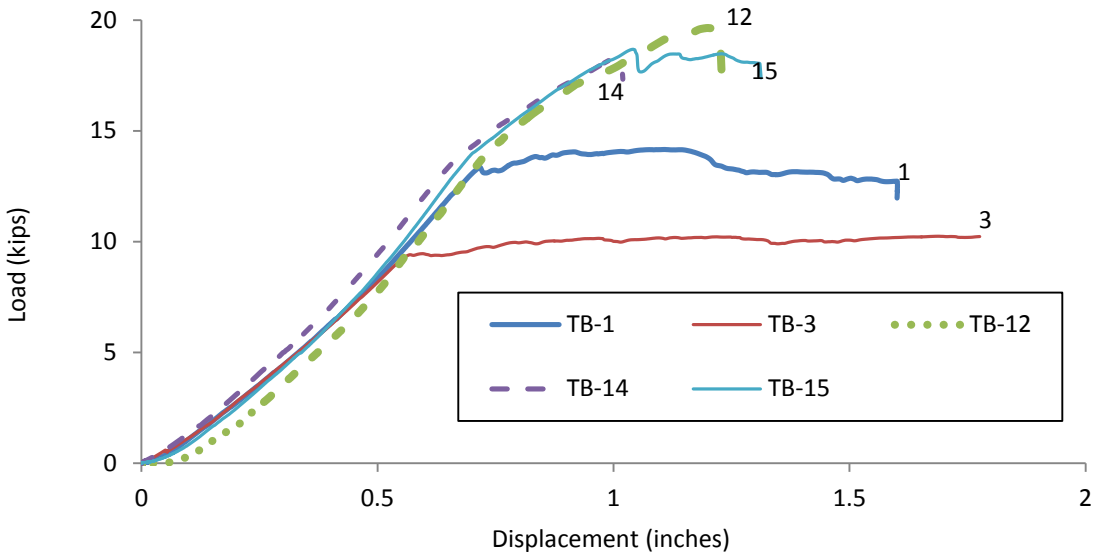

Figure 4-3: Load-deflection comparison of beams of first set and control

Figure 4-4 shows a load vs. deflection graph of the top performing repairs for the second set compared to the control beams from its set.

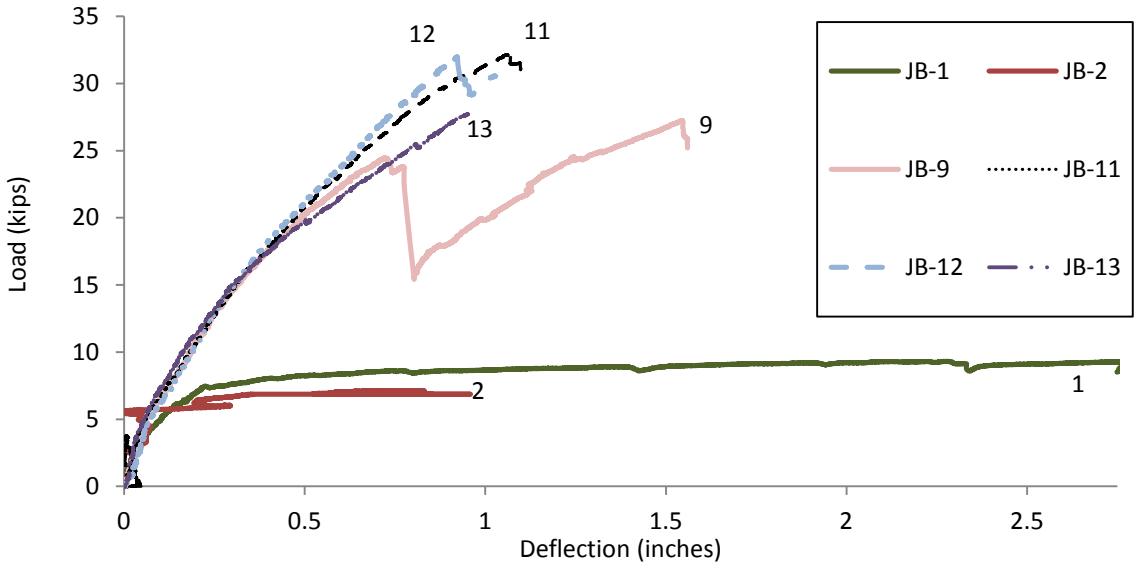

Figure 4-4: Load-deflection comparison of best performing repairs and control beams

A comparison between the failure load of damaged beam B2-2 (control damaged beam with no CFRP) and CFRP repaired beams B2-3 to B2-19 shows that the CFRP repair enhanced the flexural capacity by a range of 101% to 353%. Also, increases in the failure load of 54% to 193% were observed for the CFRP repaired pre-damaged beams B2-3 to B2-19 when compared to an undamaged control beam B2-1. Figure 4-5 and Figure 4-6 show load-deflection comparisons for the beams in the second set.

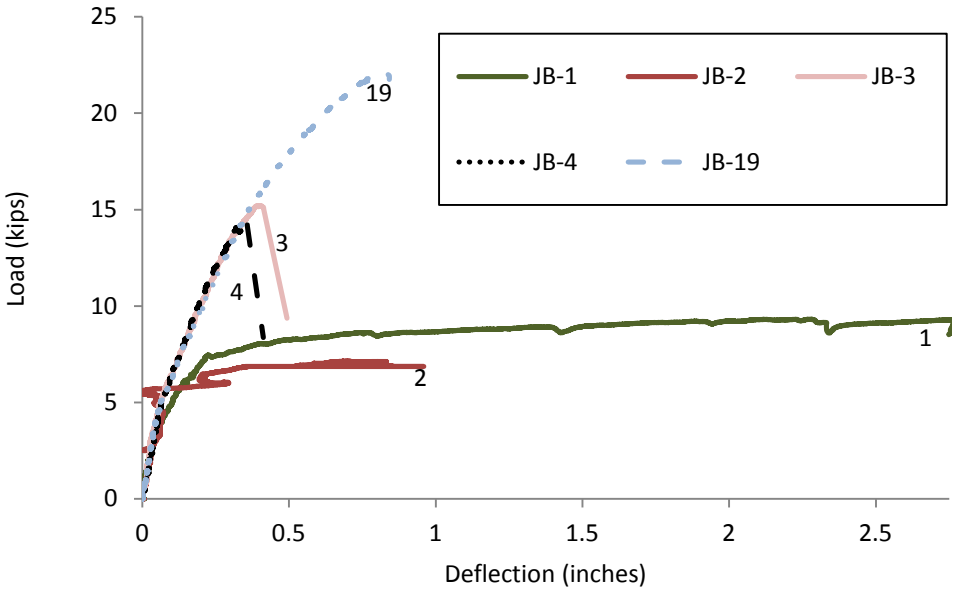

Figure 4-5: Load-deflection comparison for some beams in the second beam set (JB-1, JB-2, JB-3, JB-4, and JB-19)

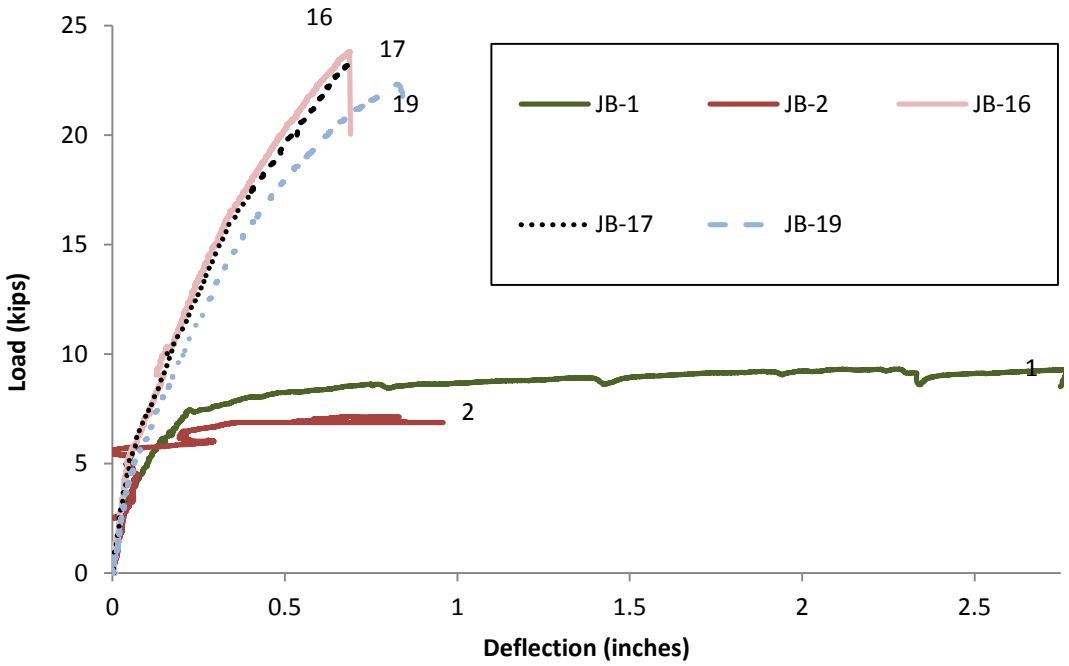

Figure 4-6: Load-deflection comparison for some beams in second set (JB-1, JB-2, JB-16, JB-17, and JB-19)

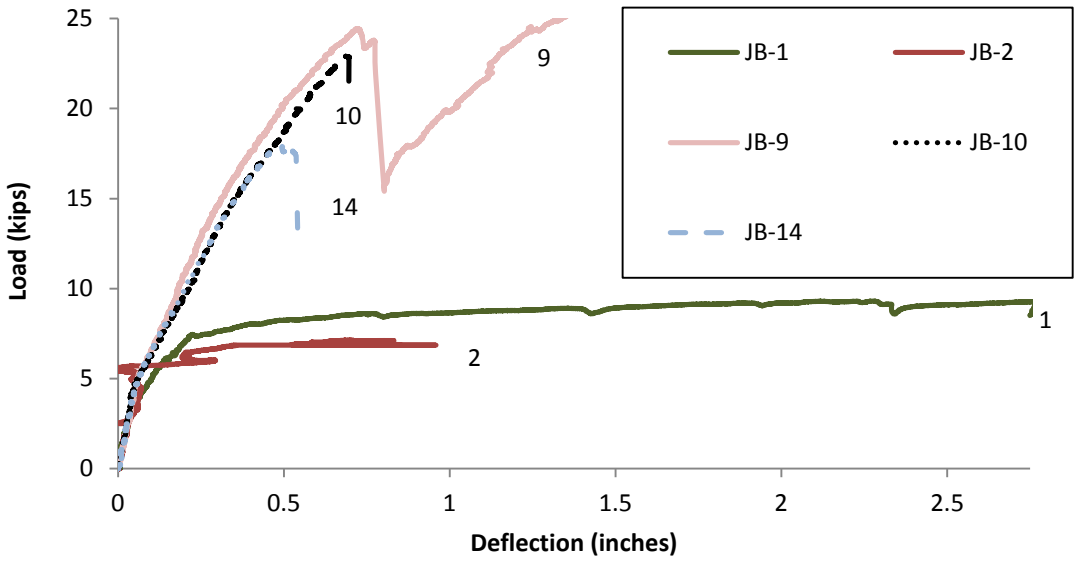

Figure 4-7: Load-deflection comparison for beams (JB-1, JB-2, JB-9, JB-10, and JB-14)

4.2.2. RC STRAIN RESULTS

For the first set of beams, Table 4-5 represents the measured soffit strains at middle of the beams. Percentages of strain reduction at specified loads due to usage of intermediate U-wrappings for the first set contacting the #4 rebar and one layer of CFRP is given in Table 4-5.

Table 4-5: Strain Decreases at Various Loads for First RC Set

Beam designation	% of max strain decreased due to intermediate anchoring		
	at 5 kip	at 10 kip	at 15 kip
B1-5	0.0%**	0.0%**	0.0%**
B1-6	9.7%	15.8%	-0.2%
B1-7	68.3%	25.6%	-8.8%
B1-8	-20.0%*	3.5%*	8.4%*
B1-9	49.9%	12.0%	24.3%
B1-10	38.4%	6.8%	-2.1%
B1-11	43.4%	8.4%	13.5%
B1-12	73.6%	22.9%	28.9%
B1-13	49.3%	12.1%	4.6%
B1-14	72.5%	33.1%	30.6%
B1-15	75.9%	20.1%	28.0%

* Strain gauges have been determined unreliable; ** Control specimen gives values of 0%

In addition to the strain results listed for the first set, the maximum strain values from the mid-span soffits of the second set are listed in Table 4-6. A comparison between a repaired beam with only end anchorage and the best performing CFRP repair which utilizes multiple intermediate anchoring U-wrappings is used to evaluate the reduction in strains at increasing

load levels. The second set of beams (B2-1 to B2-19) is also referred to as JB-1 to JB-19.

Table 4-6: Strain Decreases at Various Loads for Second RC Set

Beam designation	% of max strain decreased due to intermediate anchoring		
	at 5 kip	at 10 kip	at 15 kip
B2-5	35.5%	17.7%	17.8%
B2-6	11.5%	6.1%	10.8%
B2-7	-19.4%*	-20.9%*	-606.5%*
B2-8	31.2%	16.2%	6.5%
B2-9	31.5%	13.6%	17.5%
B2-10	21.9%	14.2%	8.9%
B2-11	40.7%	20.2%	23.7%
B2-12	28.1%	17.2%	23.8%
B2-13	-11.0%*	4.1%*	-0.7%*
B2-14	26.8%	19.0%	22.7%
B2-15	N/A	N/A	N/A
B2-16	63.6%	19.6%	14.4%
B2-17	64.0%	19.5%	22.2%
B2-18	16.0%	11.8%	10.0%
B2-19	0.0%**	0.0%**	0.0%**

* Strain gauges have been determined unreliable; ** Control specimen gives values of 0%

It can be seen by the comparison in Figures 4-8 to 4-14 that the use of intermediate U-wrappings for anchoring does suppress the strain developed in the longitudinal laminate applied to the beams soffit.

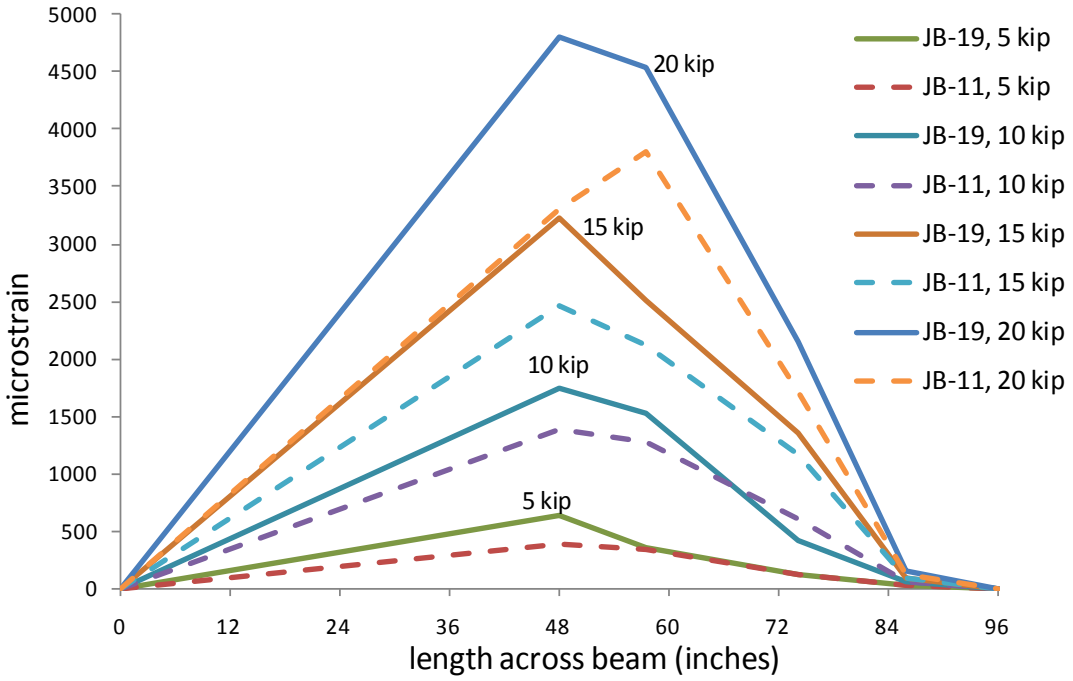

Figure 4-8: Comparison of strain developed along beams soffit for best repair and control beams

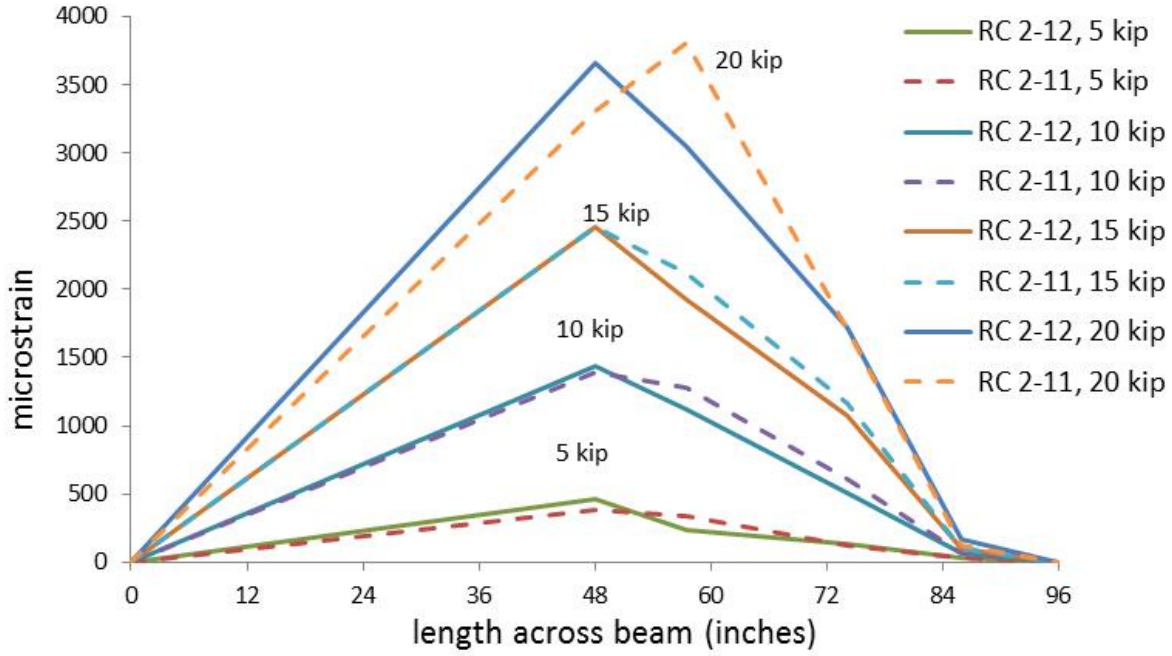

Figure 4-9: Comparison of strain developed along beams soffit for best repair and fully wrapped

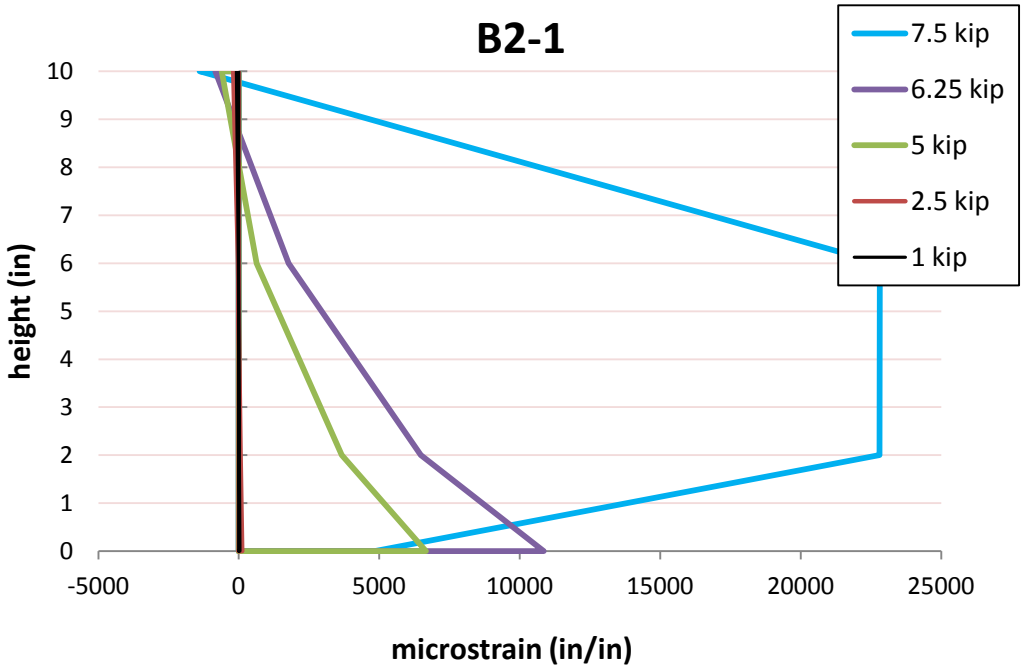

Figure 4-10: Strain per height of cross-section for control beam of second set at various loads

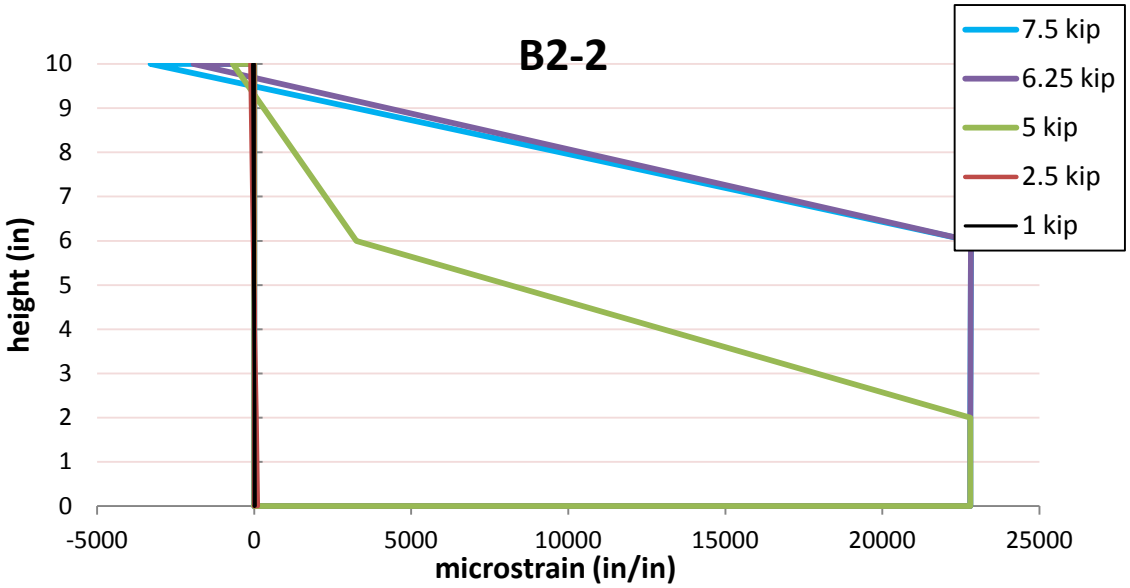

Figure 4-11: Strain per height of cross-section for control beam of JB set (second set) at various loads

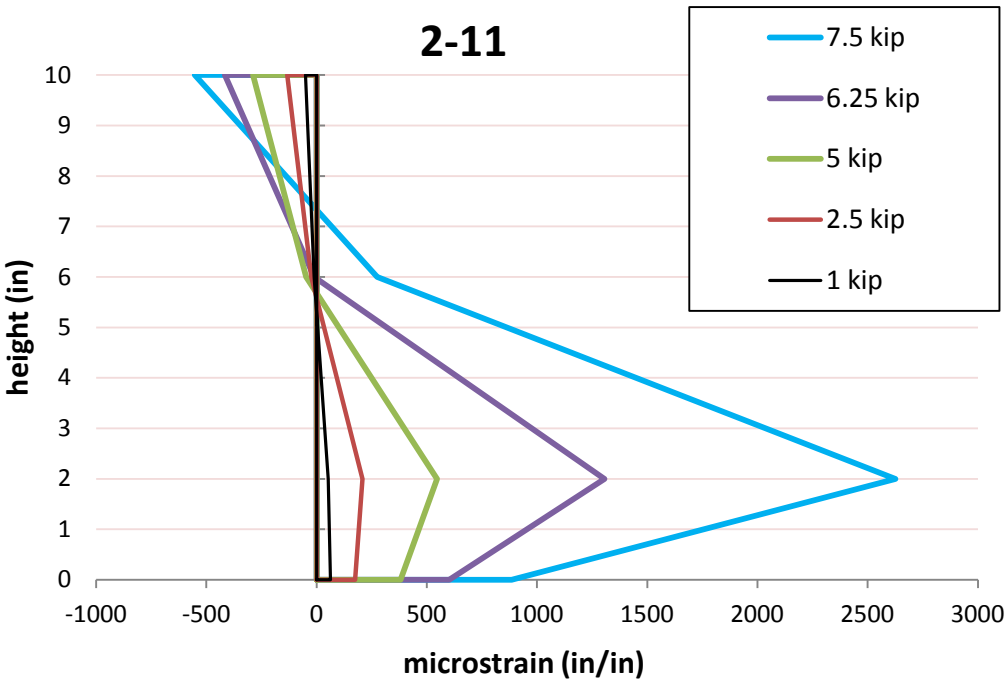

Figure 4-12: Strain per height of cross-section for repaired beam of JB set at various loads

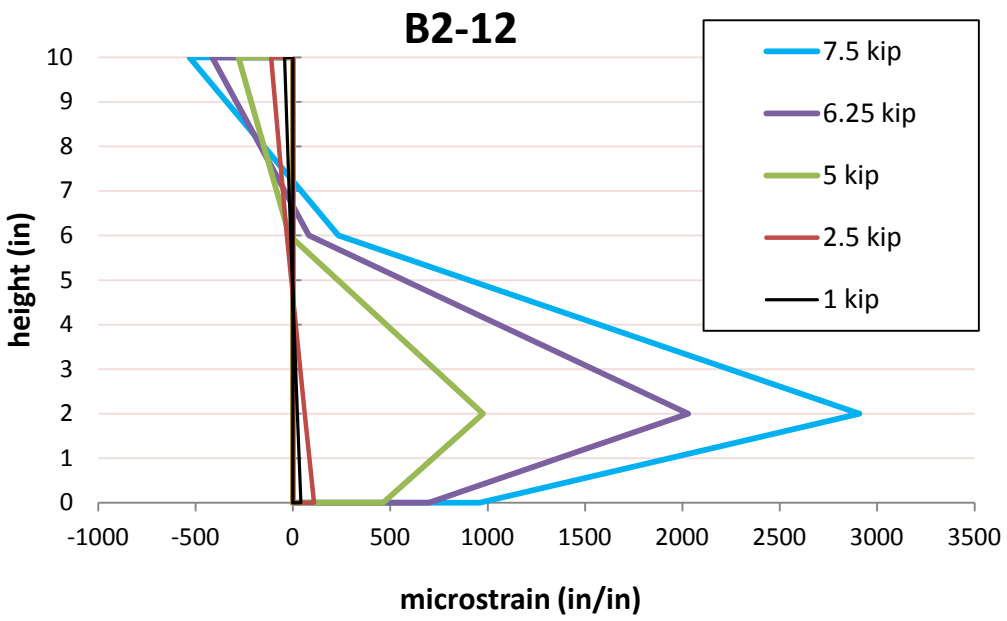

Figure 4-13: Strain per height of cross-section for repaired beam of JB set at various loads

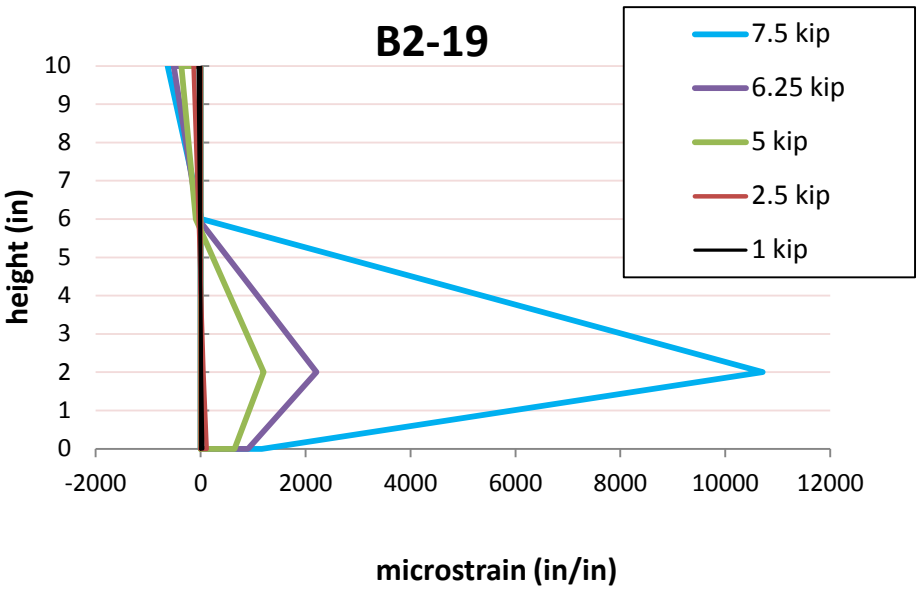

Figure 4-14: Strain per height of cross-section for repaired beam of JB set at various loads

4.2.3. RC FAILURE MODES

The failure modes observed and recorded during the flexural testing of the RC beams is presented in Tables 4-7 and 4-8.

Table 4-7: Failure Modes Recorded for First RC Set

Beam Designation	Recorded Failure Mode
B1-1	excessive flexural cracks and crack widening
B1-2	compression failure with slight delamination
B1-3	excessive flexural cracks and crack widening
B1-4	debonding failure of entire right side of CFRP
B1-5	delamination of CFRP with concrete attached
B1-6	slight debonding instantly followed by rupture
B1-7	slight debonding instantly followed by rupture
B1-8	slight debonding instantly followed by rupture
B1-9	CFRP rupture
B1-10	CFRP rupture
B1-11	slight compression cracking then rupture
B1-12	CFRP rupture
B1-13	slight compression cracking then rupture
B1-14	slight debonding on one side instantly followed by rupture
B1-15	compression failure w/ splitting of center U-wrap

Table 4-8: Failure Modes Recorded for Second RC set

Beam Designation	Failure mode
B2-1	excessive flexural cracks and crack widening
B2-2	excessive flexural cracks and crack widening
B2-3	debonding from one side of CFRP
B2-4	debonding from one side of CFRP
B2-5	debonding from one side after excessive crack formation
B2-6	shear failure
B2-7	CFRP rupture (beam only had 1 layer of CFRP though)
B2-8	slight debonding then compression failure
B2-9	excessive shear cracking then compression failure
B2-10	excessive shear cracking then compression failure
B2-11	shear failure
B2-12	CFRP rupture at mid-span
B2-13	CFRP rupture w/ zipper type failure
B2-14	shear failure
B2-15	shear failure
B2-16	shear failure
B2-17	shear failure
B2-18	shear failure
B2-19	excessive flexural cracking then debonding failure

4.3. HALF-SCALE PRESTRESSED CONCRETE GIRDERS DATA

4.3.1. HALF-SCALE LOAD-DEFLECTION RESULTS

Values of maximum load capacity, the corresponding deflections, and percent increases for the half-scale AASHTO type II girders is available and presented in Table 4-9.

Table 4-9: Max Load/Deflection Results for Half-Scale PS Girders

Girder designation	Max Load (kip)	Corresponding deflection (in)	% increase compared to damaged PS-2	% increase compared to undamaged PS-1
PS-1	75.87	6.94	22.60*	N/A
PS-2	61.88	5.38	0.00	-18.44**
PS-3	90.14	2.44	45.66	18.81
PS-4	84.75	2.14	36.94	11.70
PS-5	78.92	1.61	27.53	4.02
PS-6	100.91	2.39	63.07	33.01
PS-7	104.42	2.74	68.74	37.63
PS-8	99.16	2.29	60.24	30.70
PS-9	77.26	1.58	24.85	1.83
PS-10	87.68	2.14	41.69	15.57

* Increase of flexural capacity of PS-1 compared to that of PS-2
** Loss of flexural capacity of PS-1 due to strand cutting; a percentage of its original capacity

A comparison between the failure loads of control girder PS-2 (unstrengthened with CFRP) and the repaired girders with two layers of CFRP shows that the CFRP repairs enhanced the flexural capacity of a damaged girder by a range of 27.53% to 45.66%. Also, for girders repaired with 3 layers of CFRP, increases in the flexural capacity were measured ranging from 60.24% to 68.74% compared to control girder PS-2. Increases in the failure load of 24.85% and 41.69% were observed for the repaired girders fully wrapped with CFRP when compared to the unstrengthened control beam PS-2.

The graphical depiction of the load deflection results for each girder tested are presented in various comparisons in Figure 4-15 through Figure 4-19. The test results indicate a loss of 18.44% in flexural capacity due to damage and cutting one of the prestressing strands compared to the undamaged control girder. The CFRP repair restored the damaged girder's capacity and exceeded the capacity of the undamaged control girder by up to 37.63%. The repaired girders also had an enhancement of their flexural capacity of up to 68% compared to that of the damaged girder. The results also show that U-shaped wrapping of CFRP laminates enhanced the flexural capacity even if the U-wrapping was not continuously covering the entire girder side (not fully wrapped). By comparing the two fully wrapped beams, it is understood that overlapping transverse U-wrappings is needed to develop proper continuity; even in a direction perpendicular to the direction of the fibers.

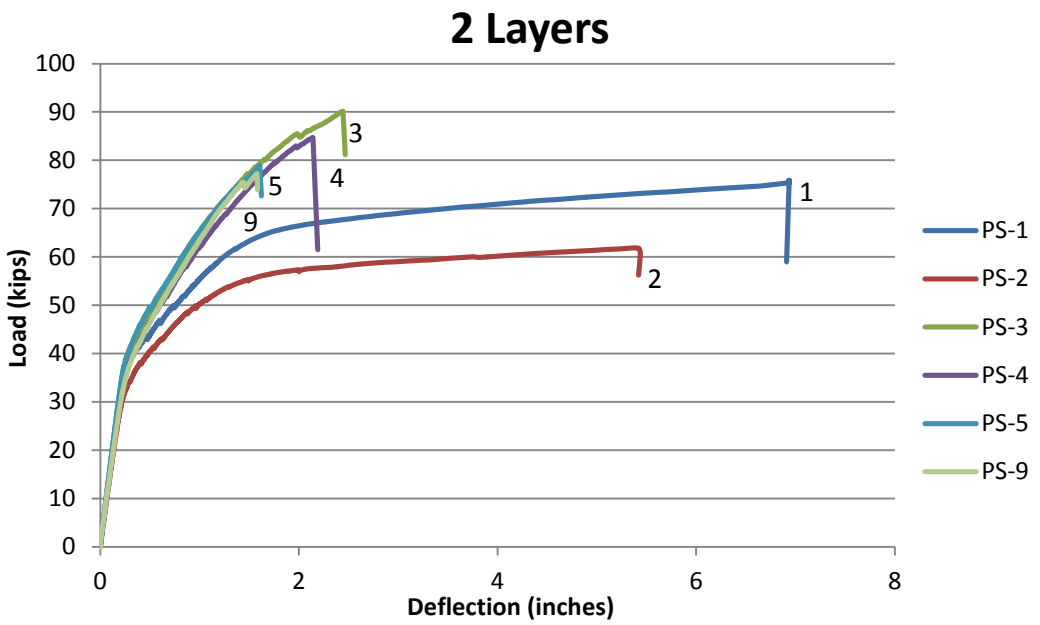

Figure 4-15: Load vs. deflection for controls and girders with 2 layers of CFRP

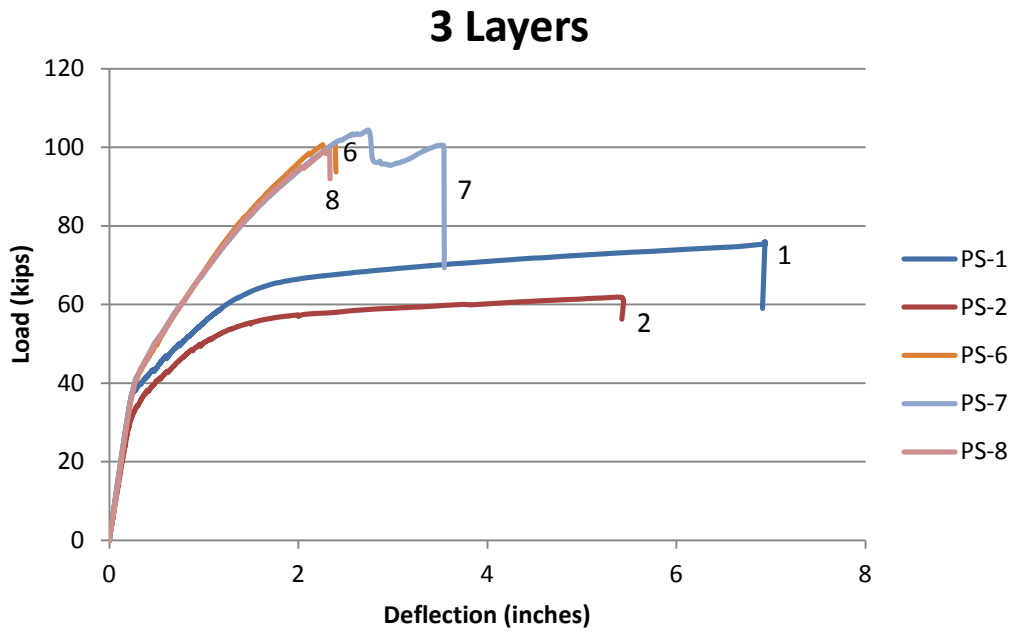

Figure 4-16: Load vs. deflection for controls and girders with 3 layers of CFRP

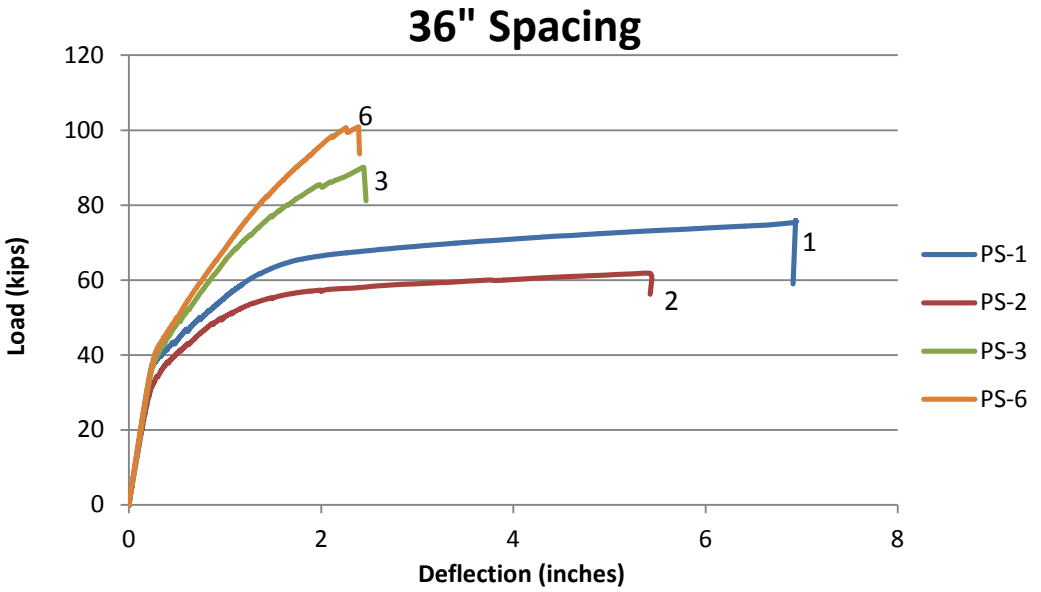

Figure 4-17: Load vs. deflection for controls and 36” spacing configurations

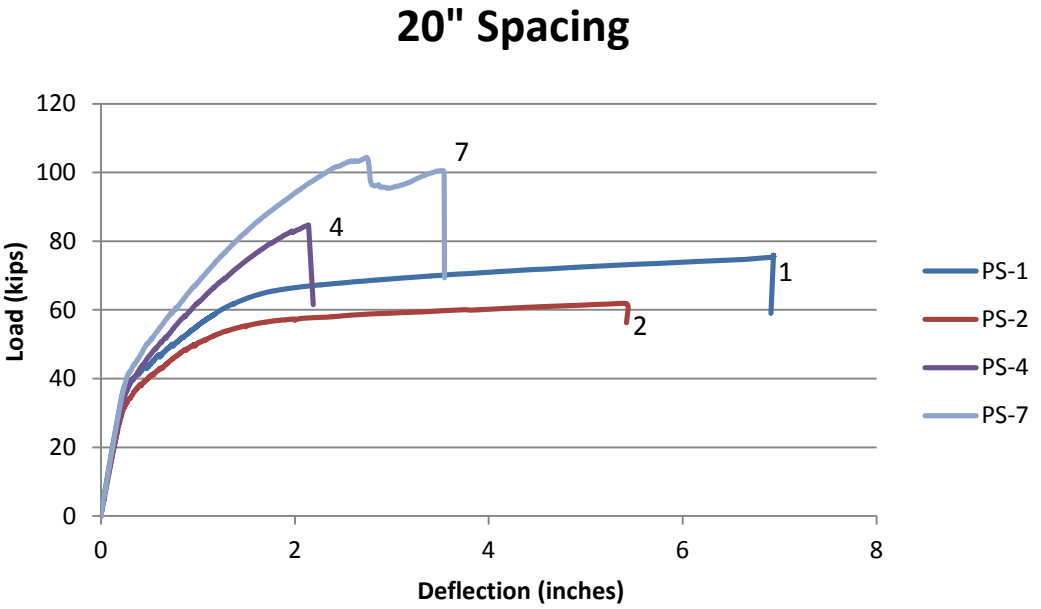

Figure 4-18: Load vs. deflection for controls and 20” spacing configurations

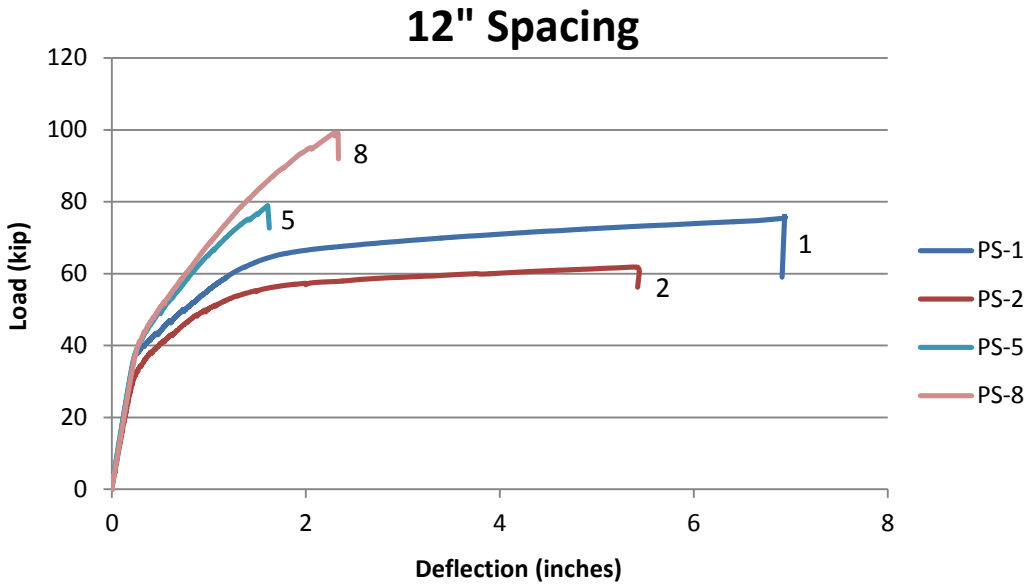

Figure 4-19: Load vs. deflection for controls and 12" spacing configurations

As seen by the results, the damage and cutting of one of the prestressing strands (Girder PS-2) resulted in 18.44% loss in flexural capacity compared to the undamaged control girder PS-1. The CFRP repair of the damaged girder PS-2 as shown in girders PS3 to PS9 restored the damaged girder's capacity and exceeded the capacity of the undamaged control girder PS-1 by up to 37.63%. The results also show that U-shaped wrapping of CFRP laminates (Girders PS-3 to PS-8) enhanced the flexural capacity even if the U-wrapping was not continuously covering the entire girder side (not fully wrapped).

4.3.2. HALF-SCALE STRAIN RESULTS

The measured strain results were recorded. The trains were measured along the height of the beam at mid-span and at the soffit of the beam along the beam length. The strains measured at a load level of 70 kip are presented in Figure 4-20. Half of the span lengths of the symmetrical girders were instrumented with a multitude of strain gauges while the other half of the span length had one strain gauge. Therefore, the profiles shown in Figure 4-20 depict much more detailed behavior on the girder right side of the center peaks.

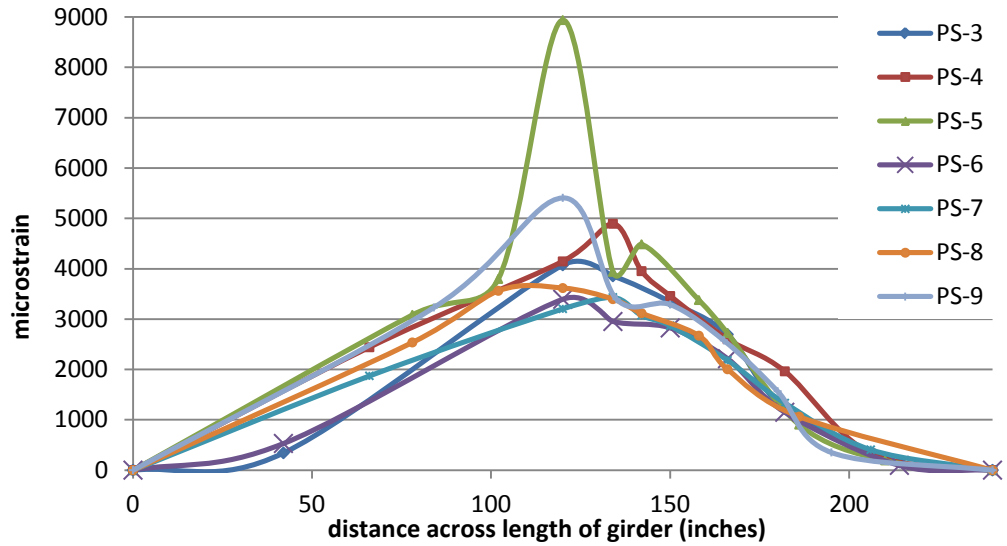

Fig. 4-20: Strain of CFRP at girder soffit vs. length for repaired girders

When discussing the strain development of the previous RC samples a percentage of reduction was calculated to evaluate the effectiveness of the repair. However, the half-scale girders did not incorporate a repair configuration with only end anchors, which is necessary to calculate a percentage decrease. Instead the effectiveness of the repair is considered by simply identifying the repair configuration that reduces strain the most. Table 4-10 presents the tensile strain values measured at mid-span at various load levels. The strains were measured at the soffit. It should be evident that PS-7 was most successful at mitigating strain development.

Table 4-10: Strain Values Measured at Various Loads for Half-Scale Girders

Beam Designation	Maximum Strain Values Recorded at Various Loads					
	at 5 kip	at 15 kip	at25 kip	at 40 kip	at 60 kip	at 70 kip
PS-1	52.58	158.51	280.33	291.40*	broke	broke
PS-2	61.32	200.39	1837.30	broke	broke	broke
PS-3	51.03	167.19	314.76	1295.52	2984.16	4075.28
PS-4	55.16	172.14	341.49	1332.85	3197.49	4146.04
PS-5	53.03	146.52	316.97	1270.22	5213.27	8939.73
PS-6	51.57	160.54	292.03	1048.55	2646.34	3393.13
PS-7	49.05	150.30	266.07	835.90	2415.59	3203.85
PS-8	52.59	161.94	281.84	942.62	2647.17	3616.50
PS-9	58.40	180.76	368.50	1357.88	3433.54	5409.16

* Strain gauges have been determined unreliable; & green equals lowest value recorded at that load

4.3.3. HALF-SCALE FAILURE MODES

The modes of failure and other documented observed behaviors are presented in Table 4-11.

Table 4-11: Failure Modes Recorded for Half-Scale Girders

Beam Designation	Failure Mode and Observations of Behavior during Testing
PS-1	flexural failure started with visible widening of flexural cracks around 60 kip, cracks widen to an estimated eighth of an inch at 68 kip, ultimately compression failure caused the beam to completely fail around 76 kip
PS-2	flexural failure started with visible widening of flexural cracks around 35 kip, cracks widen excessively around 49 kip, ultimately a large compression/shear crack from flexural side up to load at 25" off center
PS-3	debonding sound heard around 86 kip, CFRP rupture ultimately occurred at approx. 5 inches off center on the side of debonding/delamination, debonding spanned from about center of the beam to center of second u-wrap span
PS-4	debonding sounds heard around 80 kip, CFRP rupture ultimately occurred at approx. 7 or 8" inches off center on the side of debonding/delamination, debonding spanned from point of rupture to center of second u-wrap span
PS-5	debonding sounds heard around 75 kip, CFRP rupture ultimately occurred at center span, debonding/delamination spanned from just pasted fist u-wrap on one side to beginning of first on the other side
PS-6	debonding sounds heard around 95 kip, CFRP debonding/delamination spanned from just pasted center u-wrap to beginning of last u-wrap, the first u-wrap was also completely debonded-originating from top of wrap
PS-7	Load reached 105 then dropped to 95 before failure, CFRP debonding/delamination spanned from just pasted center u-wrap to end of last u-wrap, the second u-wrap was also completely debonded-originating from top of wrap
PS-8	debonding sounds heard around 95 kip, CFRP rupture ultimately occurred at center, two local debonding areas formed-one occurred in first u-wrap span on one side, the other was from first wrap to last wrap on the opposite side
PS-9	localized debonding of center u-wrappings at top of beam and perhaps other debonding sounds heard around 75 kip, ultimately CFRP rupture at center span, debonding/ delamination did occur in center section approx. 60" total

As seen in Table 4-11, the control girders experienced a classic flexural failure initiated by excessive deflection and widening of flexural cracks. A photo of a control beam experiencing excessive deflection is presented in Figure 4-21. As for the repaired girders, they experienced either CFRP debonding, CFRP rupture without debonding, or localized debonding followed by rupture of CFRP; as shown in Figures 4-22 to 4-24. Some repaired girders also experienced debonding of some of their U-wrappings, as shown in Figure 4-24 (right).

Figure 4-21: Half-scale control girder displaying excessive deflection under loading

Figure 4-22: Half-scale girder displaying debonding failure of CFRP laminates

Figure 4-23: Close-up of laminate debonding initiated by flexural crack development

Figure 4-24:(left) Rupture of longitudinal CFRP, (right) Debonding of CFRP U-wrapping

The half-scale girders were intended to be tested under fatigue for 2 million cycles but using a high fatigue load range of 10 kip to 35 kip. The repaired half-scale beams were tested in several stages to failure. After several initial loading cycles to simulate possible overloading conditions, the half-scale beams did not survive the desired 2 million cycles of loading. The half-scale girders failed prematurely at less than 1 million cycles under this overload condition.

4.3.4. HALF-SCALE FATIGUE TEST RESULTS

Figures 4-25 through 4-27 show the fatigue behavior and load deflection results for half-scale girders. The range of fatigue loading was much higher than that required by AASHTO LRFD to simulate overloading conditions. The half-scale girders only survived less than 1 million cycles of fatigue loading at about 3 Hz, with a fatigue load range of 10 kip to 35 kip. According to the data files, the fatigue cycles details are:

- PS-11 started at 4 Hz then went to 3 Hz after 2,000 cycles, then 2 Hz after 214,000 cycles
- PS-12 started at 4 Hz then went to 3 Hz after 6,000 cycles, then 2Hz after 69,000 cycles
- PS-13 started at 2 Hz and stayed there

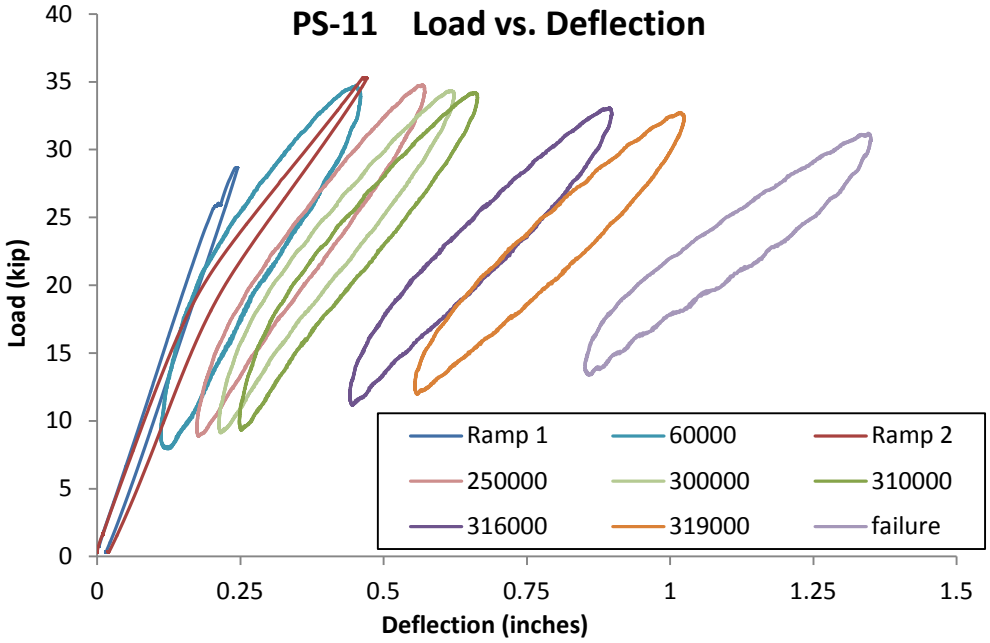

Figure 4-25: Fatigue behavior and degradation until failure for girder PS-11

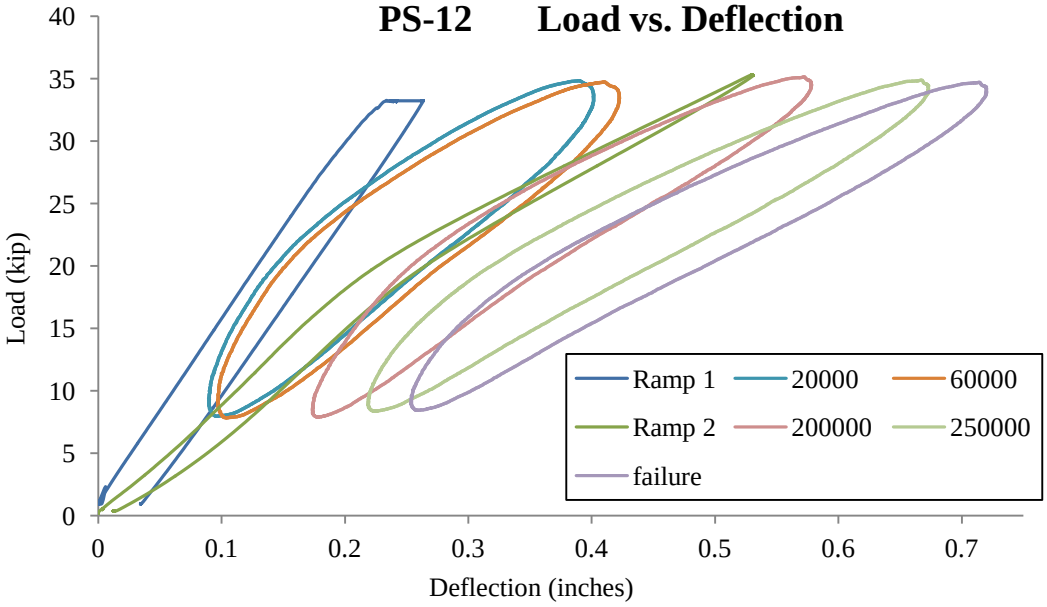

Figure 4-26: Fatigue behavior and degradation until failure for girder PS-12

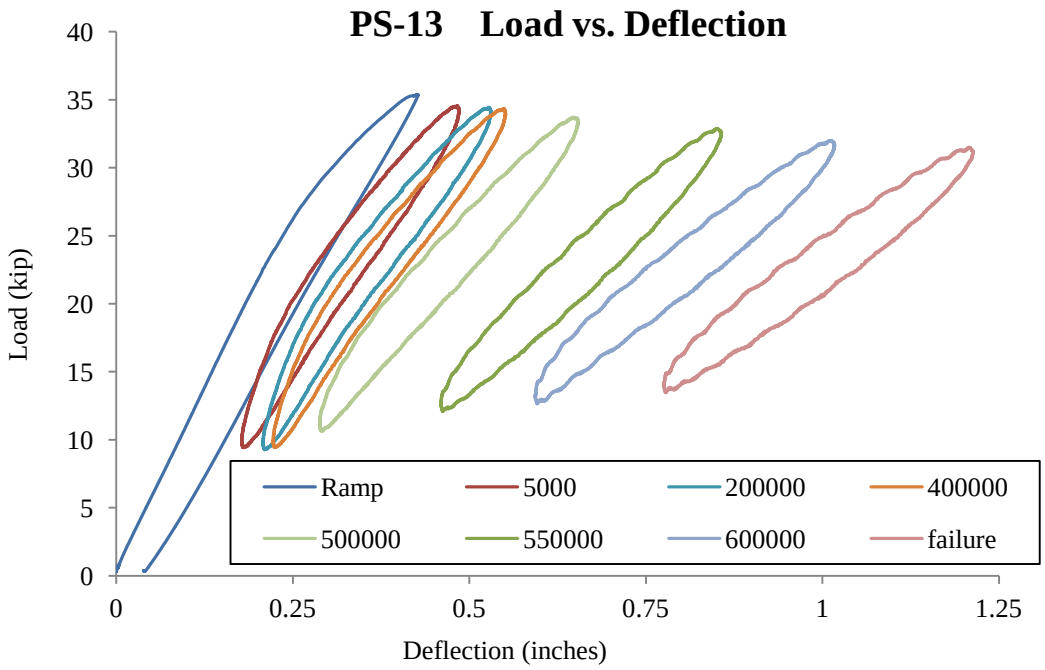

Figure 4-27: Fatigue behavior and degradation until failure for girder PS-13

Table 4-12 represents the test results for half-scale girders under fatigue loading.

Table 4-12: Fatigue Testing Results for the Half-Scale AASHTO Type II Girders

Fatigue Testing Results for the Half-scale AASHTO type II Girders			
Half-scale Girder designations	Loading Level Ranges	Loading Rates	Number of Loading Cycles Completed
PS-11	10 kip-35 kip	started at 4 Hz then to 3 Hz after 2,000 cycles, then 2 Hz after 214,000 cycles	322,000
PS-12	10 kip-35 kip	started at 4 Hz then to 3 Hz after 6,000 cycles, then 2Hz after 69,000 cycles	296,000
PS-13	10 kip-35 kip	2Hz	635,000

4.4. FULL-SCALE PRESTRESSED CONCRETE GIRDERS DATA

4.4.1. FULL-SCALE LOAD DEFLECTION RESULTS

For the static testing of full-scale girders, values of maximum load capacity, the corresponding deflections, and percent increases for the full-scale AASHTO type II girders are shown in Table 4-13.

Table 4-13: Max Load-Deflection Results for Full-Scale PSC Girders

Girder designation	Max Load (kip)	Corresponding deflection (in)	% increase compared to damaged PSC-4	% increase compared to undamaged PSC-8
PSC-4	166.83	2.41	N/A	-9.9%**
PSC-5	205.38	2.58	23.1%	10.9%
PSC-6	214.77	4.94	28.7%	16.0%
PSC-7	206.32	3.04	23.7%	11.4%
PSC-8	185.22	2.99	11.0%*	N/A
* Increase of flexural capacity of PSC-8 compared to that of PSC-4 ** Loss of flexural capacity of PSC-4 due to strand cutting; a percentage of its original capacity				

A comparison between the failure loads of control girder PSC-4 (unstrengthened with CFRP) and the repaired girders with two layers of CFRP shows that the CFRP repairs enhanced the flexural capacity of a damaged girder by an average of 25.9%. Also, for the girder repaired with three layers of CFRP, an increase in the flexural capacity were measured to be 23.7% when compared to control girder PSC-8. When comparing the failure load and behavior of control girder (damaged and unstrengthened with CFRP) and repaired girders with 2 and 3 layers of CFRP, the CFRP repair enhanced the flexural capacity by a range of 23% to 28% compared to control damaged girder with less strands. Also, for repaired girders with 2 and 3 layers of CFRP, increases in the flexural capacity were reported to range from 10 % to 16% compared to control undamaged girder. That means that the repair not only restored the flexural capacity of the damaged PSC girder but also exceeded the capacity of the undamaged girder.

The graphical depiction of the load deflection results for each girder tested are presented in various comparisons in Figure 4-28 through Figure 4-32.

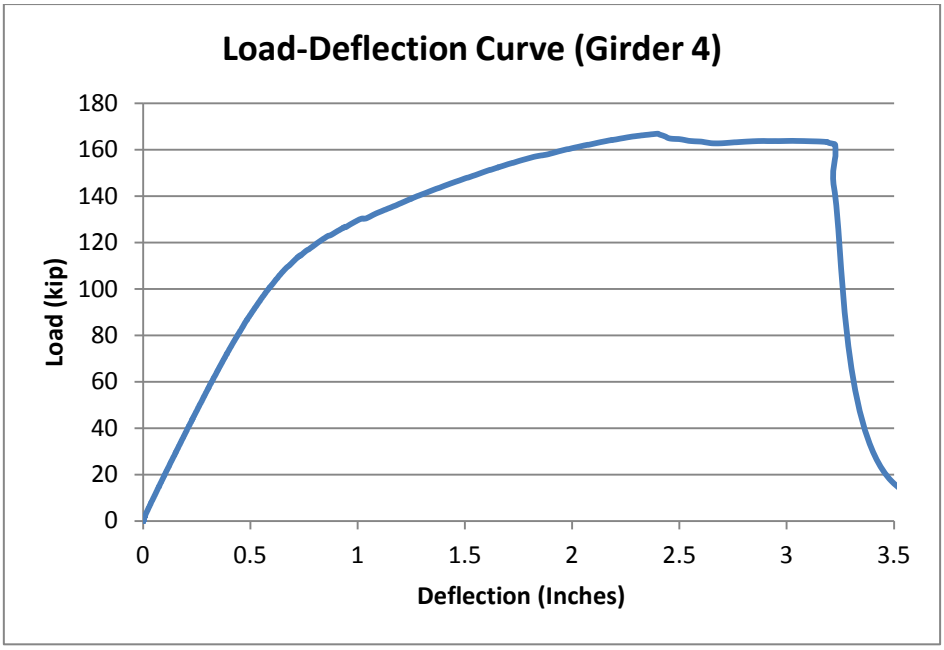

Figure 4-28: Load deflection of PSC-4

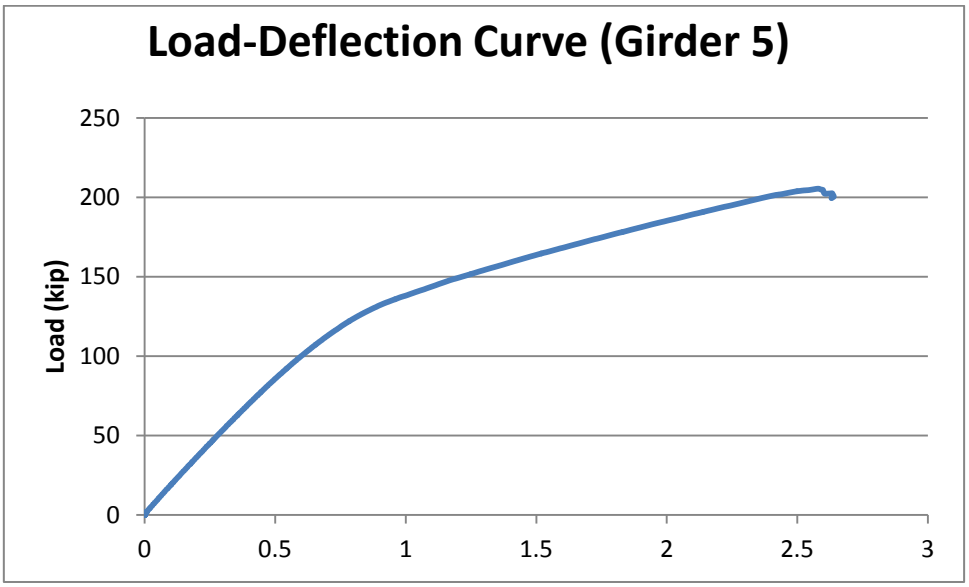

Figure 4-29: Load deflection of PSC-5

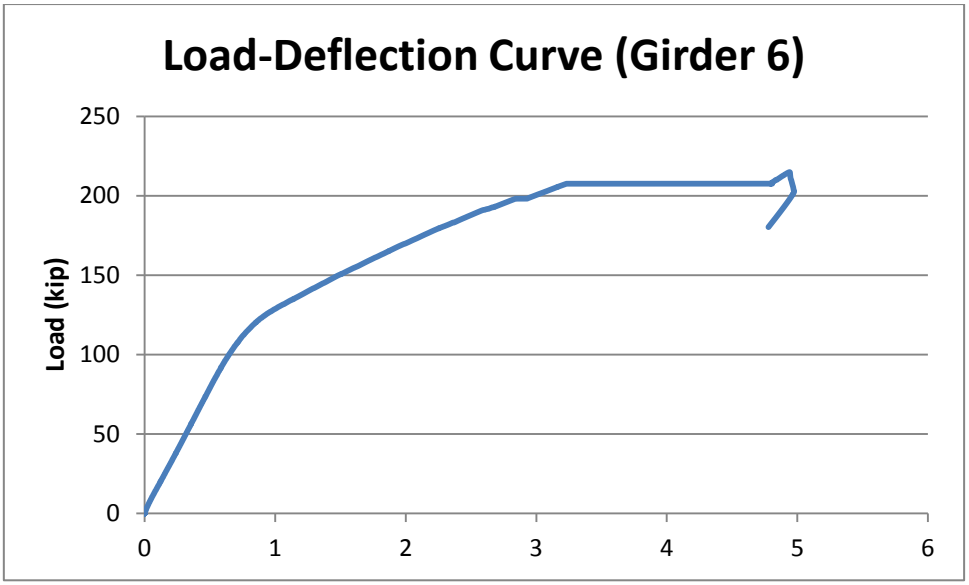

Figure 4-30: Load deflection of PSC-6

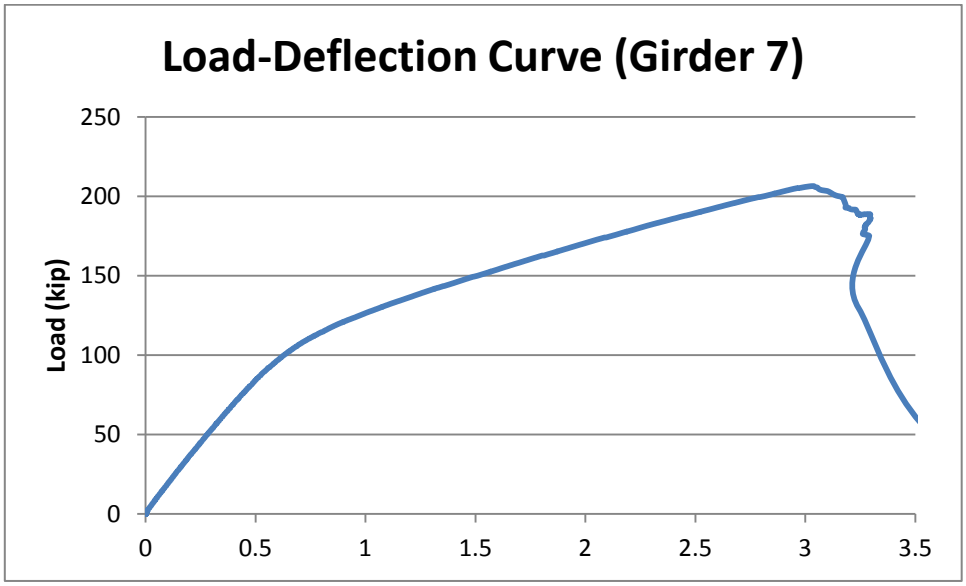

Figure 4-31: Load deflection of PSC-7

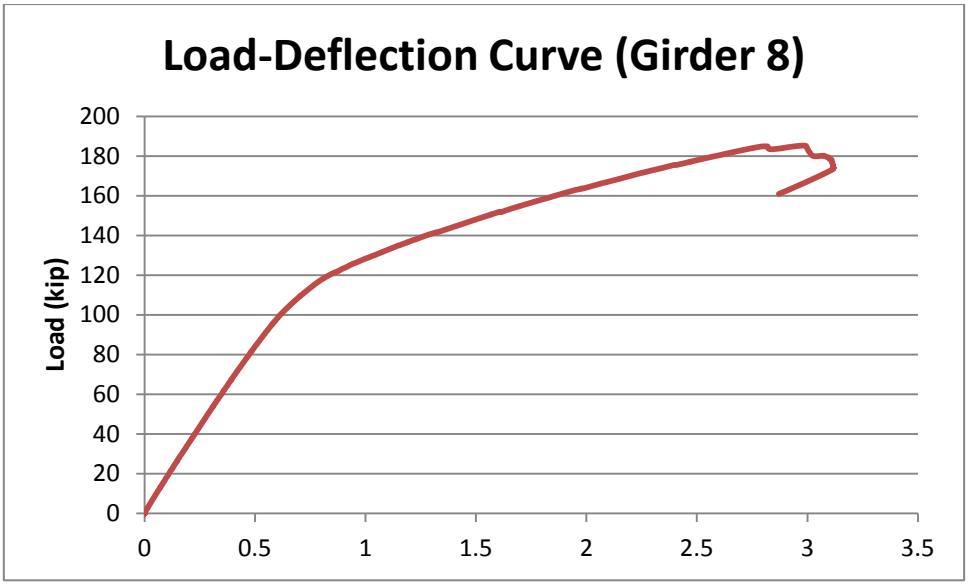

Figure 4-32: Load deflection of PSC-8

4.4.2. FULL-SCALE STRAIN RESULTS

The strain development for each full-scale girder is presented in Figure 4-33 through Figure 4-41.

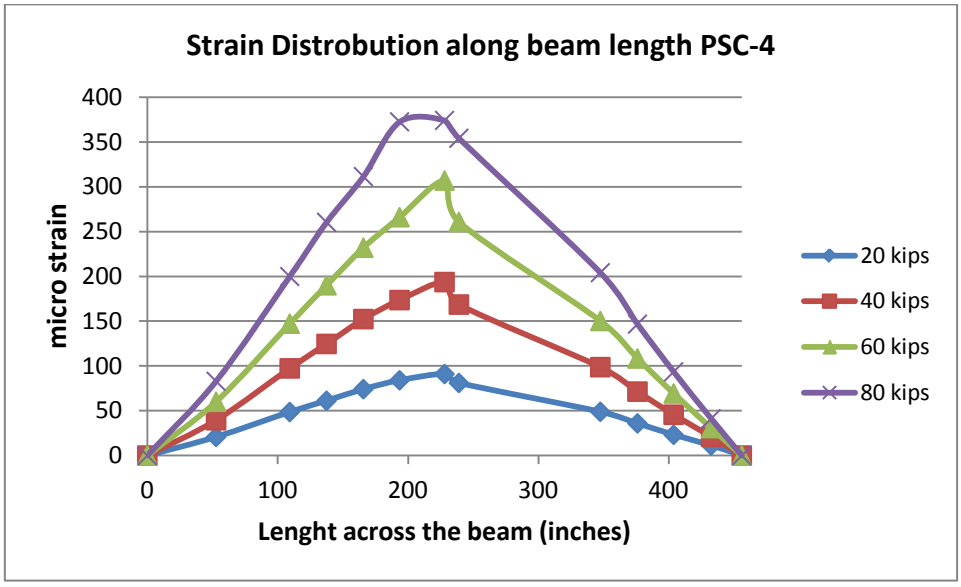

Figure 4-33: Strain development for PSC-4

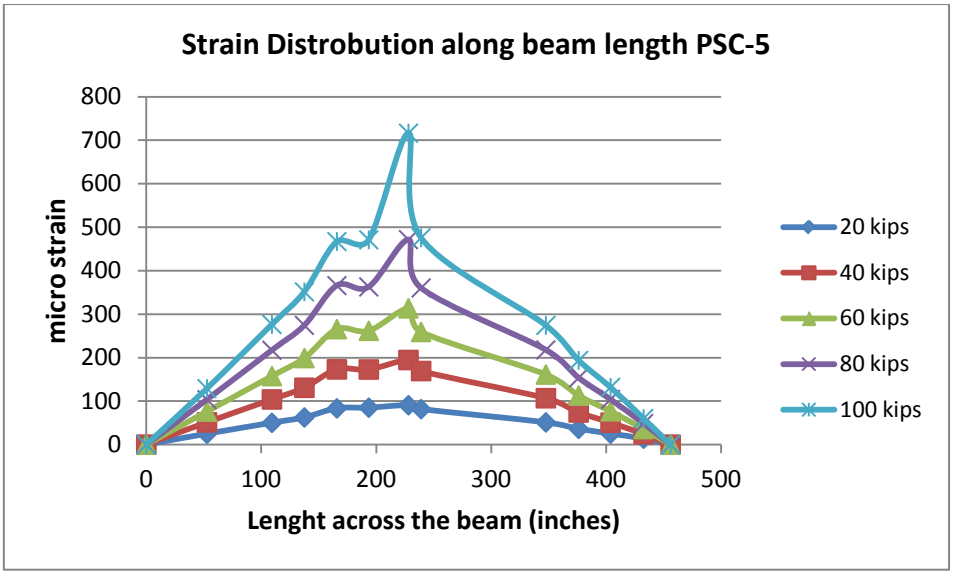

Figure 4-34: Strain development for PSC-5

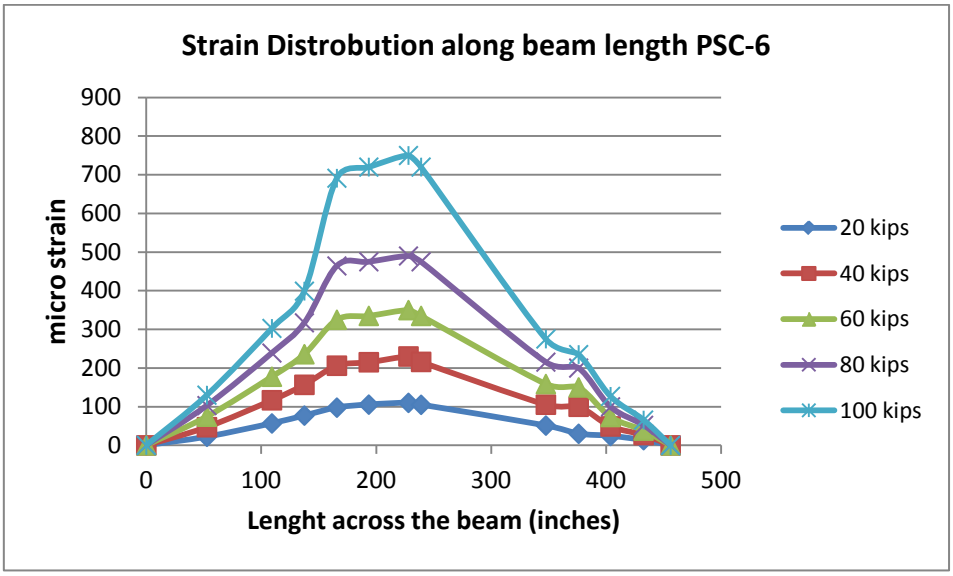

Figure 4-35: Strain development for PSC-6

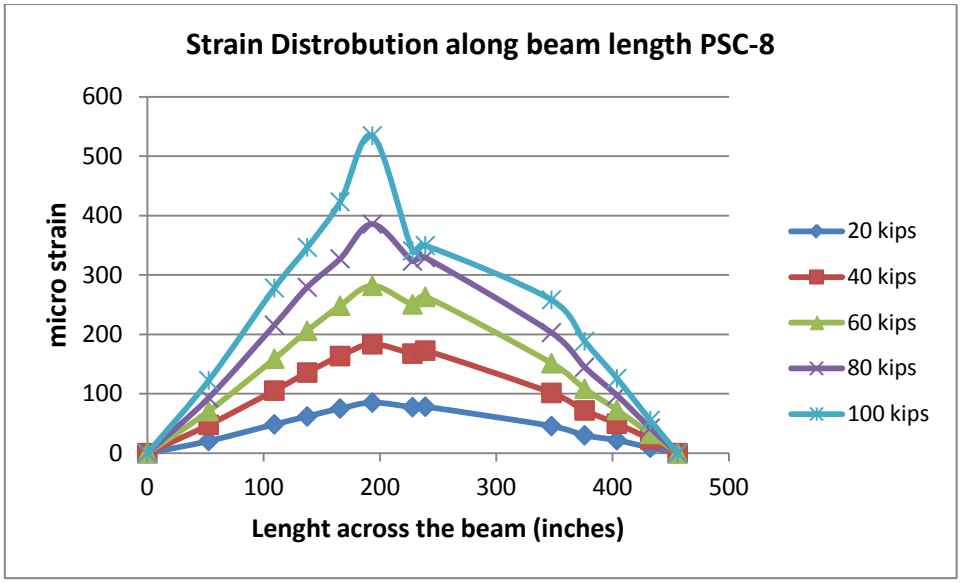

Figure 4-36: Strain development for PSC-8

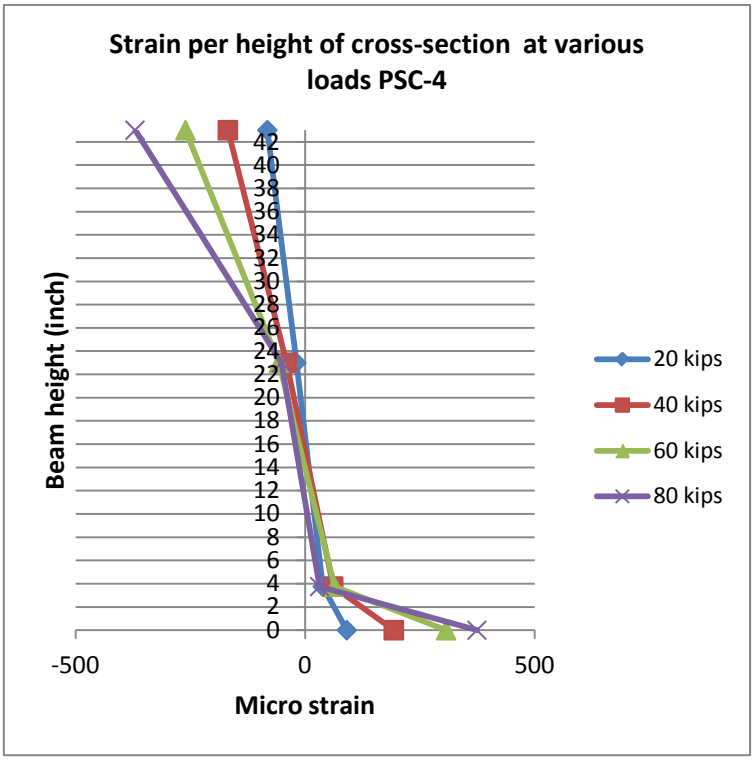

Figure 4-37: Strain development for PSC-4

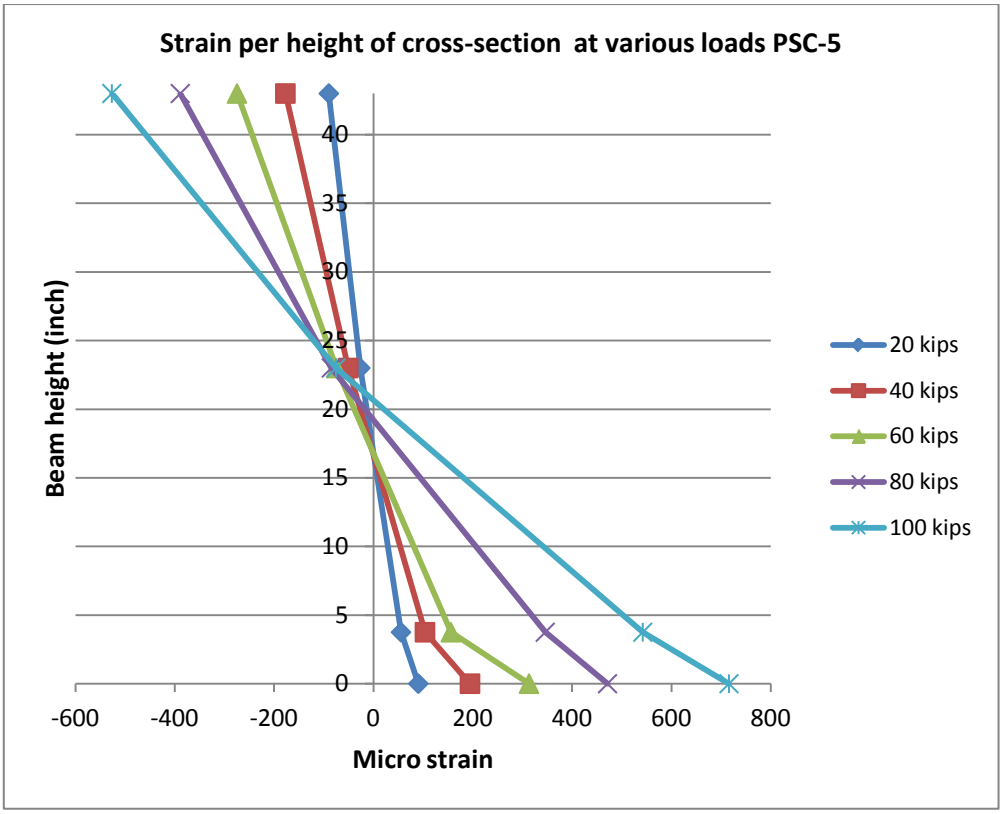

Figure 4-38: Strain development for PSC-5

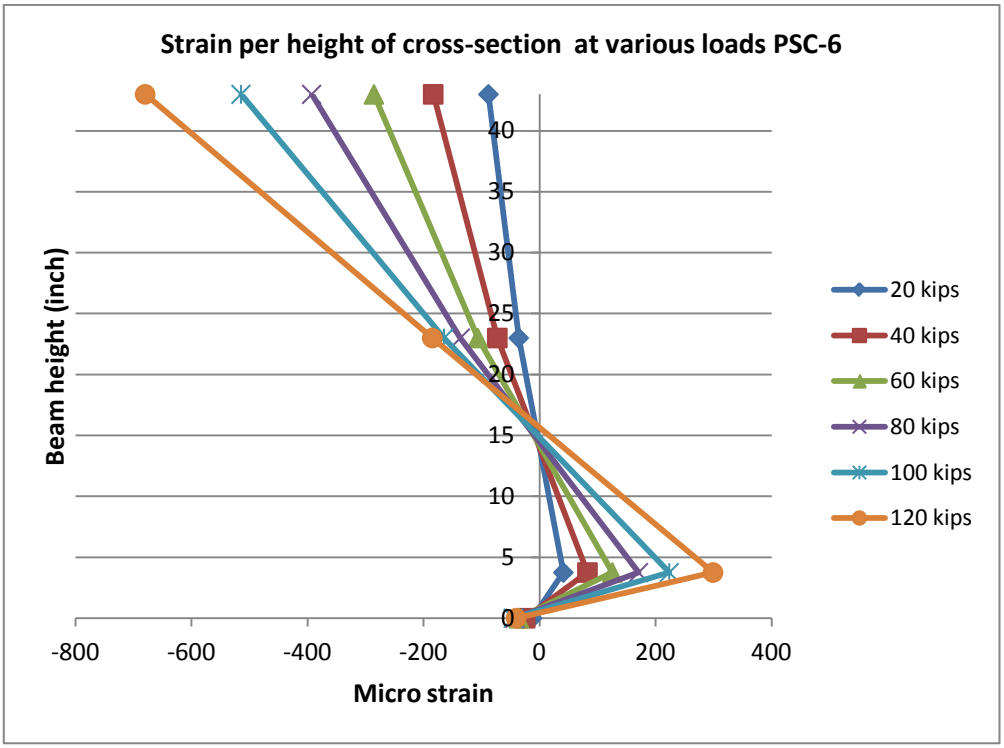

Figure 4-39: Strain development for PSC-6

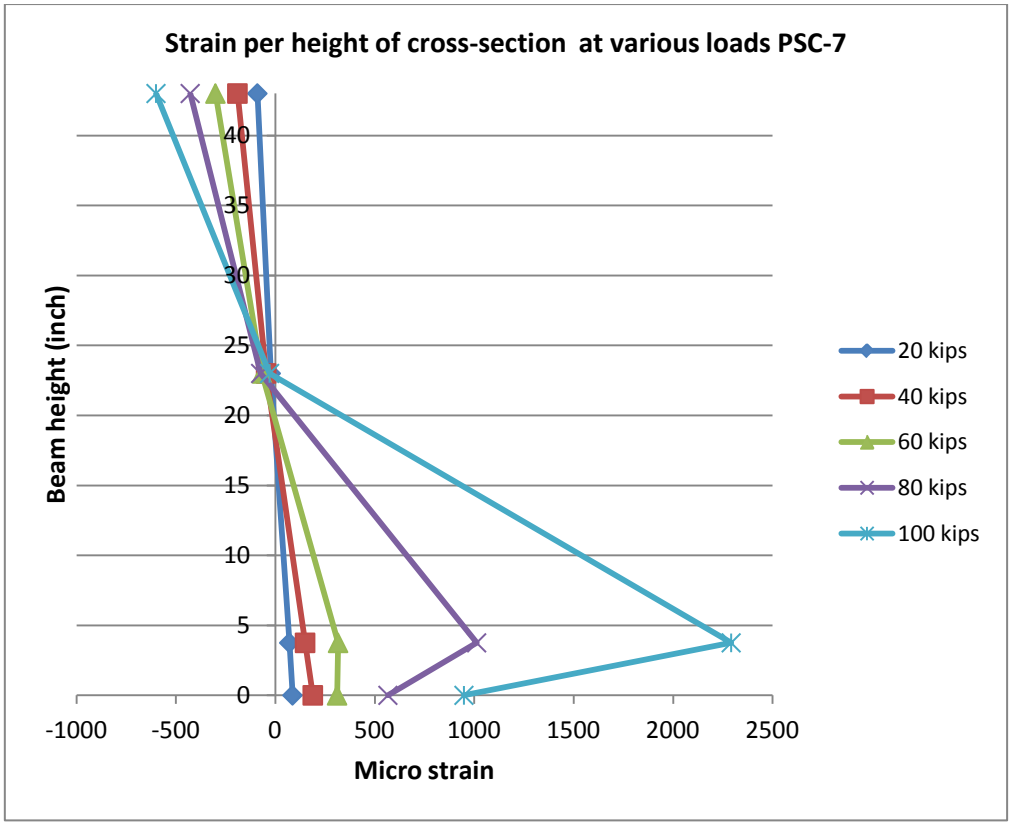

Figure 4-40: Strain development for PSC-7

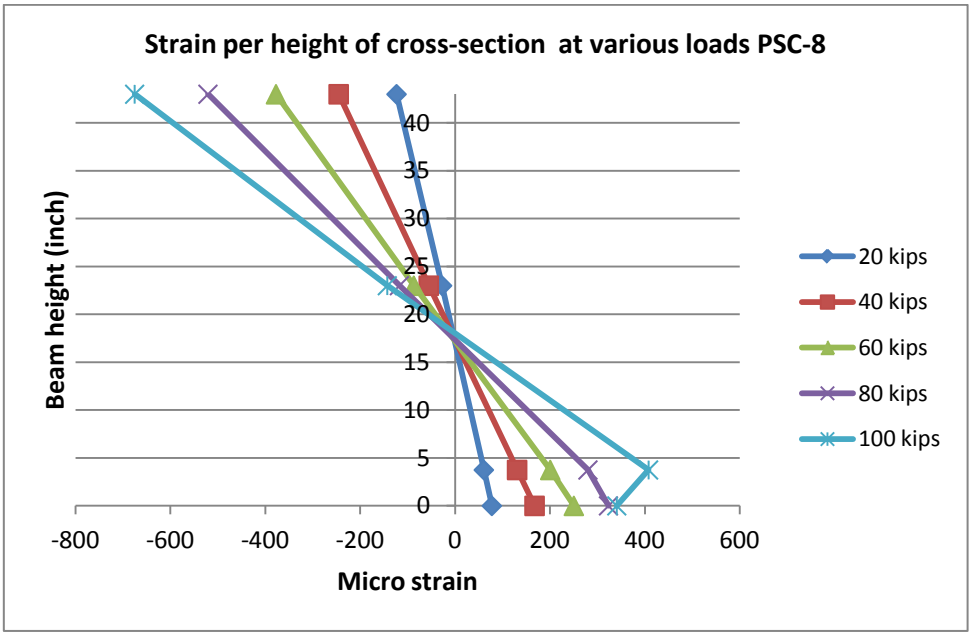

Figure 4-41: Strain development for PSC-8

4.4.3. FULL-SCALE FAILURE MODES

The failure modes for tested girders are presented in Figures 4-42 through 4-45.

Figure 4-42: CFRP pattern

Figure 4-43: Repair preparation

Figure 4-44: Failure of full-scale PSC girder by static testing

Figure 4-45: Failure of full-scale PSC girder by static testing

4.4.4. FULL-SCALE FATIGUE TESTING RESULTS

The fatigue load cycles were applied to three PSC girders. The girders survived the 2 million cycles of fatigue at 2 Hz with a load range of 20 to 45 kip for PSC-1 and PSC-2. However,

PSC-3 was subjected to a higher load range of 25 to 50 kip. All three beams showed no significant loss of stiffness or degradation. The beams were tested up to failure under static test as shown in the figures. They performed very well without any sign of degradation or weakness due to the fatigue loading.

The full-scale PSC girders were tested under the typical fatigue loading indicated in AASHTO LRFD Specifications for 2 million cycles of 2 and 3 Hz. The girder loading was cycled between the loads of 20 kip and 45 kip to simulate the dead load to the dead load plus factored fatigue live load. The last full-scale girder was loaded to a higher load range of 25 kip to 50 kip for 2 million cycles. The full-scale AASHTO II girders successfully survived the 2 million cycles of fatigue loading with a very small amount of residual deformation and little change in stiffness. Then, the girders were tested in flexure until failure under a four point loading arrangement. According to the test data, the fatigue procedures were:

- PSC-2 appears to have started at 1 Hz, then 0.5 Hz after 110,000 cycles, then 1 Hz after 282,000 cycles, then 2 Hz after 289,000 cycles
- PSC-1 started and stayed at 2 Hz
- PSC-3 started and stayed at 3 Hz

The fatigue loading procedures are shown in Table 4-14.

Table 4-14: Fatigue Testing Results for the Full-Scale AASHTO Type II Girders

Fatigue Testing Results for the Full-scale AASHTO type II Girders			
Full-scale Girder designations	Loading Level Ranges	Loading Rates	Number of Loading Cycles Completed
PSC-1	20 kip-45 kip	2Hz	2,000,000
PSC-2	20 kip-45 kip	started at 1 Hz, then 0.5 Hz after 110,000 cycles, then 1 Hz after 282,000 cycles, then 2 Hz after 289,000 cycles	2,000,000
PSC-3	25 kip-50 kip	3Hz	2,000,000

The fatigue testing results for full-scale girders are presented in Figure 4-46 through Figure 4-61.

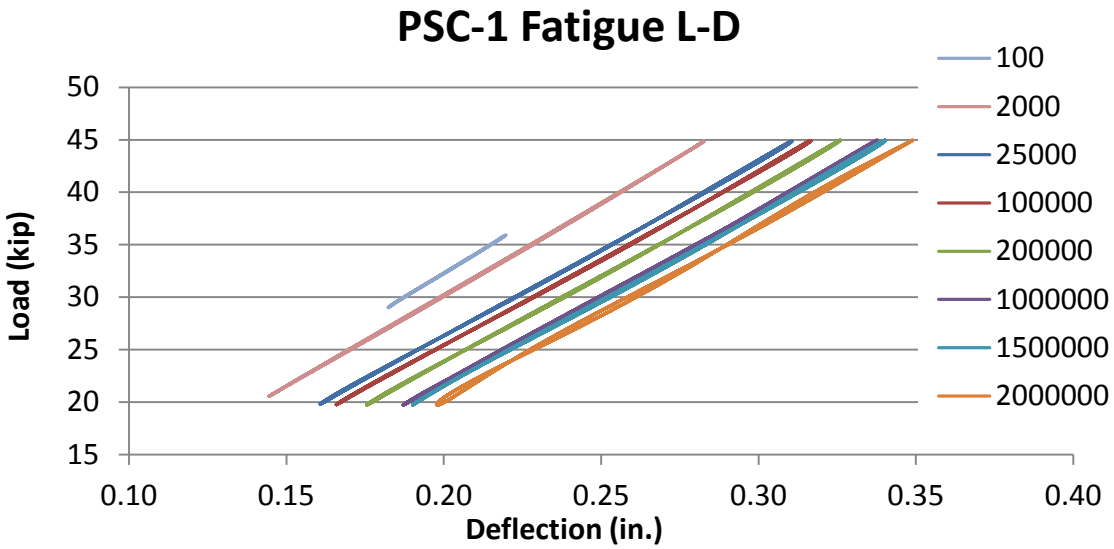

Figure 4-46: Fatigue load-deflection of full-scale girder PSC-1

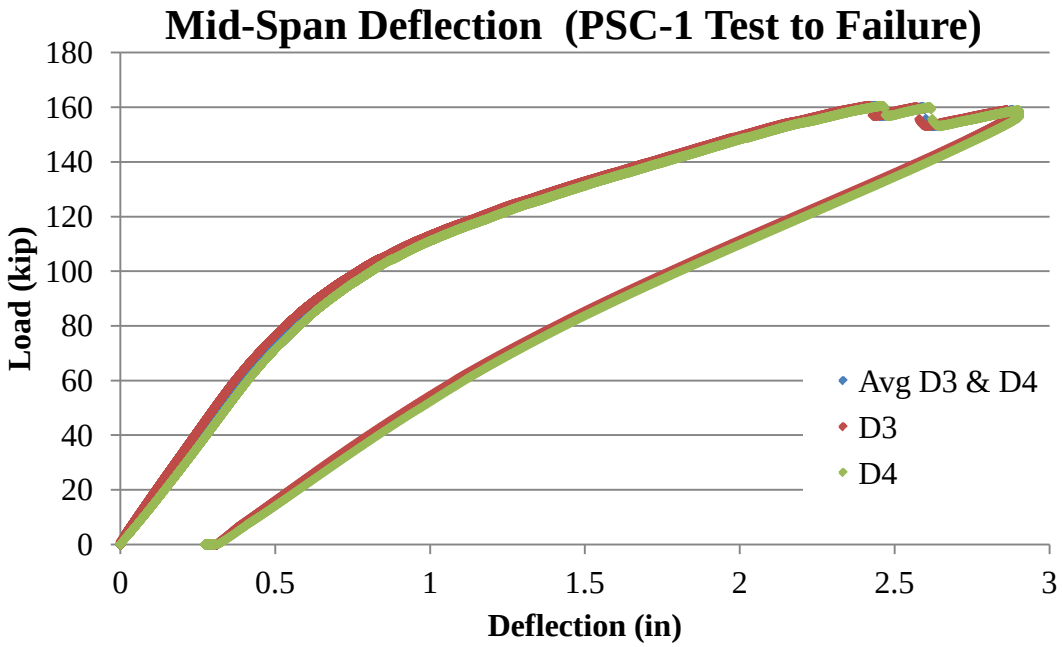

Figure 4-47: Load-deflection of PSC-1 at static failure after fatigue loading cycles

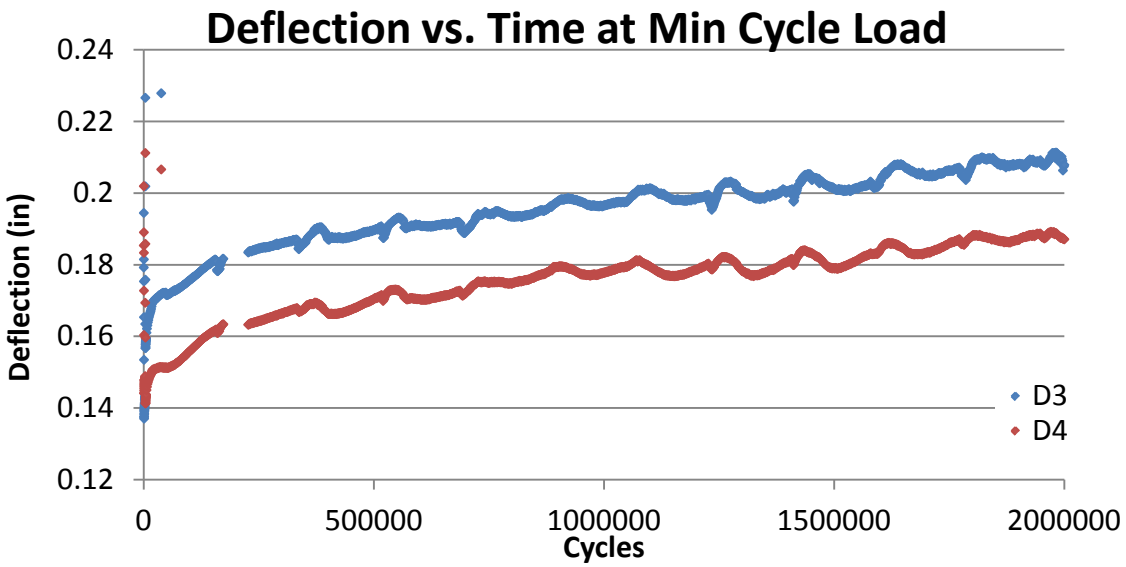

Figure 4-48: Deflection cycles of PSC-1 at min cycle load

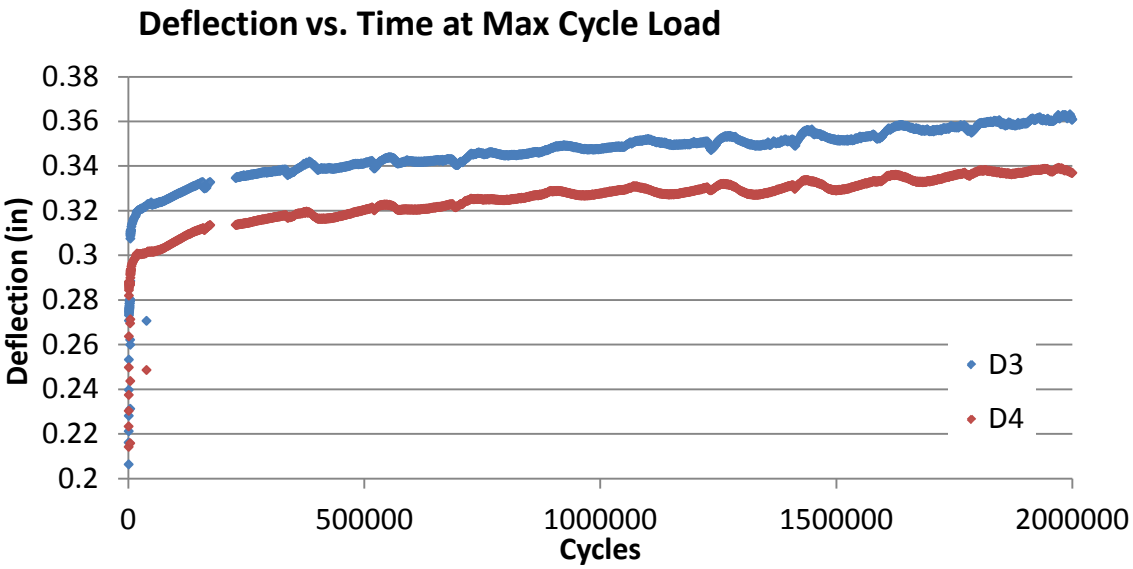

Figure 4-49: Deflection cycles of PSC-1 at max cycle load

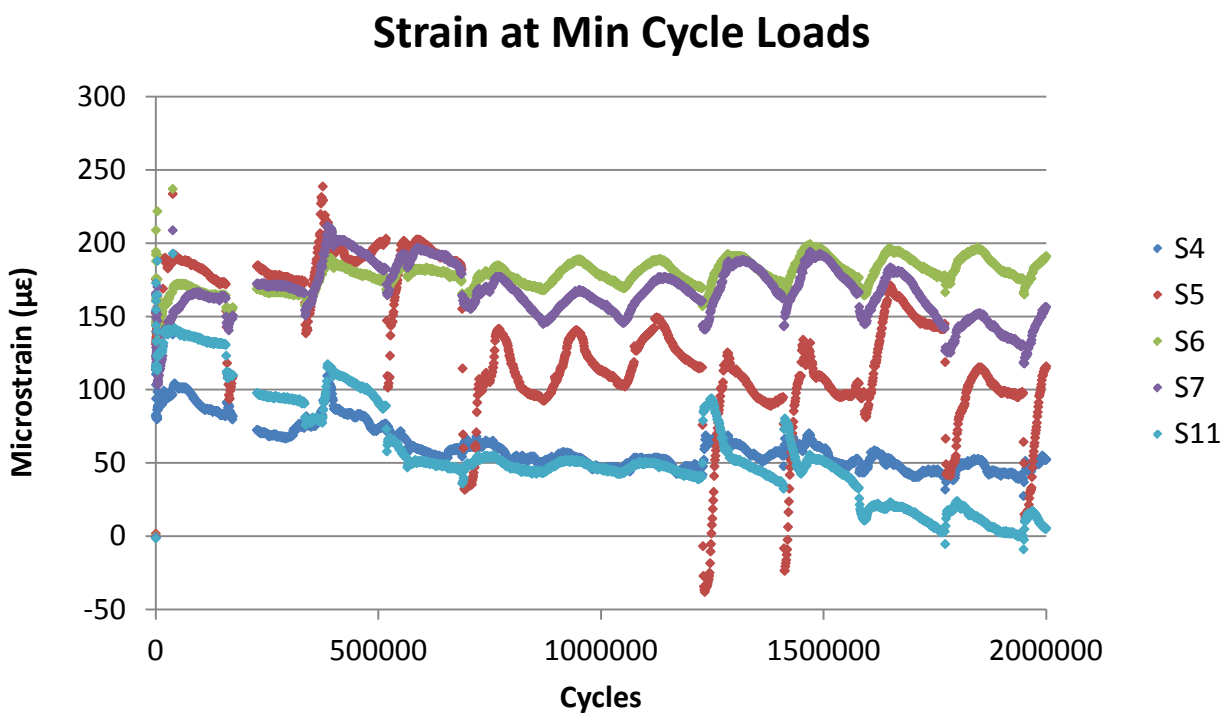

Figure 4-50: Strain cycles of PSC-1 at min cycle load

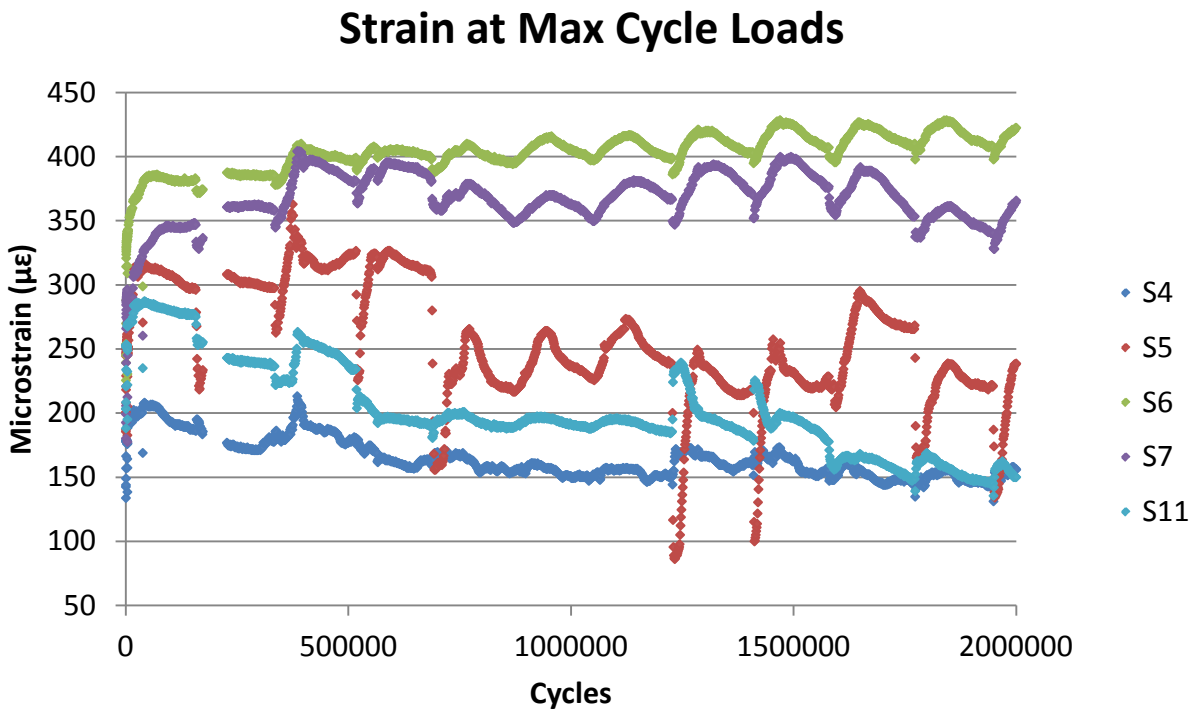

Figure 4-51: Strain cycles of PSC-1 at max cycle load

Notes of fatigue testing of Beam PSC-2:

- The engineers came into the office one morning and saw on the display that one of the deflection gauges was flat lining. It turned out that the shaft had gotten stuck at the highest point of the deflection rebound. They were not sure at what point over the weekend this occurred. They sprayed it with contact cleaner and got it working again about 7:49:20 am that morning. The gauge was D3 which is one of the two deflection gauges at mid-span. The one on the east side. It was usually the approach to take an average of D3 and D4 for center deflection.

- Another thing to take a note of is that D2 got stuck in a position that it was reading anything for a short time. That occurred somewhere around cycle count 762,240.Some spikes were noticed in the data for that gauge from working the shaft free so it would work properly again.

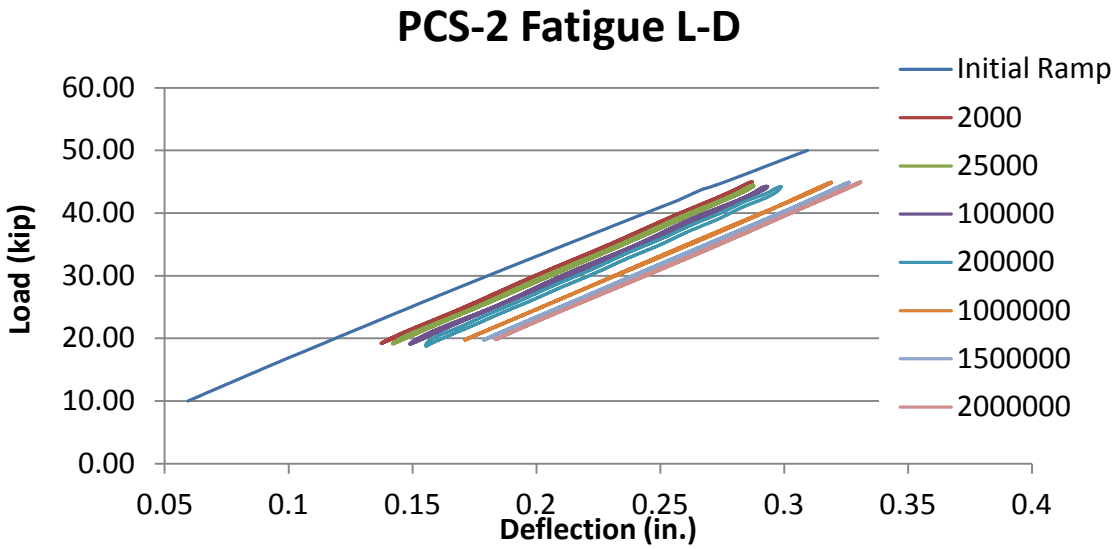

Figure 4-52: Fatigue load-deflection of full-scale girder PSC-2

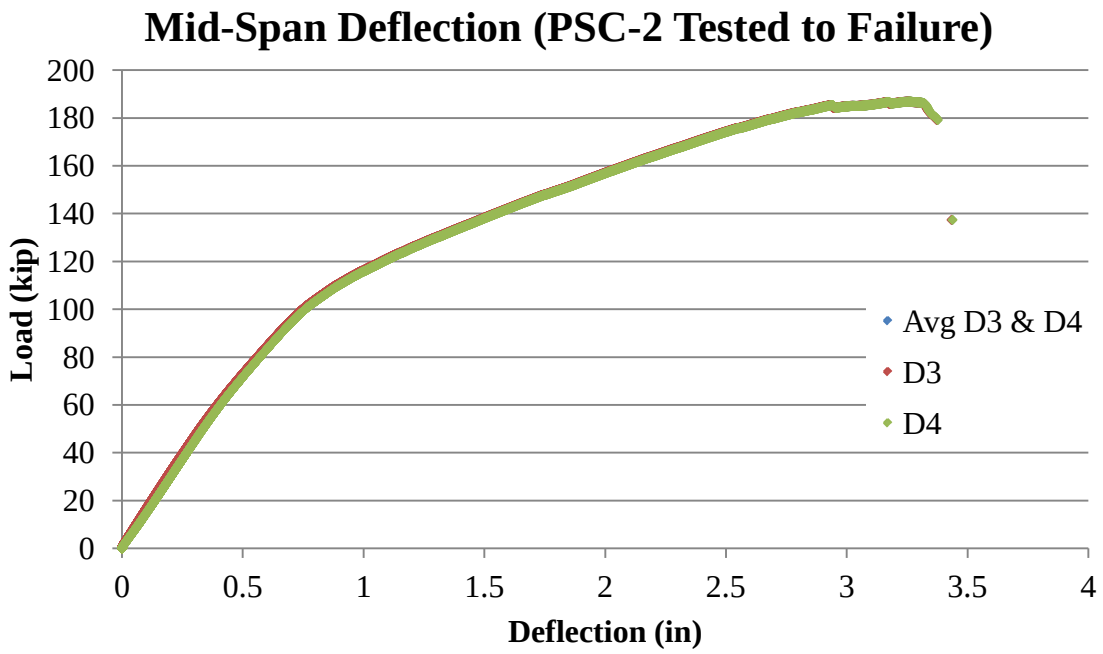

Figure 4-53: Load-deflection of PSC-2 at static failure after fatigue loading cycles

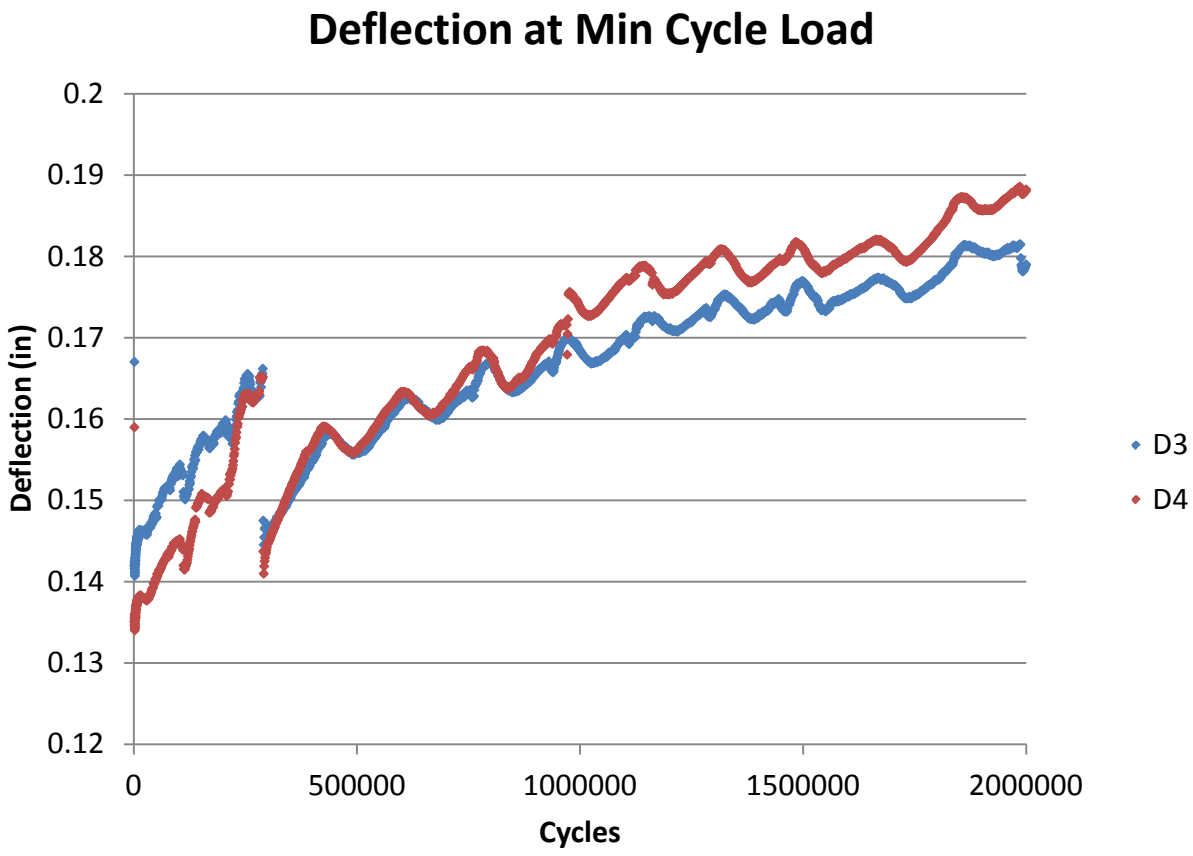

Figure 4-54: Deflection cycles of PSC-2 at min cycle load

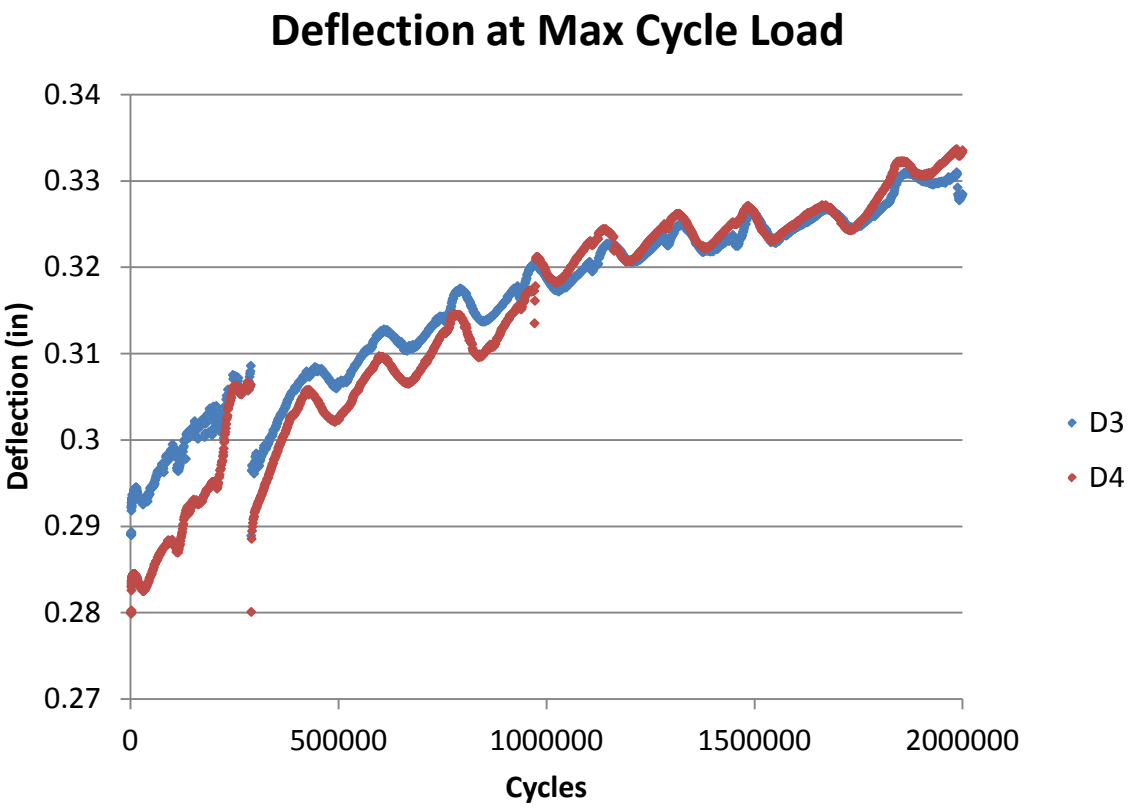

Figure 4-55: Deflection cycles of PSC-2 at max cycle load

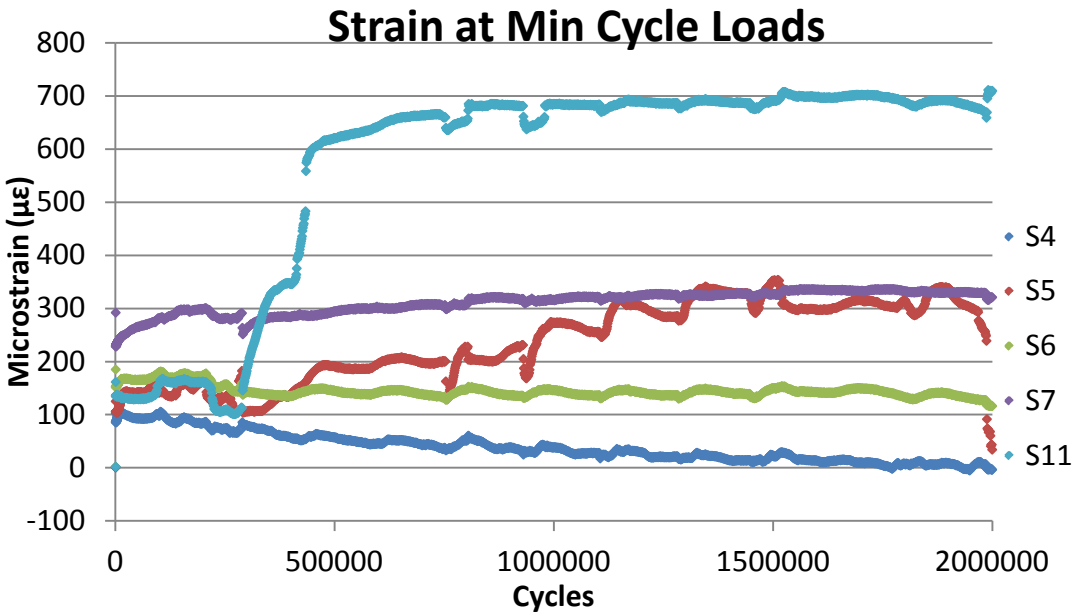

Figure 4-56: Strain cycles of PSC-2 at min cycle load

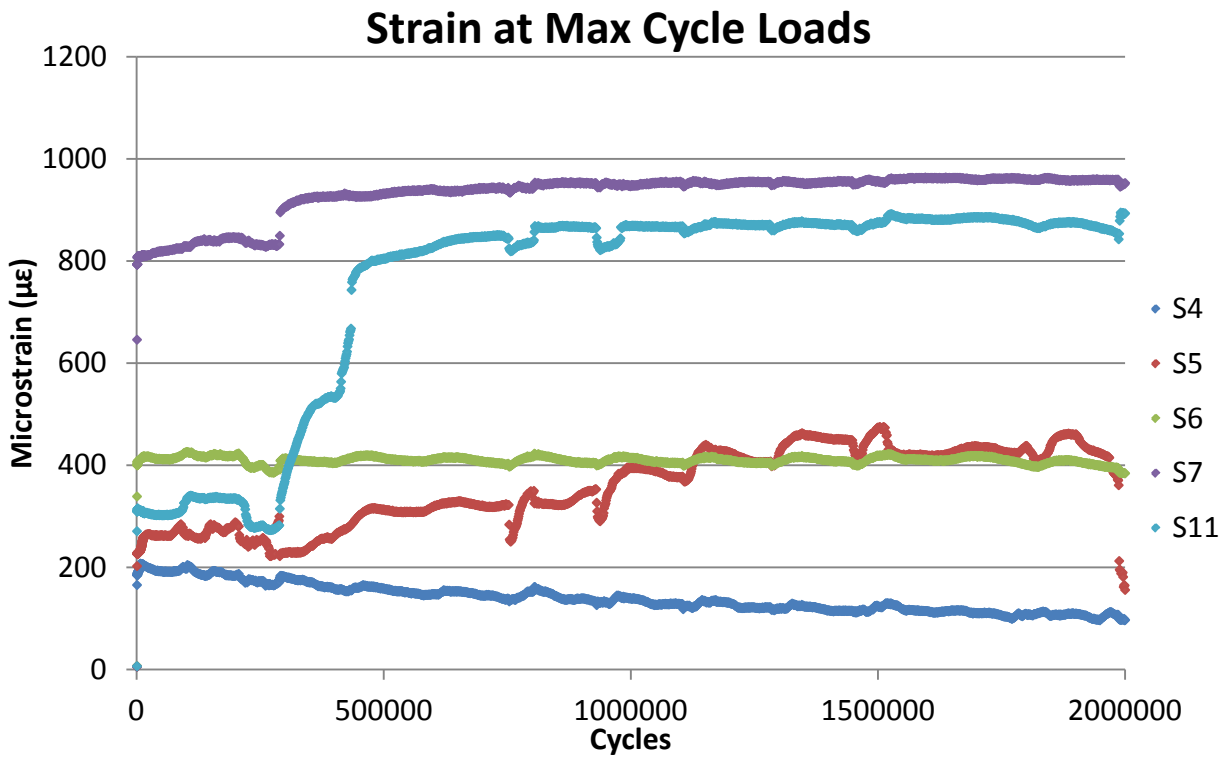

Figure 4-57: Strain cycles of PSC-2 at max cycle load

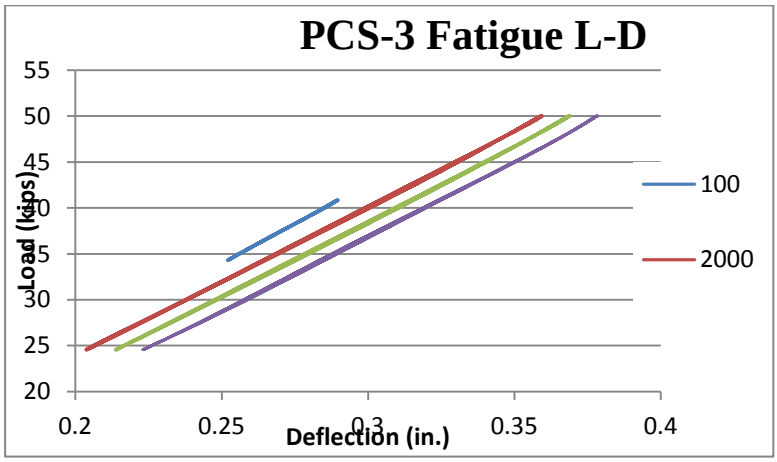

Figure 4-58: Fatigue Load-deflection of PSC-3

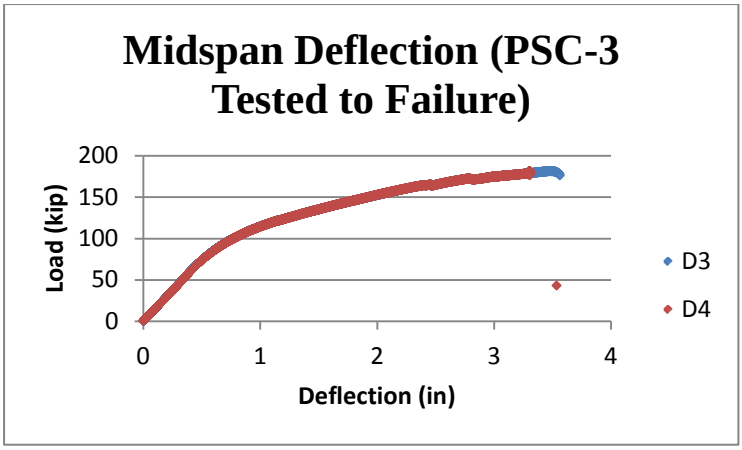

Figure 4-59: Load-deflection of PSC-3 at static failure after fatigue loading cycles

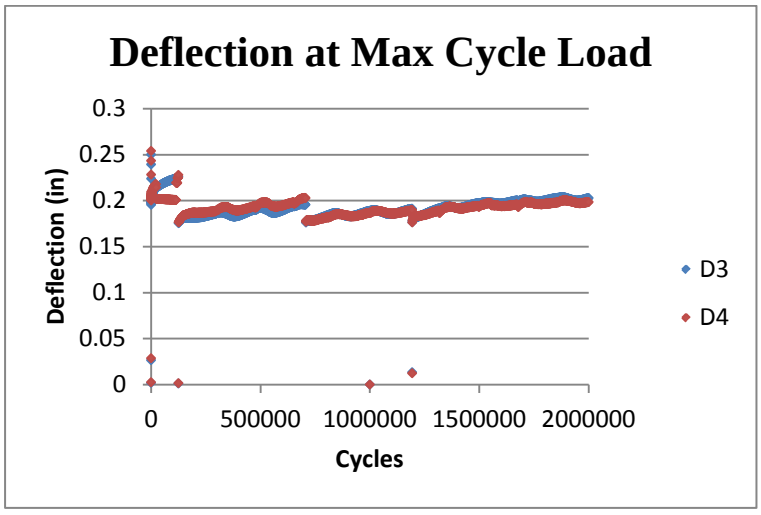

Figure 4-60: Deflection cycles of PSC-3 at max cycle load

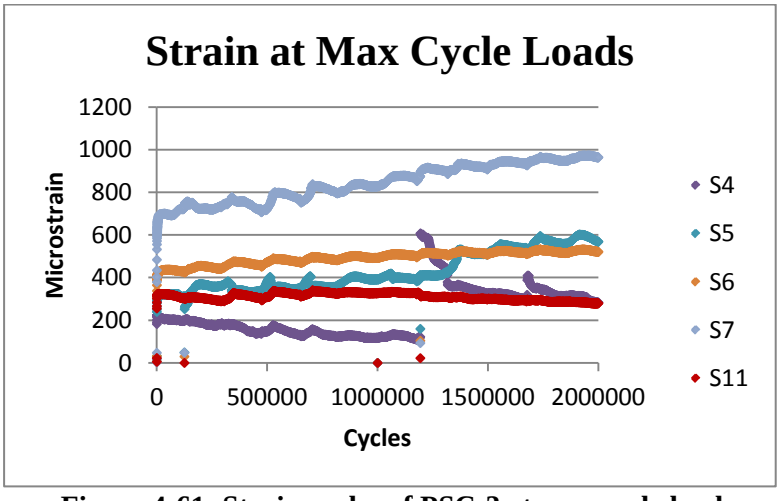

Figure 4-61: Strain cycles of PSC-3 at max cycle load

5. ANALYTICAL FINDINGS

5.1. METHOD OF ANALYSIS FOR RC BEAMS

The analysis of predicting the behaviors of RC beams strengthened with CFRP uses existing models from the ACI 440.2R-08 document and Charkas et al. 2003. The models are used to get theoretical values for maximum capacity and deflection, respectively.

5.1.1. CAPACITY PREDICTIONS

Similar to designing any structural member, the nominal moment multiplied by the phi value must be greater than the ultimate moment of the beam as seen in Eq. 1.

$$\varphi M_n \geq M_u \quad \textbf{Eq. (1)}$$

This method uses the theoretical strain at the level of the CFRP; Eq. 2 is used to calculate the theoretical strain developed at the soffit to initiate debonding.

$$\varepsilon_{fd} = 0.083\sqrt{\frac{f'_c}{nE_f t_f}} \leq 0.9\varepsilon_{fu} \quad \textbf{Eq. (2)}$$

The effective strain level in the CFRP reinforcement at the ultimate limit state controlled by concrete crushing can be found from Eq. 3.

$$\varepsilon_{fe} = \varepsilon_{cu}\left(\frac{d_f - c}{c}\right) - \varepsilon_{bi} < \varepsilon_{fd} \quad \textbf{Eq. (3)}$$

Where ε_{bi} is the initial strain and should be excluded from the strains in the FRP system. Unless all loads on the member, including the self-weight, are removed before installation, initial strains will exist.

$$f_{fe} = E_f \varepsilon_{fe} \quad \textbf{Eq. (4)}$$

Eq. 4 provides the effective maximum stress level in the CFRP that can be developed before flexural failure of the section, assuming perfectly elastic behavior. Then, based on the strain level in the CFRP reinforcements, the strain level in the non-prestressing steel can be found from Eq. 5.

$$\varepsilon_s = \left(\varepsilon_{fe} + \varepsilon_{bi}\right)\left(\frac{d-c}{d_f - c}\right) \quad \textbf{Eq. (5)}$$

The stress developed in the steel can then be determined from the strain level in the steel using its stress-strain curve as shown in Eq. 6.

$$f_s = E_s \varepsilon_s \leq f_y \quad \textbf{Eq. (6)}$$

Next, with the strain and stress levels in both the CFRP and the steel for the assumed neutral axis, the internal force equilibrium may be checked using Eq. 7.

$$c = \frac{A_s f_s + A_f f_{fe}}{\alpha_1 f'_c \beta_1 b} \quad \textbf{Eq. (7)}$$

Once an accurate neutral axis is found through iterative processes the nominal moment of the beam with CFRP applied can be calculated using Eq. 8.

$$M_n = A_s f_s \left(d \frac{\beta_1 c}{2}\right) + \psi_f A_f f_{fe} (h \frac{\beta_1 c}{2}) \quad \textbf{Eq. (8)}$$

The remaining two equations are related to predicting stresses in both the steel reinforcements and the CFRP reinforcements at service loads. Eq. 9 provides calculations for the stresses in the steel and Eq. 10 for calculations of stresses in the CFRP.

$$f_{s,s} = \frac{\left[M_s + \varepsilon_{bi} A_f E_f \left(d_f - \frac{kd}{3}\right)\right](d - kd) E_s}{A_s E_s \left(d - \frac{kd}{3}\right)(d - kd) + A_f E_f \left(d_f - \frac{kd}{3}\right)(d_f - kd)} \quad \textbf{Eq. (9)}$$

$$f_{f,s} = f_{s,s} \left(\frac{E_f}{E_s}\right) \frac{d_f - kd}{d - kd} - \varepsilon_{bi} E_f \quad \textbf{Eq. (10)}$$

5.1.2. DEFLECTION PREDICTION

Precracking stage

$$\Delta_{\text{mid-span}} = \frac{\phi_a}{24} (3L^2 - 4{L_a}^2 \quad \textbf{Eq. (11)}$$

$$\phi_a = \frac{PL_a}{2E_c I_g} \quad \textbf{Eq. (12)}$$

Post-cracking stage

$$L_g = \frac{2M_{cr}}{P} \quad \textbf{Eq. (13)}$$

$$\Delta_{\text{mid-span}} = \frac{\phi_a}{24} \left(3L^2 - 4{L_a}^2\right) + \frac{(L_g + L_a)}{6} (\phi_{cr} L_a - \phi_a L_g) \quad \textbf{Eq. (14)}$$

$$\phi_a = \frac{(\phi_y - \phi_{cr})(M_a - M_{cr})}{(M_y - M_{cr})} + \phi_{cr} M_a = \frac{PL_a}{2} \quad \textbf{Eq. (15)}$$

Post-yielding stage

$$L_y = \frac{2M_y}{P} \quad \textbf{Eq. (16)}$$

$$\Delta_{\text{mid-span}} = \frac{\phi_a}{24} \left(3L^2 - 4{L_a}^2\right) + \frac{L_y}{6} \left[\phi_{cr} \left(L_y + L_g\right) - \phi_a \left(L_y + L_a\right)\right]$$

$$+\frac{\phi_y(L_a-L_g)(L_a+L_y+L_g)}{6} \quad \textbf{Eq. (17)}$$

$$\phi_a = \frac{(M_a-M_y)(\phi_a-\phi_y)}{(M_a-M_y)} + \phi_y \quad \textbf{Eq. (18)}$$

5.2. METHOD OF ANALYSIS FOR PSC GIRDERS

5.2.1. CAPACITY PREDICTIONS

Similar to designing RC members the nominal moment multiplied by the phi value must be greater than the ultimate moment of the beam as seen in Eq. 19.

$$\varphi M_n \geq M_u \quad \textbf{Eq. (19)}$$

This method uses the theoretical strain at the level of the CFRP; Eq. 20 is used to calculate the theoretical strain developed at the soffit to initiate debonding.

$$\varepsilon_{fd} = 0.083\sqrt{\frac{f'_c}{nE_f t_f}} \leq 0.9\varepsilon_{fu} \quad \textbf{Eq. (20)}$$

The effective strain level in the CFRP reinforcement at the ultimate limit state controlled by concrete crushing can be found from Eq. 21.

$$\varepsilon_{fe} = \varepsilon_{cu}\left(\frac{d_f-c}{c}\right) - \varepsilon_{bi} < \varepsilon_{fd} \quad \textbf{Eq. (21)}$$

Where ε_{bi} is the initial strains and should be excluded from the strains in the FRP system. Unless all loads on the member, including the self-weight, are removed before installation, initial strains will exist.

If the ultimate limit state is controlled by prestressing steel rupture, the effective strain level in the CFRP can be found using Eq. 22;

$$\varepsilon_{fe} = \left(\varepsilon_{pu} - \varepsilon_{pi}\right)\left(\frac{d_f-c}{d_p-c}\right) - \varepsilon_{bi} \leq \varepsilon_{fd} \quad \textbf{Eq. (22)}$$

where ε_{pi} is found by evaluating Eq. 23.

$$\varepsilon_{pi} = \frac{P_e}{A_p E_p} + \frac{P_e}{A_c E_c}\left(1 + \frac{e^2}{r^2}\right) \quad \textbf{Eq. (23)}$$

$$f_{fe} = E_f \varepsilon_{fe} \quad \textbf{Eq. (24)}$$

Eq. 24 provides the effective maximum stress level in the CFRP that can be developed before failure of the section; assuming perfectly elastic behavior. Then, based on the strain level in the CFRP reinforcements, the strain level in the prestressing steel can be found from Eq. 25.

$$\varepsilon_{ps} = \varepsilon_{pe} + \frac{P_e}{A_c E_c}\left(1 + \frac{e^2}{r^2}\right) + \varepsilon_{pnet} \leq 0.035 \quad \textbf{Eq. (25)}$$

The net tensile strain εpnet can be calculated using Eq. 26 for concrete crushing failure modes and Eq. 27 for FRP rupture or debonding failure modes.

$$\varepsilon_{pnet} = 0.003\left(\frac{d_p - c}{c}\right) \quad \textbf{Eq. (26)}$$

$$\varepsilon_{pnet} = \left(\varepsilon_{fe} + \varepsilon_{bi}\right)\left(\frac{d_p - c}{d_f - c}\right) \quad \textbf{Eq. (27)}$$

Next, with the strain and stress levels in both the CFRP and the prestressing steel for the assumed neutral axis, the internal force equilibrium may be checked using Eq. 28.

$$c = \frac{A_p f_{ps} + A_f f_{fe}}{\alpha_1 f'_c \beta_1 b} \quad \textbf{Eq. (28)}$$

Once an accurate neutral axis is found through iterative processes the nominal moment of the beam with CFRP applied can be calculated using Eq. 29.

$$M_n = A_p f_{ps}\left(d_p \frac{\beta_1 c}{2}\right) + \psi_f A_f f_{fe}(d_f - \frac{\beta_1 c}{2}) \quad \textbf{Eq. (29)}$$

The remaining two equations are related to predicting stresses or strains in both the prestressing steel reinforcements and the CFRP reinforcements at service loads. Eq. 30 provides calculations for the strains in the steel and Eq. 31 for calculations of stresses in the CFRP.

$$\varepsilon_{pnet,s} = \frac{M_s e}{E_c I_g} \quad \text{for uncracked condition or} \quad \varepsilon_{pnet,s} = \frac{M_{snet} e}{E_c I_{cr}} \quad \text{for cracked} \quad \textbf{Eq. (30)}$$

$$f_{f,s} = \left(\frac{E_f}{E_s}\right)\frac{M_s y_b}{I} - \varepsilon_{bi} E_f \quad \textbf{Eq. (31)}$$

5.3. PRESENTATION OF RESULTS

5.3.1. REINFORCED CONCRETE RESULTS

The predictive analysis and percent differences from predictions for RC beams of the first set and the second set are presented in Table 5-1 and Table 5-2, respectively.

Table 5-1: Predictive Analysis and Percent Differences from Predictions for RC Beams (First Set)

Percent increase or decrease from predicted values		
Beam designation	Loads	Deflections
	predicted = 18.18 kip	predicted: 0.675 in
TB-5	14.25%	1.01%
TB-6	8.39%	28.02%
TB-7	8.81%	51.17%
TB-8	2.92%	33.98%
TB-9	8.45%	30.28%
TB-10	5.82%	24.84%
TB-11	3.77%	37.97%
TB-12	8.04%	55.60%
TB-13	1.27%	10.86%
TB-14	1.25%	27.46%
TB-15	2.77%	32.00%

Table 5-2: Predictive Analysis and Percent Differences from Predictions for RC Beams (Second Set)

Percent increase or decrease from predicted values		
Beam designation	LOADS:	DEFLECTIONS:
	predicted = 22.67 kip	predicted: 0.846 in
JB-5	6.41%	25.50%
JB-6	0.63%	20.66%
JB-7	25.72%	34.56%
JB-8	18.56%	37.11%
JB-9	20.19%	82.71%
JB-10	1.04%	18.86%
JB-11	42.77%	26.26%
JB-12	41.10%	9.09%
JB-13	22.44%	9.09%
JB-14	20.57%	13.25%
JB-15	8.29%	42.38%
JB-16	5.07%	1.59%
JB-17	2.63%	18.00%
JB-18	4.66%	16.07%
JB-19	1.54%	2.49%

5.3.2. HALF-SCALE PRESTRESSED RESULTS

Table 5-3 presents the predictive analysis ad percent difference from prediction for PS half-scale girders.

Table 5-3: Predictive Analysis and Percent Differences from Predictions for PS girders

Girder designation	Test Max Load (kip)	Predicted Max Load (kip)	% increase or decrease of test load compared to prediction
PS-1	75.87	81.9	decrease 7.3%
PS-2	61.88	66.5	decrease 6.9%
PS-3	90.14	79.7	increase 13%
PS-4	84.75	79.7	increase 6.3%
PS-5	78.92	79.7	decrease 0.9%
PS-6	100.91	85.6	increase 17.8%
PS-7	104.42	85.6	increase 21.9%
PS-8	99.16	85.6	increase 15.8%
PS-9	77.26	79.7	decrease 3.1%
PS-10	87.68	79.7	increase 10.0%

5.3.3. FULL-SCALE PRESTRESSED RESULTS

Table 5-4 presents the predictive analysis ad percent difference from prediction for PSC full-scale girders.

Table 5-4: Predictive Analysis and Percent Differences from Predictions for PSC Girders

Girder designation	Tested Max Load (kip)	Tested Max Deflection (in)	Predicted Max Load (kip)	% increase or decrease compared to prediction
Fatigue Loaded Girders Ultimate Failure Test after Cycling				
PSC-1	160.52	2.44	188.43	14.8% (Decrease)
PSC-2	186.88	3.26	198.89	6.0% (Decrease)
PSC-3	181.61	3.39	207.57	12.5% (Decrease)
Statically Tested of Girders (Predicted Cracking Load 111.65 kip)				
PSC-4	166.83	2.40	164.52	1.4% (Increase)
PSC-5	205.37	2.58	212.53	3.4% (Decrease)
PSC-6	214.77	3.42	234.99	8.6% (Decrease)
PSC-7	206.32	3.03	198.89	3.7% (Increase)
PSC-8	185.22	2.99	187.97	1.5% (Decrease)

6. CONCLUSIONS

6.1. REINFORCED CONCRETE BEAMS

1. The use of CFRP laminates in repair of laterally damaged beams increases load-carrying capacity for the beams while reducing ductility.

2. The repaired beams with CFRP longitudinal strip without transverse U-wrappings result in premature CFRP debonding.

3. A significant increase of load-carrying capacity of about 68% can be achieved by using the CFRP longitudinal soffit laminates combined with U-wrappings.

4. The ACI 440.2R-08 document provides adequate to conservative capacity estimations for repair designs, provided that transverse U-wrappings are used appropriately to mitigate early debonding failures.

5. The use of CFRP laminates with different lengths at the soffit indicated that the longitudinal CFRP reinforcement should extend as far as possible within the span and should terminate no closer than specified in the ACI 440.2R-08 for development length requirements.

6. In case the CFRP shear enhancements are not needed, the configuration of transverse U-wrappings with spacing between them has shown to provide similar flexural benefits when compared to a fully wrapped beam.

7. Evenly spaced transverse U-wrappings provide efficient configuration for CFRP flexural enhancement repairs to mitigate debonding.

8. Without consideration for shear enhancements, the optimum spacing for transverse anchoring is theorized to be a distance of two thirds to twice the height of the beam. Yet, the recommendation is to keep the spacing between the transverse U-wrapping to one half to two third the height of the beam.

9. When repairing laterally damaged beams having a loss of steel reinforcements, it is necessary to cover the damaged section with transverse and longitudinal strips to reduce the crack opening and propagation in the critical region, which initiates early debonding.

6.2. HALF-SCALE PRESTRESSED CONCRETE GIRDERS

1. Impact damaged AASHTO Type II girders with ruptured strands and loss of concrete section can be successfully repaired using externally bonded CFRP laminates to restore the original flexural capacity.

2. The longitudinal CFRP strips applied to the girder soffit along with U-wrapping instead of full wrap proved to be an excellent repair alternative for damaged girders.

3. The use of CFRP laminates in repair of laterally damaged girders reduces deflection and

increases load-carrying capacity for the girders.

4. A significant increase of girders' load-carrying capacity of about…% can be achieved by using the CFRP longitudinal soffit laminates combined with U-wrappings.

5. Different U-wrapping configurations with varied spacing have proven to significantly enhance the flexural capacity of damaged prestressed concrete girders and prevent premature debonding of longitudinal laminates.

6. A comparison between the failure load of a control girder (with cut strand and unstrengthened with CFRP) and repaired girders with 2 layers of CFRP shows that CFRP repair enhanced the flexural capacity by 27.53% to 45.66%.

7. For repaired girders with 3 layers of CFRP, increases in the flexural capacity were reported to range from 60.24% to 68.74% when compared to control girder (with cut strand and unstrengthened with CFRP).

8. An increase in the failure load of 24.85% to 41.69% was observed for the fully CFRP wrapped repaired girders compared to the unstrengthened control girder.

9. Proper CFRP repair design in terms of the number of CFRP longitudinal layers and U-wrapping spacing could result in obtaining significant enhancement for the capacity and desired failure modes for the repaired girders.

10. Favorable failure modes of the repaired girders can be maintained using a CFRP repair configuration utilizing spacing between the U-wrappings to prevent undesirable modes of failure such as debonding of the longitudinal CFRP strips from the girder concrete soffit. If shear improvement are not needed, spacing close to that of the depth of the composite girder can be applied for the U-wrap configuration design to constitute a safe CFRP repair.

11. The optimum spacing for transverse anchoring is determined to be a distance of one half to two thirds the height of the girder.

12. Debonding of some U-wrappings was experienced at high loading levels after restoring the girders' virgin flexural capacity. Therefore, it is recommended that another CFRP strip be applied in the longitudinal direction at the top of the girder web to anchor the top end of the U-wrappings. That will mitigate premature failure of girders.

13. The repaired CFRP girders experienced a more brittle failure than control undamaged beams having no CFRP. That requires caution in the design.

14. Test results show that with proper detailing, CFRP systems can be designed to restore the flexural capacity and maintain the desired failure mode of concrete crushing in the compressive zone.

15. When repairing laterally damaged girders having a loss of concrete and ruptured prestressing strands, it is necessary to cover the damaged section with transverse and longitudinal strips to restrain the crack opening and propagation in the critical region,

which initiates early debonding.

6.3. FULL-SCALE PRESTRESSED CONCLUSIONS

1. The original failure mode of a prestressed bridge girder can be maintained when utilizing non-prestressed fabric CFRP repair applications.

2. The original capacity of a damaged bridge girder can be restored and enhanced using non-prestressed fabric CFRP repair applications.

3. Damaged prestressed bridge girders repaired using non-prestressed fabric CFRP laminates suffer little degradation even after more than two million cycles of fatigue loading that simulated service load conditions.

4. The longitudinal CFRP laminate applied to the girder soffit along with U-wrapping anchored with a longitudinal CFRP strip at the top ends of U-wrappings proved to be an excellent repair alternative for damaged girders.

5. Evenly spaced transverse U-wrappings provide very efficient configuration for CFRP flexural enhancement repairs to mitigate debonding.

6. The CFRP repair restored the lost flexural capacity of the damaged girder. The CFRP repair also enhanced the flexural capacity for the repaired girders by a range of 23% to 28% compared to that of the control damaged girders.

7. The CFRP repair not only restored the lost flexural capacity of the damaged girders but also enhanced their flexural strength than that for undamaged control girder by about 10% to 16%.

8. Without consideration for shear enhancements, the optimum spacing for transverse anchoring is recommended to be between a distance of one half to two thirds the height of the AASHTO girder (or one half the height of the entire composite cross-section).

9. When repairing laterally damaged girders having a loss of concrete and ruptured prestressing strands, it is necessary to cover the damaged section with transverse and longitudinal strips to restrain the crack opening and propagation in the critical region which initiates early debonding.

10. Proper CFRP repair design in terms of the number of CFRP longitudinal layers and U-wrapping spacing could result in obtaining significant enhancement for the capacity and desired failure modes for the repaired girders.

11. Favorable failure modes of the repaired girders can be maintained using a CFRP repair configuration utilizing spacing between the U-wrappings to prevent undesirable modes of failure such as debonding of the longitudinal CFRP strips from the girder concrete soffit.

6.4. CONCLUSIONS FOR PROCEDURE OF DESIGN PRACTICE

The following sets of procedures are derived from considerations provided by the ACI

440.2R-08 and have been confirmed or revised based on this research project or the previously confirmed research conducted by others. These following procedures are provided specifically for the repair of laterally damaged concrete bridge girders repaired with non-prestressed unidirectional CFRP fabric.

6.4.1. CFRP REPAIR DESIGN CALCULATIONS

1. The first action to be taken is to evaluate the structural member affected by the lateral damage. The evaluation should document the existing dimensions of the structural members; the location, and size of cracks and spalls; the location and extent of any corrosion of reinforcing steel; the presence of any active corrosion; the quality and location of existing reinforcing steel; the in-place compressive strength of the concrete; and the soundness of the concrete, particularly the concrete cover in all areas where the FRP system is going to be bonded to the concrete.

2. Next, use the information which was gathered from the evaluation in step 1 and verify that a non-prestressed CFRP repair system is applicable to the level of damage sustained. Where the damage levels may include *Minor Damage, Moderate Damage, Severe Damage*, or *Severe I*; provided that the loss of prestressing force is less than 25% where the levels of damage are defined as:

Minor Damage: defined as; concrete with shallow spalls, nicks and cracks, scraps and some efflorescence, rust or water stains. Damage at this level does not affect a member's capacity. Repairs are for aesthetic or preventative purposes.

Moderate Damage: will include; larger cracks and sufficient spalling or loss of concrete to expose strands. Moderate damage does not affect a member's capacity. Repairs are intended to prevent further deterioration.

Severe Damage: is classified as; any damage requiring structural repairs. Typical damage at this level includes significant cracking and spalling, corrosion and exposed and broken strands.

Severe I: the experienced damage requires structural repair that can be affected using a non-prestressed or post-tensioned method. This may be considered as repair to affect the strength (or ultimate) limit state.

3. If a non-prestressed repair system is applicable from step 2, check that the damaged member's existing strength is sufficient to resist a level of load described by ACI440.2R-08 equation 9-1 or if the structure requires a fire rating it must satisfy ACI440.2R-08 equation 9-2.

$$(\phi R_n)_{existing} \geq (1.1S_{DL} + 0.75S_{LL})_{new} \qquad \text{(ACI Eq. 9-1)}$$

Where $(\phi R_n)_{existing}$ is the existing strength of the damaged structural member. Similarly, S_{DL} and S_{LL} are the dead and live loads expected on the repaired structural member.

$$R_n \geq S_{DL} + S_{LL} \qquad \text{(ACI Eq. 9-2)}$$

Where Rn is the nominal resistance of a member at an elevated temperature as determined in ACI 216R and the loads are as previously defined.

4. If appropriate equation in step 3 is satisfied, open affiliated Excel spreadsheet and enter dimensional values and material properties in the yellow cells of the input tab. A display of the input tab is shown below in figure 6-1

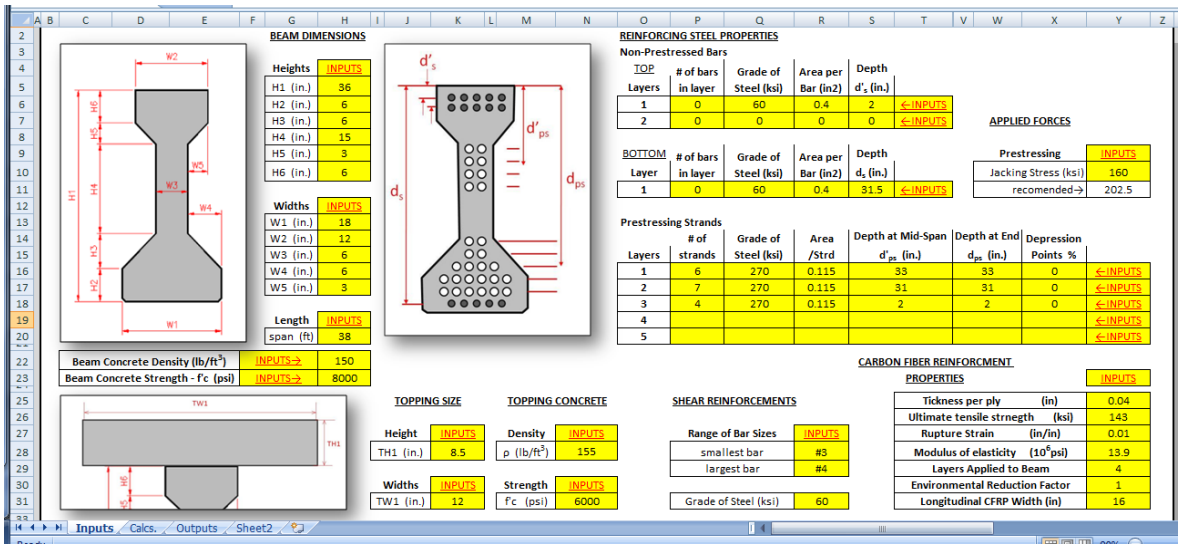

Figure 6-1: Display of input tab from affiliated Excel spreadsheet

5. After entering all values required for input tab check the output tab and verify that the calculated ultimate moment is at least equivalent to that of the girder of interest prior to damage. If calculated ultimate moment is not sufficient return to input page and increase the width or number of layers of the CFRP, if ultimate moment exceeds that of the undamaged girder in question return to input page and decrease the same values. Repeat until most desirable width and number of layers is selected. Figure 6-2 shows output tab of Excel spreadsheet.

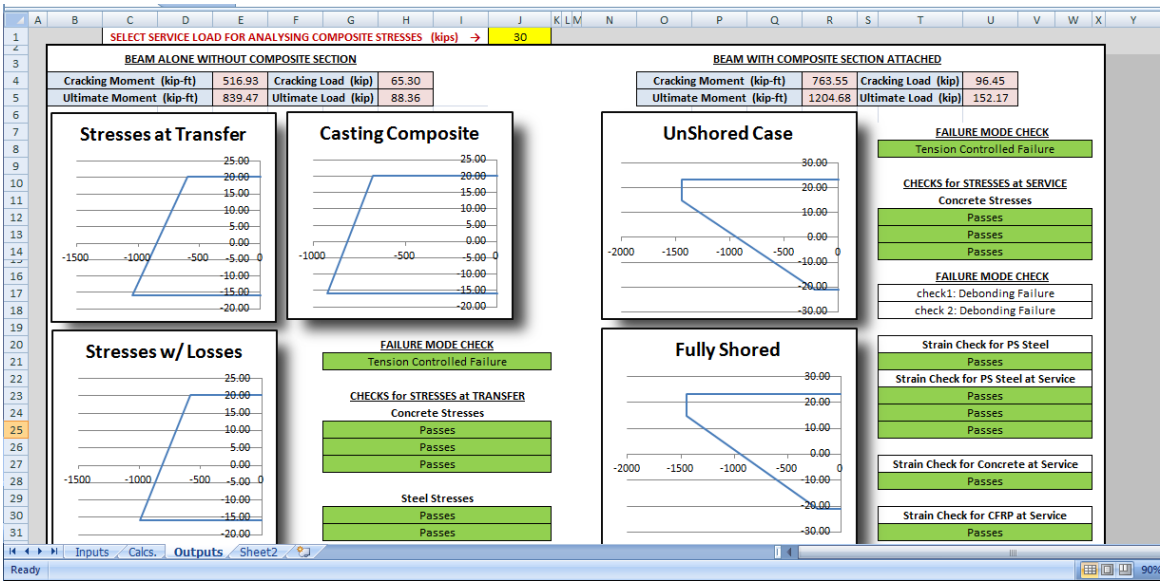

Figure 6-2: Display of output tab from affiliated Excel spreadsheet

6. After the desired level of strengthening is established with the use of the provided Excel spreadsheet determine the maximum spacings of the transverse U-wrapping by multiplying the height of the girder plus the composite deck by ½ if capacity enhancements are not required.

7. If the desire of the repair is also to provide strength enhancements for expected increased loading, follow the calculations and procedures listed in chapter 12 of the ACI440.2R-08 for shear design to establish the maximum spacings of the transverse U-wrappings using the enhanced properties of the structural member. (the smaller value of step 6 and 7 should be used if step 7 is applicable)

8. Determine the minimum length between transverse U-wrappings by computing the critical length related to the bond capacity in ACI equation 13-2.

$$l_{df} = 0.057\sqrt{\frac{nE_f t_f}{\sqrt{f'c}}} \qquad \text{(ACI Eq. 13-2)}$$

$$l_{df} = \sqrt{\frac{nE_f t_f}{\sqrt{f'c}}}$$

Where l_{df} is the critical length, n is the number of layers, E_f is the modulus of elasticity of the CFRP, t_f is the thickness of the fibers, and $f'c$ is the compressive strength of the concrete girder.

9. If step 7 was applicable and the maximum spacings are less than the width of the CFRP U-wrappings or the value calculated in step 8 a fully wrapped arrangements of the transverse layers is recommended.

6.4.2. IMPLEMENTING THE CALCULATED DESIGN VALUES

1. Provide the first longitudinal layer extending the entire span of the damaged girder's soffit and each subsequent layer provided should be one foot shorter than the previous until the desired number of layers determined in step 5 of section 6.3.1. is reached.

2. Provide longitudinal layers on the bottom flange of the girder approximately equal to 60% of the beams span centered over the damaged area. If the number of layers used on the girder's soffit is greater than 1 then 2 layers shall be used on the bottom flanges otherwise only 1 is required. Additional layers should be one foot shorter than the previous as in step 1.

3. Provide one longitudinal layer on the web of the girder over the damaged area. This layer could be as short as a few feet but must be greater than calculated length. The intention is

to cover any area affected by the damage to prevent crack propagations in the critical region.

4. Provide overlapping transverse U-wrappings covering the damaged area of the girder and provide spaced U-wrappings between the damaged area and the supported ends of the girder. The spacings should be adjusted between the minimum and maximum lengths determined so that each longitudinal layer terminates underneath one of the transverse U-wrappings. The number of layers provided for each transverse section should follow the guidelines in the ACI 440.2R-08 and the NCHRP Report 514. The additional layers of U-wrapping do not change sizes and they should extend at least up to the top of the web.

6.4.3. APPLYING THE CFRP REPAIR

1. Surface Preparation: In general, the surface must be clean, dry and free of protrusions or cavities, which may cause voids behind the composite. Discontinuous wrapping schematics typically require a light sandblasting, grinding or other approved methods to prepare for bonding. Sharp corners should be ground down to a radius of approximately .5 inches.

2. Mixing: Pour the contents of component B into the pail of component A. Mix thoroughly for five minutes with a low speed mixer at 400-600 RPM until uniformly blended. If material is too thick, heat unmixed components by placing containers in hot tap water or sunlight until desired viscosity is achieved. The epoxy may also be thickened in the field to the desired consistency by adding fumed silica.

3. Application: Apply epoxy to surface as a primer coat. Then, uniformly saturate the fabric by hand and apply to the surface. Next, using a roller or a trowel, press the fabric to surface and work out any air voids or pockets of thick epoxy.

4. Quality Control: If voids behind the cured CFRP laminates are present, use the same epoxy and inject it into voids using traditional injection methods.

5. If a more detailed application procedure is required it is recommended to refer to section 3.3 of this document, instructions provided by the manufacturer of the product being used, or the information in the ACI440.2R-08.

7. DELIVERABLES

7.1. PRACTITIONER SUMMARY

This document was prepared to provide the basic information needed to identify the most suitable CFRP configuration for prestressed concrete (PSC) girder repair. The document ultimately presents some optimum repair designs and discusses their benefits and limitations; which depend on the level of damage sustained by the girder and the desired intentions for recovered or enhanced capacities. The included information describes how to evaluate the level of damage, how to determine if CFRP repair applications are appropriate, how to determine/design the most suitable repair configuration, how to apply the determined CFRP repair, and how to maintain it.

The included provisions were manly adopted and derived from four primary sources, the ACI 440.2R-08, the NCHRP Report 514, the FDOT Structural Manual, and the associated research involving non-prestressed unidirectional CFRP fabric composites.

7.2. DAMAGE / CONDITION ASSESSMENT

After being notified of a damaged bridge girder it is first essential to thoroughly evaluate the structural member affected. The evaluation should document the existing dimensions of the structural members; the location and size of cracks and spalls; the location and extent of any corrosion of reinforcing steel; the presence of any active corrosion; the quality and location of existing reinforcing steel; the in-place compressive strength of the concrete; and the soundness of the concrete (particularly the concrete cover). The inspector evaluating the member should also note the cause of the damage (overloading, overheight collision, environmental hazards, etc...). The evaluated damaged condition of the PSC bridge girder should then be classified as Minor, Moderate, or any class of Severe as they are defined in Table 7-1.

Table 7-1: Descriptions of Common Damages and Their Associated Classifications

Damage Classification	Description of Sustained Damage Sufficient for the Association with the Classification Designation
Minor	Concrete with shallow spalls, nicks and cracks, scraps and some efflorescence, rust or water stains. Damage at this level does not affect a member's capacity. Repairs are for aesthetic or preventative purposes.
Moderate	Concrete will have larger cracks and sufficient spalling or loss of concrete to expose strands. Moderate damage does not affect a member's capacity. Repairs are intended to prevent further deterioration.
Severe	Any damage requiring structural repairs. Typical damage at this level includes significant cracking and spalling, corrosion and exposed or broken strands.
Severe I	The experienced damage requires structural repair that can be affected using a non-prestressed or post-tensioned method. This may be considered as repair to affect the strength (or ultimate) limit state.
Severe II	The experienced damage requires structural repair involving replacement of prestressing force through new prestressing or post-tensioning. This may be considered as a repair to affect the service limit state in addition to the ultimate limit state.
Severe III	The experienced damage is too extensive. Repair is not practical and the member or element must be replaced.

7.3. REPAIR SYSTEM SELECTION

There are a number of available FRP composite systems used in repair or strengthening structural members, however it is recommended that all FRP applications used for repairing damaged bridge girders have carbon as the primary reinforcement (CFRP). Various CFRP repair application methods and their associated benefits/ limitations are presented in Table 7-2.

Table: 7-2: Various CFRP Repair Methods, Their Benefits and Limitations

Repair Methods Considered	**Maximum Level of Damage Suitable**	**Applicable Beam Geometries**	**Constructability/ Speed of Repair**
Pre-Cured CFRP	Severe I	All	Easy/ fast
CFRP Fabrics	Severe I (up to 22% loss of PS force)	All	Easy/ fast
NSM CFRP Bars	Severe I	I-B, otherwise limited	Difficult/ moderate
Prestressed CFRP	Severe II (replace lost PS force)	All	Difficult/moderate
Post-tensioned CFRP	Severe II (replace lost PS force)	All	Moderate/moderate
Girder Replacement	Severe III	All	Difficult/ very slow
All CFRP repair applications can be implemented when Minor or Moderate damages exist			

Using the evaluated damage classification of the structural member and Table 2-1 it can be quickly determined what the appropriate CFRP repair systems are. However, consideration

should be given to the fact that all though it has been demonstrated that prestressed and post-tensioned CFRP repairs utilize the carbon fiber material more efficiently, the difficulties and cost of implementation are more significant than the cost of extra CFRP material needed for non-prestressed applications.

Thus, the following information has been provided based on well documented experimental and analytical research concerning externally bonded non-prestressed unidirectional fabric CFRP. From this research it is recommended that the Tyfo® Fibrwrap® System from the Fyfe Co. LLC be used. Specifically, the Tyfo® SCH-41 composite using the Tyfo® S epoxy. If a repair system other than CFRP fabrics is required it is recommended to reference the ACI 440.2R-08 for proper repair considerations.

7.4. CFRP REPAIR DESIGN

The following repair design provisions were either adopted, altered, or derived from four primary sources; the ACI 440.2R-08, the NCHRP Report 514, the FDOT Structural Manual, and the associated research involving non-prestressed unidirectional CFRP fabric composites.

7.5. EXTERNALLY BONDED LAMINATES

It is recommended that a wet layup system is used and that the resin and adhesive shall be a thermo-set epoxy formulation specifically designed to be compatible with the fibers. As mentioned previously it is recommended to use any approved CFRP laminates such as the Tyfo® SCH-41 composite using the Tyfo® S epoxy from the Fyfe Co. LLC.

To design the CFRP repair, follow calculations and considerations in the ACI Committee 440.2R-08 ("Guide for the Design and Construction of Externally Bonded FRP Systems for Strengthening Concrete Structures") and other listed guidelines in this study. Loads shall be obtained using LRFD.

A. In addition to recommendations of ACI 440.2R-08 "Chapter 5 - Shipping, storage, and handling", use the associated information provided in Section II, Chapter 3 of the NCHRP 514 document.

B. Several types of FRP wrapping schemes are used to increase the flexure and shear strength of prestressed concrete girders. In all wrapping schemes, the FRP system can be installed continuously along the span of a member or placed as discrete strips. The use of continuous FRP reinforcement that completely encases a member is an efficient wrapping scheme; however, it could be discouraged since it might potentially prevent migration of moisture. Therefore, using longitudinal soffit CFRP and several U-wrappings at certain spacing proved to be a good repair alternative. It also helps prevent debonding of the soffit longitudinal laminates.

C. In addition to the requirements in the ACI 440.2R-08 "and the NCHRP 514 document, transverse CFRP reinforcement shall be provided at the termination points of each ply of CFRP flexural reinforcement. In addition, transverse U-wrapping reinforcement shall be provided at a maximum spacing of two-thirds of the girder height or one-half of the entire composite section height. The U-wrappings are provided along the length of the member

from end to end of the CFRP reinforcement. Intermediate transverse reinforcement shall extent to the top of the web. It is necessary to cover the damaged section with transverse and longitudinal strips to restrain the crack opening and propagation in the critical region which initiates early debonding.

7.5.1 EXTERNALLY BONDED DESIGN DETAILS

Soffit CFRP Lengths: The longitudinal reinforcements should extend a minimum distance equal to the full development length of the prestressing strands and can extend the entire span of the girder.

Overlapping/ Staggering: A lap joint shall be constructed when an interruption occurs in the direction of the fibers. Splices of FRP laminates should be provided only as permitted on drawings, specifications, or as authorized by the licensed design professional as recommended by the system manufacturer. The length of the lap splice shall be as specified by the contract documents, but must be at least 152 mm (6 in). Staggering of lap splices on multiple plies and adjacent strips shall be required unless permitted by contract documents. No lap joint is necessary in the transverse direction unless specified in the contract documents.

Alignment: Fiber orientation and straightness significantly affect the performance of a unidirectional FRP system. Misalignment may occur because of improper rolling or wrong placement of fiber sheets. Fiber misalignment is known to affect the strength more significantly than the elastic modulus. Fiber sheets must be handled with care according to the manufacturer recommendations to protect them from damage and to avoid misalignment or breakage of the fibers by pulling, separating, or wrinkling them or by folding the sheets. Alignment of fiber laminates and any necessary overlaps in multiple layers also affect the performance of the FRP system. Tolerances for misalignment of fibers are set according to current practice and the expected behavior based on classical laminate theory. The fiber plies shall be aligned on the structural member according to the contract documents and any deviation in the alignment more than 5° (approximately 87 mm/m or 1 in/ft) is not acceptable. Once installed, the fibers shall be free of kinks, folds, and waviness.

Anchoring of soffit longitudinal laminates with U-wrapping: Anchoring of fiber sheets helps prevent delamination failure of the FRP system. Different methods can be used to anchor the fiber sheets. When possible, U-wrappings may provide additional anchorage against premature delamination of the FRP system. Anchoring of FRP sheets to the concrete substrate shall follow the method specified in the contract documents or approved by the engineer. When using mechanical clamps and fasteners, care shall be taken to avoid damage to the FRP system or to the concrete substrate.

Anchoring of U-wrapping with longitudinal strip: A longitudinal CFRP strip should be provided at the top ends of U-wrappings to anchor them and prevent their premature debonding.

Tension Struts: In order to control shrinkage and flexural cracking, additional longitudinal sheets should be provided along the length of the repaired area covering the top and outside areas of the bottom flange. If the level of damage extends into the web, these tension

struts can be provided to cover that section as well.

7.6. CONSTRUCTION/ INSTALLATION

In wet layup systems, shear and flexural reinforcement shall have no more than four layers.

7.6.1. CONCRETE REPAIR AND SURFACE PREPARATION

All defective areas of concrete substrate shall be removed according to ACI 546R-96 and ICRI No. 03730, using appropriate equipment such as an air- or an electric-powered jack hammer or saw, at a sufficient depth of at least 12.7 mm (1/2 in) beyond the repair area to expose sound aggregates. If any reinforcing or prestressing steel is exposed in the process and either it is deteriorated or its bond with the concrete is broken in the process, an additional nominal depth of 19 mm (3/4 in) or at least 6.4 mm (1/4 in) larger than the largest aggregate in repair material shall be cut from its underside. If any deterioration is noticed in the repair area, its source shall be located and treated to the satisfaction of the engineer prior to restoring the section. Upon removing defective concrete, and before restoring the section, the substrate shall be cleaned from any dust, laitance, grease, oil, curing compounds, impregnations, foreign particles, wax, and other bond-inhibiting materials.

7.6.2. REPAIR OF DEFECTIVE REINFORCEMENT

All defective reinforcement shall be repaired according to ICRI No. 03730 and to the satisfaction of the engineer. FRP systems shall not be applied to concrete suspected of containing corroded reinforcement. Corroded or otherwise defective reinforcement that is to be supplemented shall be cleaned and prepared thoroughly by abrasive cleaning to a near white appearance. Damaged reinforcement that needs to be replaced shall be cut at sufficient length, according to the contract documents and the approval of the engineer, to ensure full section and sound material in the remaining portion. Splice for the ruptured or cut reinforcing or prestressing steel shall be provided at sufficient length, according to the contract documents and approval of the engineer.

Mechanical Anchorage: Mechanical anchorage of the repair material with the substrate shall be placed if specified in the contract documents. Anchors shall be secured in place by tying to other secured bars and shall not protrude outside concrete surface. If that is not possible, the concrete surface shall be built up to cover the protrusions.

7.6.3. RESTORATION OF CONCRETE CROSS-SECTION

The area of removed concrete substrate, and any void larger than 12.7 mm (1/2 in.) in diameter and depth, shall be filled with repair material that conforms to ICRI No. 03733. The repair material shall have a compressive strength equal to or greater than that of the original concrete, but no less than 31 and 38 MPa (4,500 and 5,500 psi) at 7 and 28 days, respectively. The design mix for all repair materials shall be approved by the engineer. The bond strength of the repair material to the existing concrete shall be a minimum of 1.4 MPa (200 psi) in the pull-off test according to ASTM D4541. The concrete substrate and the exposed reinforcing or prestressing steel shall be clean, sound, and free of surface moisture and frost before restoring the section. Before placement of patching materials, a water-based epoxy

cementitious bonding agent shall be applied to concrete and exposed reinforcement. Also, cracks within solid concrete in the substrate shall be stabilized using epoxy injection methods, as specified in Section 4.4.3. If the water leak through cracks or concrete joints is significant, water protection and a water conveyance and weep holes shall be provided before restoring the section. The repair material shall be cured a minimum of 7 days before installing the FRP system unless its curing and strength are verified by tests.

7.6.4. SURFACE PREPARATION

All necessary repair and restoration of a concrete section shall be approved by the engineer prior to surface preparation. In these specifications, contact-critical applications are treated in the same way as bond-critical applications. An adhesive bond with adequate strength shall always be provided between FRP and concrete. Surface preparation shall also promote continuous intimate contact between FRP and concrete by providing a clean, smooth, and flat or convex surface. Surface preparation for near surface mounted FRP bars or strips is specified in Section 4.4.4. Surface preparation for FRP shell systems where grout is pumped into the gap between the shell and the existing column surface is specified in Section 4.4.5. All surface preparations shall be approved by the engineer before installing the FRP system.

Surface Grinding

All irregularities, unevenness, and sharp protrusions in the surface profile shall be grinded away to a smooth surface with less than 0.8-mm (1/32-in.) deviation. Disk grinders or other similar devices shall be used to remove stain, paint, or any other surface substance that may affect the bond. Voids or depressions with diameters larger than 12.7 mm (1/2 in.) or depths greater than 3.2 mm (1/8 in.), when measured from a 305-mm (12-in.) straight edge placed on the surface, shall be filled according to Section 4.4.5.

Chamfering Corners

All inside and outside corners and sharp edges shall be rounded or chamfered to a minimum radius of 12.7 mm (1/2 in.) as per ACI 440.2R-02. Ridges, form lines, and sharp or roughened edges greater than 6.4 mm (1/4 in.) shall need to be ground down or filled with putty, as specified in Section 4.4.5. Obstructions and embedded objects shall be removed before installing the FRP system if required by the engineer.

Crack Injection

All cracks in the surface of concrete or the substrate that are wider than 0.25 mm (1/100 in.) shall be filled using pressure injection of epoxy according to ACI 224.1R. Smaller cracks may also require resin injection in aggressive environments. Follow ACI 224R-01 crack width criteria for various exposure conditions. The FRP system shall be installed no earlier than 24 hours after crack injection. Any surface roughness caused by injection shall be removed as per Section 4.4.1.

Surface Profiling

After surface grinding, any remaining unevenness in the surface greater than that specified in

Section 4.4.3, including out-of-plane variations, fins, protrusions, bug holes, depressions voids, and roughened corners, shall be filled and smoothed over using putty made of epoxy resin mortar or polymer cement mortar with strength equal to or greater than the strength of the original concrete. The patching material shall be cured a minimum of 7 days before installing the FRP system unless its curing and strength are verified by tests.

Surface Cleaning

Substrate concrete and finished surface of concrete shall be cleaned to the approval of the engineer. Cleaning shall remove any dust, laitance, grease, oil, curing compounds, wax, impregnations, stains, paint coatings, surface lubricants, foreign particles, weathered layers, or any other bond-inhibiting material. If power wash is used, the surface shall be allowed to dry thoroughly before installing the FRP system. The cleaned surface shall be protected against redeposit of any bond-inhibiting materials. Newly repaired or patched surfaces that have not cured a minimum of 7 days shall be coated with a water-based epoxy paint or other approved sealers.

7.6.5. INSPECTION AND INSTALLATION OF CFRP SYSTEM

Before starting the project, the manufacturer's certifications for all delivered and stored FRP components will be inspected for conformity to the contract documents. Testing in this section is for acceptance and not for qualification. For qualification testing, consult with the AASHTO Materials Specifications for FRP Systems. Materials testing will be conducted on witness panels of wet layups. Testing may include tensile strength and modulus, glass transition temperature (T_g), pot life, adhesive shear strength, lap splice strength, and hardness, according to ASTM standards, such as ASTM D3039.

Installation of CFRP should follow the guidelines of the ACI 440.2R-08 and the NCHRP 514 document.

7.6.6. INSPECTION AND QUALITY CONTROL AFTER CFRP APPLICATION

In the case of bonded FRP laminates, inspections should focus on the condition of the bond. It is necessary to develop recommended field procedures, evaluation guidelines, and reporting standards for periodic inspection of in-service FRP systems.

8. REFERENCES

1. ACI Committee 440, "ACI 440.2R-08 Guide for the Design and Construction of Externally Bonded FRP Systems for Strengthening Concrete Structures", American Concrete Institute, Farmington Hills, MI, 2008, pp. 80.
2. Agarwal, A.K. and Chen, C., “Bridge Vehicle Impact Assessment”, Project #C-07-10, New York State Department of Transportation, 2008.
3. Al-Rousan, R.; Issa, M., Fatigue performance of reinforced concrete beams strengthened with CFRP sheets, *Construction and Building Materials* vol. 25 issue 8 August, 2011. p. 3520-3529
4. Charkas, H., Rasheed, H.A., and Melhem, H. (2003). “Rigorous procedure for calculating deflections of fiber-reinforced polymer-strengthened reinforced concrete beams.” *ACI Struct. J.*, 100(4), 529-539.
5. Di Ludovico, M., “Experimental Behavior of Prestressed Concrete Beams Strengthened with FRP”, Report CIES 03-42, University of Missouri-Rolla, MO., 2003.
6. Di Ludovico, M., Nanni, A., Prota, A., & Cosenza, E. (2005). Repair of Bridge Girders with Composites: Experimental and Analytical Validation. ACI Structural Journal, 102(5), 639-648.
7. ElSafty, A., and Graeff, M., “Investigating the Most Effective CFRP Configuration in Repairing Damaged Concrete Beams due to Collision”, The 13th International Conference on Civil, Structural and Environmental Engineering Computing, Crete, Greece, CC2011/2011.
8. El-Tawil, S. and Okeil, A. M. (2002), "LRFD Flexural Provisions For PSC Bridge Girders Strengthened with CFRP Laminates," *ACI Structural Journal*, Vol. 99, No. 2, March-April, pp. 300-310.
9. Feldman, Lisa R., Jirsa, James O., and Kowal, Edward S.. "Repair of Bridge Impact Damage.", *Concrete International*, 20.2 (1998): 61-66.
10. Fu, C.C., Burhouse, J.R. and Chang, G. L., “Study of Overheight Vehicles with Highway Bridges”, *Transportation Research Board*, 2003.
11. Grace, Abdel-Sayed, Soliman, and Sale, “Strengthening Reinforced Concrete Beams Using Fiber Reinforced Polymer CFRP Laminates,” *ACI Structural Journal*, V. 96, No. 5, Sept.-Oct. 1999.
12. Grace, N. F., and Abdel-Sayed, G., “Construction and Evaluation of Full-Scale CFRP Prestressed Concrete DT-Girder,” Proceeding of the Sixth International Symposium of FRP Reinforcement for Concrete Structures, Singapore, July 2003.
13. Green, P. S., Boyd, A. J., and Lammert, K., CFRP Repair of Impact-Damaged Bridge Girders, Volume I: Structural Evaluation of Impact Damaged Prestressed Concrete I Girders Repaired with FRP Materials (Florida Department of Transportation Report BC354-55), University of Florida, Gainesville, FL, 2004.
14. Hanchey, C. M. and Exley, S. F. (1990). “Overheight Vehicle Warning Systems in Mississippi”, *ITE Journal*, 60(6), 24-29.
15. Harik, I.E., Shaaban, A.M., Gesund, H., Valli, G.Y.S., and Wang, S.T., (1990), “United States Bridge Failures, 1951-1998”, *Journal of Performance of Constructed Facilities*, Volume 4. No. 4, November 1990, Pages 272-277
16. Harries, K.A., 2009, “Structural Testing of Prestressed Concrete Girders from the Lake View Drive Bridge, *ASCE Journal of Bridge Engineering*, V. 14, No. 2, pp. 78-92.
17. Kasan, J. L., “Structural Repair of Prestressed Concrete Bridge Girders”, MSCE Thesis, University of Pittsburgh, Pennsylvania, 2009.

18. Kasan, J.L. and Harries, K. A., “Repair of Impact-Damaged Prestressed Concrete Bridge Girders with Carbon-Fiber-Reinforced Polymers” in Asia-Pacific Conference on FRP in Structures 2009, APFIS, Seoul, Korea, 2009.
19. Klaiber, F. W., T. J. Wipf, F. M. Russo, R. R. Paradis, and R. E. Monteega, Field/Laboratory Testing of Damaged Prestressed Concrete Girder Bridges, Iowa DOT Project HR-397, Final Report, Ames, Iowa, December 1999
20. Klaiber, W. F., Wipf, T. J. and Kempers, B. J., “Repair of Damaged Prestressed Concrete Bridges Using CFRP”, Mid-Continent Transportation Research Symposium, Iowa State University, 2003
21. NCHRP R-655, National Cooperative Highway Research Program, “Recommended Guide Specification for the Design of Externally Bonded FRP Systems for Repair and Strengthening of Concrete Bridge Elements” WASHINGTON, D.C., 2010
22. NCHRP R-514, National Cooperative Highway Research Program, “Bonded Repair and Retrofit of Concrete Structures Using FRP Composites - Recommended Construction Specifications and Process Control Manual” WASHINGTON, D.C., 2004
23. Nanni, A., Huang, P.C. and Tumialan, J.G., “Strengthening of Impact-Damaged Bridge Girder Using FRP Laminates”, 9th Int. Conf., Structural Faults and Repair, July 2001, Engineering Technics Press, London, UK.
24. Rosenboom, O. and Rizkalla, S., "Behavior of Prestressed Concrete Strengthened with Various CFRP Systems Subjected to Fatigue Loading", *ASCE Journal of Composites for Construction*, November/December 2006, Vol. 10, Issue 6, pp. 492-502.
25. Rosenboom, O. A., Miller, A. D., and Rizkalla, S., “Repair of Impact-Damaged Prestressed Concrete Bridge Girders using CFRP Materials”, *ACSE Journal of Bridge Engineering*, 2011.
26. S. El-Tawil, A. Okeil, M. Shahawy, (2001). Static and Fatigue Analyses of RC Beams Strengthened with CFRP Laminates. *Journal of Structural Engineering, ASCE*, Vol. 125, No. 9, September 1999, pp. 1009-1019.
27. Schiebel, S., R.Parretti, and Nanni, A., “Repair and Strengthening of Impacted PC Girders on Bridge”, Report A4845, Missouri Department of Transportation, 2001.
28. Shanafelt, G.O. and Horn, W.B., “Damage Evaluation and Repair Methods for Prestressed Concrete Bridge Members”, NCHRP Report 226, Project No. 12-21, *Transportation Research Board*, Washington, D.C., 1980.
29. Shanafelt, G.O. and Horn, W.B., “Guidelines for Evaluation and Repair of Prestressed Concrete Bridge Members”, NCHRP Report 280, Project No. 12-21(1), *Transportation Research Board*, Washington, D.C., 1985.
30. Shin, Y. and Lee, C., “Flexural Behavior of Reinforced Concrete Girders Strengthened with Carbon-Fiber-Reinforced Polymer Laminates at Different Levels of Sustaining Load”, *ACI Structural Journal*, V. 100, No.2, March-April 2003.
31. “Span Damage Rate Rising.” (1988). Michigan Roads and Construction, 85(50), 3.
32. Stallings, J.M., Tedesco, J.W., El-Mihilmy, M., and McCauley, M., “Field Performance of FRP Bridge Repairs”, *Journal of Bridge Engineering*, V. 05, No.5, 2000, pp. 107-113.
33. Tumialan, J.G., Huang, P.C, and Nanni, A., “Strengthening of an Impacted PC Girder on Bridge A10062”, Final Report RDT01-013/RI99-041, Missouri Department of Transportation, 2001.

9. APPENDIX 1: PREPARATION AND TESTING OF PRESTRESSED CONCRETE GIRDERS

Figure 9-1 shows the sawing to simulate the concrete damage for the girder. Figure 9-2 shows the repaired concrete. Figures 9-3 and 9-4 show the girder preparation and CFRP wrapping application.

Figure 9-1: Sawing in actual PSC girder

Figure 9-2: Repair of the concrete damage

Figure 9-3: Girder preparation for wrapping

Figure 9-4: CFRP wrapping application

Figure 9-5 shows testing preparation and girder set-up. Figure 9-6 shows girder failure under loading.


Figure 9-5: Testing preparation and set-up


Figure 9-6: Girder failure under loading